

Head versus tail:
germ cell-less initiates axis formation via
homeobrain and *zen1* in a beetle

Dissertation

for the award of the degree

“*Doctor rerum naturalium*”

Division of Mathematics and Natural Sciences

of the Georg-August-Universität Göttingen

within the doctoral program Genes and Development

of the Georg-August University School of Science (GAUSS)

submitted by

Salim Ansari

from Seorahi, India

Göttingen 2017

Thesis Committee

Prof. Dr. Gregor Bucher (advisor)

(Dept. of Evolutionary Developmental Genetics, Johann-Friedrich-Blumenbach Institute of Zoology and Anthropology)

Prof. Dr. Reinhard Schuh

(Dept. of Molecular Developmental Biology, Max Planck Institute for Biophysical Chemistry)

Prof. Dr. Jörg Großhans

(Dept. of Developmental Biochemistry, University Medical Faculty Göttingen)

Members of the Examination Board

Referee: Prof. Dr. Gregor Bucher

(Dept. of Evolutionary Developmental Genetics, Johann-Friedrich-Blumenbach Institute of Zoology and Anthropology)

2nd Referee: Prof. Dr. Reinhard Schuh

(Dept. of Molecular Developmental Biology, Max Planck Institute for Biophysical Chemistry)

Further members of the Examination Board

Prof. Dr. Jörg Großhans

(Dept. of Developmental Biochemistry, University Medical Faculty Göttingen)

Dr. Nico Posnien

(Dept. of Developmental Biology, Johann-Friedrich-Blumenbach Institute of Zoology and Anthropology)

Prof. Dr. Ralf Heinrich

(Dept. of Cellular Neurobiology, Johann-Friedrich-Blumenbach Institute of Zoology and Anthropology)

Prof. Dr. Daniel Jackson

(Dept. of Geobiology, Courant Research Centre)

Date of oral examination: 21.09.2017

Declaration

I hereby affirm that the doctoral thesis entitled,

"Head versus tail: *germ cell-less* initiates axis formation via *homeobrain* and *zen1* in a beetle"

prepared on my own and with no other sources and aids than quoted.

_____ Göttingen, August 7th, 2017.

Salim Ansari

To my Family and Friends

Acknowledgments

Throughout my studies, I was lucky to be surrounded by amazing, joyful and honest people which certainly shaped me as a person and guided me during this educational journey.

My sincere gratitude to my supervisor and mentor Prof. Gregor Bucher for his constant support, guidance, encouragement and freedom to pursue my own interests and ideas. When I landed in Germany (first official foreign visit) I had the expectation that I need to maintain a barrier with Professors or higher ranked people. But this myth has been kaput since I met him. He has been very kind and supportive, and at the same time humorous like a friend. I was happy to share not only lab life problems but also outdoor problems. His contribution throughout these years of my PhD has made the experiences productive and stimulating.

Many thanks to Prof. Reinhard Schuh and Prof. Jörg Großhans for being the member of my thesis committee and for all the suggestions, support and encouragement.

I would like to thank Prof. Ernst Wimmer and Dr. Nico Posnien for all the suggestions and support during the PhD. I would like to thank Prof. Martin Klingler, Dr. Michael Schoppmeier and Matthias Teuscher for hosting me in Erlangen and making sure everything went well. I would also like to thank the whole iBeetle community for their support, sharing expertise, and insightful discussions and meetings.

My sincere thanks to Inga Schild who happened to be the first person I met in Germany. She has helped me with all the bureaucracy stuff, from getting an apartment to get registered at Göttingen University. Dr. Daniela Großmann become my first supervisor in Germany who taught me not only how to inject the beetles but also how to remain motivated and cheerful all the time. She has helped me understanding the German culture and in return I hope I was able to present a glimpse of Indian culture. Many thanks to Dr. Marita Büscher for being the well-wisher and helping me out from scientific to non-

scientific problems. I have enjoyed all the non-scientific discussion from political to religious issues.

All these years of PhD studies were full of surprises, pleasant experiences, parties and memories. The credit goes to my labmates whom I literally call 'savemate' for creating the wonderful environment and always being ready to help. During this work I have been blessed to know many noble mates who never let me feel that I am living in foreign land. My warmest thanks to Peter, Max, Janna, Yong, Julia, Felix Kaufholz, Jürgen, Magdalena, Bicheng, Georg, Jonas, Hassan, Musa, Felix Quade, Atika, Kolja, Montse, Micael, Christoph, Ingrid and Constanza who were always supportive whenever I bugged them for help.

My special thanks to Peter and Max for helping me out in day to day problems. I have enjoyed those moments either on the spikeball playground or at the Playstation.

All the members of Lab3, Lab2 and Lab1 are very much appreciated for their constant support and scientific discussion. Thanks to Hanna for being a perfect student and for effort and patience. I would like to thank Prateek Sir, Md. Salim, Manoj, Parth, Anupam, Chandra, Mukesh Sir, Aman, Achintya and the Indian community in Göttingen for creating the cheerful and lively atmosphere outside of the lab life. I have been fortunate to make many good friends through sports who always tried to give me competition. I would like to heartily thank them for exploring Europe with me and for those crazy holidays. Parth, Anupam, Manoj, Chandra have been joyful and energetic travel companion in exploring the beauty of Europe. Many thanks to my friends in India (JNUites and Seorahikars) who were always supportive and encouraging and believed in me. I used to call them whenever I was disheartened. They were kind enough to discuss the undiscussable things secretly and used to make me laugh a lot.

The congenial environment and help with paper work provided by the secretaries, Birgit Rossi, Constanze Gerhards, Selen Pfändner, Merle Eggers, and Bettina Hucke are highly acknowledged and I am deeply grateful to them. Big thanks to Birgit, Beate Preitz and

Merle for all those suggestions and appreciation for my cooking. I would like to thank Constanza for inviting me on Christmas Eve which was very exciting to experience the culture.

My sincere thanks to Claudia Hinner, Elke Küster, Katrin Kanbach, Helma Griess and Angelika Löffers for technical support. I am very grateful to Claudia for tolerating me as a lab neighbor and helping me with those emergency dsRNAs and ISH request. Beate was always kind to solve microscope issues and taught me handling of the microscopes.

I truly appreciate and am grateful to the DFG, GGNB and Göttingen University for providing me a PhD salary. This was the fuel which kept me going and help me to become financial independent. On a different note, I will remember the Göttingen life, its very atmosphere, smiling people, freedom of expression and culture.

Friends are the family you choose. If you fall, I will pick you up...after I'm done laughing. By an unknown friend

Contents

1 Summary	1
2 Introduction	3
2.1 A genome-wide RNAi screen in <i>Tribolium castaneum</i>	3
2.2.1 RNAi screen vs classic genetic screen	6
2.3 Axis specification in insects.....	7
2.3.1 A-P axis specification and patterning in <i>Drosophila</i>	8
2.4 Evolution of anterior axis formation	12
2.4.1 <i>bicoid</i>	12
2.4.2 <i>panish</i>	13
2.5 Long vs short germ development.....	13
2.6 A-P axis specification and patterning in <i>Tribolium castaneum</i>	15
2.6.1 Zygotic genes	17
2.7 <i>germ cell-less</i>	19
2.8 <i>homeobrain</i>	22
3 Material and Methods	24
3.1 Model organism	24
3.2 The iBeetle screening procedure	25
3.3 iBeetle Database annotation.....	31
3.4 Phylogenetic analysis.....	32
3.5 Cloning.....	33
3.6 Fixation.....	34

3.7 Whole mount <i>in situ</i> hybridization	34
3.7.1 <i>In situ</i> probe	34
3.7.2 Mounting	35
3.8 RNAi	35
3.8 Image processing	36
3.9 Generation of a Tc-Gcl polyclonal antibody	36
3.9.1 Cloning	36
3.9.2 Protein expression and purification	38
3.9.3 Antibodies	38
3.9.4 Antibody staining of <i>Tribolium</i> embryos	39
3.10 Ovary analysis	39
3.10.1 Ovary WMISH	39
3.10.2 Ovary antibody staining	40
3.11 qRT PCR	40
3.11.1 RNA extraction	40
3.11.2 cDNA synthesis	40
3.11.3 Analysis	41
4 Result	42
4.1 Part I: The iBeetle screen	42
4.1.1 Screening	42
4.1.2 Selection criteria for head phenotypes	45
4.1.3 Rescreening: I	48
4.1.3 Rescreening: II	50
4.1.4 Initial analysis of novel head patterning genes	52

4.1.4.1 Phylogenetic analysis, RNAi phenotype and expression pattern of <i>Tribolium fat.</i>	53
4.1.4.2 Phylogenetic analysis, RNAi phenotype and expression pattern of <i>Tribolium multiple epidermal growth factor-like domain protein 8.</i>	56
4.1.4.3 Phylogenetic analysis, RNAi phenotype and expression pattern of <i>Tribolium protein kinase D3.</i>	59
4.1.4.4 Phylogenetic analysis, RNAi phenotype and expression pattern of <i>Tribolium E3 ubiquitin protein ligase HUWE1.</i>	62
4.1.4.5 Phylogenetic analysis, RNAi phenotype and expression pattern of <i>Tribolium amun.</i>	65
4.1.4.6 Phylogenetic analysis, RNAi phenotype and expression pattern of <i>Tribolium neurogenic protein big brain.</i>	68
4.1.4.7 Phylogenetic analysis, RNAi phenotype and expression pattern of <i>Tribolium polycomb group protein Psc.</i>	71
4.1.4.8 Phylogenetic analysis, RNAi phenotype and expression pattern of TC007939.....	74
4.1.5 Head patterning genes after genome-wide screen	75
4.2 Part II: The Gcl project	76
Research article.....	77
Abstract	77
Main text	78
New genes in AP-axis formation	80
<i>Tc-gcl</i> acts upstream in anterior patterning	82
Tc-Gcl may not act via Wnt signaling alone	82
Zygotic genes contribute to axis formation.....	84
A model for axis formation in short germ embryos	85
Zygotic regulation instead of gradients.....	86
Main Figures	88

Methods	93
Extended Data	97
5 Discussion	110
5.1 Part I: The iBeetle screen.....	110
5.1.1 The iBeetle screen- a new way to identify novel genes for many insect biological processes	110
5.1.1.1 Reasons for false positives	112
5.1.1.2 Reasons for false negatives	113
5.1.1.3 Results of the iBeetle project posed the following new questions to be answered in the future	114
5.1.2 Lesson from the rescreening	116
5.1.3 Prioritization of the final candidates for detailed analysis	117
5.2 Part II: The Gcl project	121
5.2.1 Finding of <i>Tc-gcl</i> and <i>Tc-hbn</i>	121
5.2.2 Where and how does Tc-Gcl Work?.....	122
5.2.2.1 How does Tc-Gcl control the maternal <i>Tc-axin</i> expression?.....	124
5.2.3 Hypothesis of anterior localization of maternal <i>Tc-axin</i> mRNA	125
5.2.4 Tc-Gcl may not be involved in the germ cell development.....	126
5.2.3 Role of Tc-Hbn in anterior patterning.....	126
5.2.4 Mechanism behind double abdomen formation	127
5.2.4 Zygotic control of axis specification in insects.....	128
5.2.5 Outlook	129
6 References	131
7 Appendix	152
7.1 List of <i>Tc</i> genes	152

7.2 Vectors used during the study 154

7.3 Phylogenetic trees of *Tc-gcl* and *Tc-hbn*..... 156

8 Curriculum vitae 158

1 Summary

The iBeetle screen project: Christiane Nüsslein-Volhard and Eric Wieschaus performed the first saturated forward genetic screen using random mutagenesis to identify genes important for embryonic development in *Drosophila melanogaster*. However, the *Drosophila* larval head turns outside in during embryogenesis as a result this involuted head lacks phenotypic markers for identification of defects. Moreover, perturbation of *Drosophila* head development often interferes with head involution making it difficult to identify the primary phenotype. Therefore, we decided to study head development in an alternative model organism with an insect typical head, *Tribolium castaneum*. In order to identify all genes required for head development, the genome-wide iBeetle RNAi screen has been performed. I participated in the second phase of this screen to not only identify head related phenotypes but also muscle, ovary, stink gland and other phenotypes. After completion of screening phase with 865 screened genes, I was able to identify eight novel head patterning genes from 3,500 genes during the rescreening phase. Moreover, I performed the preliminary study of all eight genes which include phylogenetic analysis, RNAi phenotype and expression pattern analysis.

The Gcl project: Axis formation is an essential, early processes during bilaterian development. Classical manipulation like cytoplasm leakage, cytoplasm ligation, UV irradiation and RNase treatment showed that global organizing centres operate from both ends of insect eggs and establish the anterior-posterior (A-P) axis. Christiane Nüsslein-Volhard and co-workers identified the first anterior global pattern organizer (*-bicoid*) from *Drosophila melanogaster* in 1987. Bicoid is a morphogen that autonomously patterns the

anterior structure in a concentration dependent manner to pattern the A-P axis. However, *bicoid* is limited to higher flies and neither anterior determinants nor a molecular mechanism that establishes A-P polarity in less short germ insects like beetles have been discovered. In an ongoing genome-wide RNAi screen in the short germ beetle *Tribolium castaneum*, two genes namely *Tc-germ cell-less* (*Tc-gcl*) and *Tc-homeobrain* (*Tc-hbn*) were identified whose knockdown resulted in larvae with a double abdomen phenotype similar to *Dm-bicoid* and *Dm-hunchback* double mutants in *Drosophila*. *Dm-gcl* is known to be involved in germ cell development at the posterior pole, but not for anterior patterning in *Drosophila*. Surprisingly, I found that *Tc-gcl* is involved in A-P axis formation at the anterior pole in *Tribolium*. The *Drosophila* ortholog of the second gene (-Hbn) did not have phenotypic or functional information available. I was able to show that *Tc-hbn* plays an important role in axis formation in *Tribolium*. This is the first report where zygotic genes are required for axis formation in insects as they do in vertebrates. Specifically, duplication of functional SAZ (segment addition zone) either during blastoderm stage or postblastoderm stage provide the evidence of zygotic control of axis formation. The first double anterior phenotype for short germ insects was observed after double knockdown of *Tc-caudal* and *Tc-pangolin*. Moreover, Wnt signaling needs to be repressed anteriorly during early embryogenesis for proper anterior development in *Tribolium* similar to vertebrates (but not in *Drosophila*). We introduce a novel technique that will help overcoming a major problem of RNAi studies in the emerging model organisms. Often, RNAi leads to lethality or sterility of the mother before offspring can be analyzed. In this study, I was able to show that VSR (viral suppressor of RNAi) transgenic line (developed by Julia Ulrich), which ubiquitously expresses an RNAi inhibitor, can rescue the sterility of the mother without compromising the zygotic phenotypes. Based on my finding, I established the most comprehensive model for insect axis formation outside of *Drosophila*.

2 Introduction

2.1 A genome-wide RNAi screen in *Tribolium castaneum*

Although insects are the most species rich class of animals, only one species *Drosophila melanogaster* contributes most to our understanding of insect biology. There are both technical and practical reasons that established *Drosophila* as the best studied insect model organism. Practical reasons include a short generation time, easy and cheap stock keeping, and a large number of progeny throughout the year. Technical reasons include tools for saturated genetic screens, a multitude of genetic tools, a well annotated genome and many collections of transgenic and mutant lines and antibodies (Hales et al., 2015; Nüsslein-Volhard and Wieschaus, 1980; St Johnston, 2002). However, *Drosophila* does not represent in many aspects the biology of most insects because of its derived situation. Researchers have tried to perform forward genetic screens in more typical insect species such as *Nasonia vitripennis* and *Tribolium castaneum* (Pultz et al., 2000; Sulston and Anderson, 1996; Trauner et al., 2009). However, these genetic screens were not able to reach saturation because of technical reasons: for example a lack of balancer chromosomes and difficult stock keeping. Therefore most insect biology knowledge comes from *Drosophila*. So far, researchers have been using candidate gene approaches in these alternative model organisms to study the variety of biological process. The candidate genes were selected based on findings in *Drosophila* and other established model organisms that gave an opportunity to study the role of the orthologs in these alternative model organism (Bolognesi et al., 2008; Bucher and Klingler, 2004; Posnien et al., 2011). However, this approach has the following restrictions. First, it limits the functional studies to those genes that are conserved. Second, it limits the identification of novel genes or species specific genes. Third, it also limits the study of biological process which are absent in established model organisms. Fourth, candidate gene approach reached saturation but components of biological process were still missing. (Schmitt-Engel et al., 2015a).

These limitations prompted researchers to perform unbiased genome-wide screening in more representative insects. This has been complemented by breakthroughs in genetic manipulation that allowed to do functional genetics in alternative model organism as well. (This has been complemented by breakthroughs in genetic manipulation tools that allowed to perform second comprehensive screen in novel organism.) Particularly, reverse genetics based on next generation sequencing and RNA interference (RNAi) open up the opportunity to do unbiased genome-wide screening in the red flour beetle, *Tribolium castaneum* (Schmitt-Engel et al., 2015a). *Tribolium* is well suited for genome-wide RNAi screening because of following reasons. *Tribolium* shows a strong RNAi response that often phenocopies a null phenotype. Environmental RNAi in *Tribolium* is systemic (i.e. the effect spreads throughout the body) and parental RNAi (i.e. the effect is transferred to the next generation) is possible as well. *Tribolium* has a well annotated genome and an updated gene set with splice variants information based on RNA sequencing (RNA-Seq) data. In addition, *Tribolium* is amenable for transposon mediated insertion, CRISPR/Cas genome editing and in vivo imaging (Benton et al., 2013; Berghammer et al., 2009a; Bucher et al., 2002; Gilles et al., 2015; Schinko et al., 2010; Trauner et al., 2009; *Tribolium* Genome Sequencing Consortium et al., 2008).

Biological reasons are following: *Tribolium castaneum* belongs to the coleopterans which is more species rich than diptera (*Drosophila*). *Tribolium* development shows more insect typical features than *Drosophila*. For instance, *Tribolium* has short germ embryos, larval legs, a non-involuted head and extra-embryonic tissues. In addition, *Tribolium* is a pest of stored grain products and provides the chance to serve as a model organism for the study of other economical important coleopteran pest species like the boll weevil, the bark beetles and (possibly) others. (Panfilio, 2008; Posnien et al., 2010; Schröder et al., 2008; Sokoloff, 1972; *Tribolium* Genome Sequencing Consortium et al., 2008).

The iBeetle screen, a genome-wide RNAi screen, is a collaboration of the German *Tribolium* community which aims to analyze the loss of function effect of every gene in the *Tribolium* genome. The iBeetle project has following three main purposes.

1. To identify genes from processes which are either not present in *Drosophila* (stink gland, embryonic leg development, etc.) or are difficult to study (involted head, somatic stem cells etc.) (Li et al., 2013; Panfilio, 2008; Posnien et al., 2010; Snodgrass, 1954).
2. To establish *Tribolium* as an efficient complementary screening platform which will allow to identify the genes of conserved processes (e.g. muscle development in *Drosophila*) which were not identified in established model organisms due to evolutionary changes such as species specific gene loss or redundancy of gene duplication (Schmitt-Engel et al., 2015).
3. To overcome the exhausted candidate gene approach (All the predicted genes through candidate gene approach were analyzed in *Tribolium* but there are still many novel factors to be discovered) and to achieve a saturated screen in *Tribolium* (Fu et al., 2012a; Savard et al., 2006).

In first phase of the iBeetle screening, larval and pupal screens were performed in parallel and covered 30% of *Tribolium* genome (Schmitt-Engel et al., 2015a). Larval screen aims to identify metamorphosis phenotypes by injecting dsRNA in female larvae-L6. The pupal screen aims to identify embryonic phenotypes by injecting dsRNA in female pupae. I became part of the iBeetle project in the second phase of screening where we only performed pupal screening. The second phase of the pupal screen refers to screening the function of random genes in those biological process that includes embryogenesis, muscle formation, ovary development and stink gland biology. Screening includes the injection of dsRNA and subsequent analysis for above mentioned phenotypes which took around 14 months. The following confirmation of selected candidates for detailed analysis took approximately another 4 months. With the funding from BAYER Crop Science, the iBeetle project aims to cover the whole *Tribolium* genome by the end of 2019. In addition, iBeetle base (<http://ibeetle-base.uni-goettingen.de>) and FlyBase (<http://flybase.org>) have mutual links to share the relevant information (Dönitz et al., 2013, 2015)

2.2.1 RNAi screen vs classic genetic screen

The major conclusion of the first half of the iBeetle screening is that RNAi screens have certain advantage over classical forward genetics. For example, RNAi screens do not require balancer chromosome and laborious stock keeping work (Berghammer et al., 1999). In the iBeetle screening, all the phenotypic information as well as genetic information are electronically stored in the iBeetle base that is accessible for anyone and phenotypes can be easily reproduced without exchange of any further information. The identity of the knocked down genes are already known contrary to classical forward screens (Dönitz et al., 2015). RNAi can be easily performed at different development stages to identify the early and late functions of genes separately. In addition, parental RNAi is able to knockdown both maternal and zygotic gene function and as a result reveals phenotypes not found by the zygotic null mutants produced by classical forward screens. RNAi could be used to generate the hypomorphic phenotypes for lethal and pleiotropic genes, identification of those phenotypes that led to genetic compensation due to mutations. Moreover, the penetrance of RNAi phenotypes is high (around 80%) compared to classic genetic screens (around 25%) (Bucher et al., 2002; Rossi et al., 2015; St Johnston, 2002). On the other hand, an RNAi screen does not give null phenotypes which is seen in classical screen.

The iBeetle screening has led to the identification of novel genes for many biological processes which would have not been possible by the candidate gene approach. For instance, *Tc-Rbm24* was found to be involved in muscle development of *Tribolium*. Interestingly, the ortholog of *Tc-Rbm24* is absent in *Drosophila* but present in vertebrates and required for muscle development. Moreover, the iBeetle screen has identified several genes in those biological processes which are either absent in *Drosophila* or were not possible to identify by differential gene expression analysis (e.g. stink gland physiology)(Li et al., 2013; Schmitt-Engel et al., 2015a; Siemanowski et al., 2015).

2.3 Axis specification in insects

One of the most important steps during bilaterian embryonic development is setting up the anterior-posterior (A-P) and dorsal-ventral (D-V) axes. A-P axis and D-V axis correspond to the head to tail and the back to belly axis, respectively. Axis specification and pattern formation have fascinated developmental biologists since the nineteenth century. Many organisms evolved to have different mechanisms to establish the A-P axis. For example, *C. elegans* uses the spatial information of the sperm pronucleus while the chicken uses gravitational information (Gilbert, 2014). Insects have been used extensively to study this process. Early in the nineteenth century it was suggested that the instruction signal of axis specification operates from thoracic region (Haget 1953). This hypothesis was challenged by many researchers. For example, Yajima showed that depending on the orientation of the embryo, vertical centrifugation was able to produce double head (abdomen replaced with head) or double abdomen (head replaced with abdomen) phenotypes in *Chironomus dorsalis* (Yajima, 1960). Sander showed the axis duplication (double head and double abdomen) phenotype in *Euscelis plebre* by classical manipulation (pricking, transplantation and ligation) (Sander, 1961). Yajima and Kalthoff observed a double malformation phenotype using UV irradiation and RNase treatment (Kalthoff, 1971; Kalthoff and Sander, 1968; Yajima, 1964). The generation of this striking phenotype in a variety of insects using different classical manipulations led to the hypothesis of a two gradient system active at both poles to specify the A-P axis. Both the anterior and posterior poles, and the middle portion of the embryo were suggested to be formed through the interaction of oppositely localized global organizing centres (Kalthoff, 1971; Kalthoff and Sander, 1968; Sander, 1961; Yajima, 1960, 1964). In spite of the remarkable and informative phenotypes induced by classic manipulation in both lower dipterans and higher dipterans, scientists were not able to discover the factors (genes) which are responsible for A-P axis formation and patterning of insects. However, they speculated that nucleic acids could be involved in this process. (Frohnhofer et al., 1986).

2.3.1 A-P axis specification and patterning in *Drosophila*

A number of mutants generated in classical forward genetic screens showed axis duplication as well as anterior and posterior deletion phenotypes which led to the discovery of the components for A-P axis specification (Mohler and Wieschaus, 1986; Nüsslein-Volhard and Wieschaus, 1980; Schupbach and Wieschaus, 1986). This ground-breaking discovery of early embryonic development was honoured with the Noble prize (for medicine in 1995) to Christiane Nüsslein-Volhard, Eric Wieschaus and Edward Lewis. *Drosophila* possess polytrophic meroistic ovarioles where nurse cells reside with developing oocytes in a follicle chamber (Bünnig 2006). These nurse cells provide maternal factors as well as the cellular machinery (e.g. organelles) for the developing oocytes via cellular interconnections (St Johnston and Nüsslein-Volhard, 1992). Axis specification initiates by the posteriorly localized tissue growth factor alpha ($TGF\alpha$) ligand-Grk protein which provides the signal to neighboring follicle cells through epidermal growth factor receptor (EGFR)- Torpedo during early stages of oogenesis (Roth and Lynch, 2009). As a result of EGF signalling, these neighboring cells become posterior follicle cells, which in turn send back the signals to developing oocytes which leads to the polarization of microtubules. Repolarization of microtubules networks results in the asymmetry movement of oocyte nucleus along with *grk* mRNA to the dorsal anterior region and localization of maternal determinants *bicoid* and *oskar* mRNAs to the anterior and the posterior pole respectively. Par-1, LGL (works with Par-1), dynein regulators-BicaudalD (BicD) and Egalitarian (Egl), and other factors are required for polarization of microtubules and establishment of polarity. Grk protein is required again during the mid-stage of oogenesis to induce the dorsal follicle cells fate and establish the dorsal ventral axis. Mutation in Grk-EGFR signalling, factors that required for polarization of microtubules and other factors (e.g. spindle genes, Notch signalling factors) can affect the localization of maternal determinants and asymmetry movement of oocyte nucleus and as a result disturb the A-P and D-V axis formation. For example, *bicoid* mRNA is localized at both poles in *gurken* mutants (Driever and Nüsslein-Volhard, 1988a; Ephrussi et al., 1991; Roth and Lynch, 2009). The uniform *Drosophila* embryo is patterned

into smaller domains progressively during development by a hierarchical gene cascade. These gene sets are classified into following categories.

Maternal effector genes: Functional mutation of maternal effector genes affects many segments. The mRNAs of anterior determinant *bicoid* (*bcd*) and posterior determinant *nanos* (*nos*) are localized at the anterior and posterior pole respectively through their 3' UTR (Driever and Nüsslein-Volhard, 1988a, 1988b; Dubnau and Struhl, 1996; Ephrussi et al., 1991; Hülskamp et al., 1990; Irish et al., 1989; Rivera-Pomar et al., 1996). For example, Exuperantia and Swallow proteins localized the *bicoid* mRNA at the anterior pole (Frohnhofer and Christiane Niisslein-Volhard, 1987). However, the mRNAs of *hunchback* (*hb*) and *caudal* (*cad*) are ubiquitously distributed within eggs (Fig. 2.1A). After fertilization, anteriorly localized *bcd* mRNA is translated and establishes the A-P Bcd protein gradient. An A-P gradient of Bcd morphogen covers the anterior half of the embryo and loss of Bcd results in embryo with a duplicated telson in place of head, thorax and anterior abdominal segments. Bcd has both instructive and permissive function. Its instructive role is to form anterior structures by activating anterior zygotic gap genes in a concentration dependent manner along with its target Hb (Driever, 1993; Simpson-Brose et al., 1994). Its permissive role is to prevent the formation of posterior structures at the anterior pole by repressing the translation of *cad* mRNA in the anterior part by binding to its 3' UTR which result in the opposite Cad gradient (Rivera-Pomar et al., 1996). Loss of both Bcd and Hb maternal information produce the double abdomen phenotype (double abdomen polarity) and a similar phenotype can be observed when *nos* is ectopically expressed at the anterior pole (Frohnhofer and Nüsslein-Volhard, 1986). The mutations in *bicaudal*, *BicaudalC*, *BicaudalD*, *ik2*, *bullwinkle*, *alice* and at least in four more loci result in double abdomen phenotypes with varying penetration and expressivity. For example, *ik2* mutants have disturbed actin cytoskeleton organization in the oocyte which results in mislocalization of *oskar* and *gurken* mRNAs and produce bicaudal and ventralized embryos (Luschnig et al., 2004; Mohler and Wieschaus, 1986; Shapiro and Anderson, 2006). Moreover, Bcd can also repress the Nos function when ectopically expressed at the posterior pole which results in

symmetrical double heads (embryos with double head in opposite polarity) (Driever et al., 1990; Gavis and Lehmann, 1992; Simpson-Brose et al., 1994). A P-A gradient of Nos forms from posteriorly localized *nos* mRNA. The Nos gradient activates the posterior gap genes and repress the translation of *hb* mRNA in the posterior part which result in a Hb A-P gradient (Fig. 2.1B) (Driever and Nüsslein-Volhard, 1988b; Dubnau and Struhl, 1996; Hülskamp et al., 1990; Irish et al., 1989a; Rivera-Pomar et al., 1996) (Fig. 1A-B). (Driever, 1993).

Drosophila torso like (tsl) is expressed at both poles in follicle cells of the oocytes. This localized *tsl* activates the ubiquitously expressed *torso (tor)* receptor at both terminal trough *trunk* ligand (Mineo et al., 2015; Savant-Bhonsale and Montell, 1993). Activation of *tor* receptor initiates the receptor tyrosine kinase (RTK/Ras/MAPK) pathway which neutralizes the ubiquitous transcriptional repressor- Capicua this leads to de-repression of zygotic genes- *tailless (tll)* and *huckebein (hkb)* at both terminal (de las Heras and Casanova, 2006). In summary, the terminal maternal genes- *torso* and *torso like* - pattern terminal non-segmented structures of embryo via torso-mediated MAPK pathway (Furriols and Casanova, 2003; Lu et al., 1993; Martin et al., 1994). Loss of *Torso* signalling results in loss of acron and telson (including last abdomen segment) (Klingler et al., 1988).

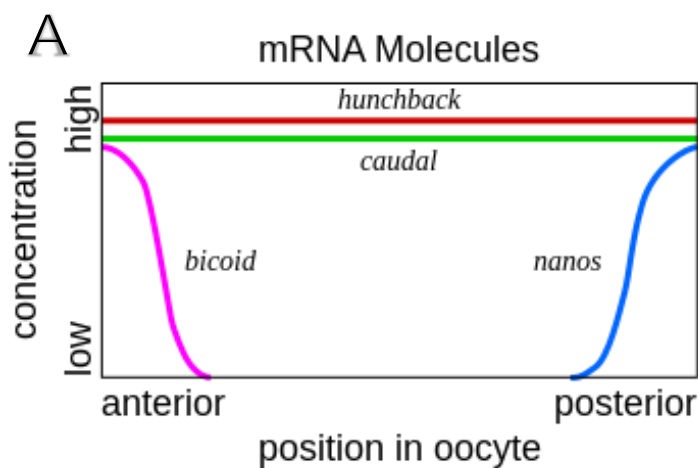
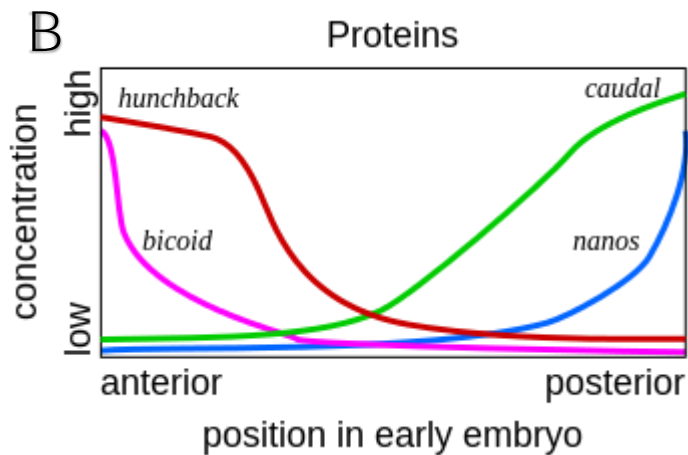


Figure 2.1 Maternal gradient along the A-P axis in *Drosophila*. (A) Distribution of maternal effector mRNAs in the oocyte by nurse cells. (B) Gradient of maternal effector proteins in early embryo. Bcd and Hb form A-P gradient and Nos and Cad form the opposing gradient. Taken from Developmental biology book by Scott F. Gilbert.



Gap genes: Gap genes [*hb*, *giant (gt)*, *Krüppel (Kr)*, *knirps (knl)*] are the targets of the maternal genes and the first zygotic expressed genes. They subdivide the embryo into smaller regions. Mutation in these genes results in gaps in the larval body because of the loss of consecutive segments. For example, the Torso maternal system activates *huckebein (hkb)* and *tailless (tll)* which pattern the terminal regions with other genes (Bronner and Jackle, 1991; Strecker et al., 1986). There is a special class of head gap genes [*Orthodenticle (otd)*, *empty spiracles (ems)*, *buttonhead (btd)*] which are activated by the Bcd morphogen but are independent from this segmentation cascade (Cohen and Jürgens, 1990).

Pair rule genes: Primary pair rule genes [*hairy (h)*, *even skipped (eve)*, *runt (run)*] form the seven stripes along the A-P axis by combinatorial activation and repressive action of gap genes. A mutation in pair rule genes cause the loss of alternative segments. Specific enhancer sequences and regulatory mechanisms of these genes play an important role in the establishment of the striped expression pattern (Fujioka et al., 1999; Pankratz and Jackle, 1990; Reinitz and Sharp, 1995). Secondary pair rule genes [*odd-skipped (odd)*, *paired (prd)*, *sloppy paired (slp)* and *fushi tarazu (ftz)*] are regulated by the primary pair rule genes and also form seven stripes (Carroll et al., 1988; Manoukian and Krause, 1992).

Segment polarity genes such as [*wingless (wg)*, *engrailed (en)* and *hedgehog (hh)*] pattern the embryo into 14 segments and determine parasegment boundaries of all future trunk

segments. Loss of function of these genes affects every segment. At this stage, the developing embryo is no longer syncytial but nuclei are surrounded by membrane. Anterior expression of *wg* and posterior expression of *en* at the compartment boundaries control and maintain each others activities through *hh* signaling (Baker, 1988; DiNardo et al., 1985; Ingham et al., 1988; Sanson, 2001). Regulation of segment polarity genes is identical in all segments except in anterior most head segments (procephalon). Every procephalic segment shows distinct segment polarity regulation (Gallitano-Mendel and Finkelstein, 1997).

The combinatorial activity of gap and pair rule genes regulate the homeotic gene expression. In parallel to the segments are patterned by gene cascade, homeotic genes provide identity to every segment. Mutations in these genes disturb the identity of that particular segment (Garcia-Fernandez, 2005; Harding and Levine, 1988; Irish et al., 1989b). Note: can shorten the information from pair rule till here.

2.4 Evolution of anterior axis formation

2.4.1 *bicoid*

Bcd is a homeodomain containing protein that patterns the anterior structure during embryogenesis. It contains a lysine residue at 50th position (K50) which is required for DNA and RNA recognition and an arginine at 54th (R54) required for RNA recognition (Baird-Titus et al., 2006). The *bcd* gene is located upstream of *zenküllt* (*zen*) gene within the Hox-C cluster. The *bcd* is present in higher (cyclorrhaphan) flies with exception of tephritid and glossinid flies (Klomp et al., 2015). In non-cylorrhaphan flies *Hox3* gene is synthesized by nurse cells and uniformly distributed in the egg as well expressed zygotically in extraembryonic tissues. The *Hox3* gene was duplicated and evolved into *bcd* and *zen* gene in the stem of cyclorrhaphan flies. In the process of divergence and subfunctionalisation of *hox3* gene, *zen* retained the zygotic expression and function in extraembryonic tissues but *bcd* evolved into an anterior maternal determinant. In summary, *bcd* is a molecular

innovation of higher flies and believed to have evolved from a tandem duplicated *zen* gene (Dearden and Akam, 1999; McGregor, 2005; Stauber et al., 1999).

2.4.2 *panish*

In spite of being the global pattern organizer and playing crucial role during axis specification and patterning, Bcd is limited to the cyclorrhaphan flies. However, classic experiments and the regulation of *Tc-hb* and *Tc-cad* mRNAs by Dm-Bcd suggest the presence of Bcd like molecule for anterior patterning in lower dipteran, beetles, wasp etc. (Brown et al., 2001; Wolff et al., 1998). Recently Panish, structurally different from Bcd, was discovered to pattern the anterior in the from *Chironomous riparius* midge. Panish is maternally anteriorly deposited to the freshly laid eggs and forms the A-P gradient in the early blastoderm stage. Knockdown of Panish produces a symmetrical double abdomen cuticle (Bicaudal phenotype) like the double mutant of *bcd* and *hb* in *Drosophila*. The *panish* gene name is derived from the Wnt signaling effector *pangolin/tcf (pan)* gene because of a common C-clamp domain. But Panish lacks both the HMG (high mobility group) and the β catenin domain of Pan. How Panish specifies and patterns the anterior region is not known. However, Klomp et al. suggested that it could have permissive function and act by opposing the establishment of posterior gene regulatory network (GRN) at the anterior pole (Klomp et al., 2015). This suggests the rapid evolution of structurally different anterior patterning in true flies. However, these two species are long germ insects while axis formation in short germ insects is not understood so far. Moreover, no factor has been reported until now, the knockdown of which would lead to a duplication of posterior structures like bicaudal phenotype in short germ insects.

2.5 Long vs short germ development

Long germ development refers to the simultaneous specification of all future segments in germ anlagen before gastrulation. This type of embryo was also called large germ because most of the embryo is filled with germ anlagen (Davis and Patel, 2002; Krause, 1939). This

mode of development is present for instance in *Drosophila melanogaster* (Dipteran) and *Nasonia vitripennis* (Hymenopteran). The amount of extraembryonic membrane is highly reduced in these species and in *Drosophila* referred to as amnioserosa. However, this mode of development is neither the ancestral nor the most common type in insects (Fig. 2.2A).

Short germ development refers to the simultaneous formation of anterior germ anlagen (for instance head and thorax) before gastrulation. Abdominal segments develop progressively from a posterior growth zone (or segment addition zone). So, the patterning of anterior segments occurs in a syncytial environment but abdominal segments form sequentially in a cellular environment. This embryo was also called small germ because the early embryo is filled with only a small portion of germ anlagen. Anterior regions of the blastoderm consist of extraembryonic serosa and amnion and the germ anlagen are mostly restricted to posterior-ventral side (Davis and Patel, 2002; Krause, 1939). This mode of development is present in *Tribolium castaneum* (Coleopteran) and *Oncopeltus fasciatus* (Hemipteran) (Fig. 2.2B).

Short germ is ancestral and long germ has evolved independently several times. However, the type of ovaries- panoistic (germ cells differentiate into oocyte only) or meroistic (germ cells differentiate into nurse cells and oocyte) - could have played an important role during their evolution.

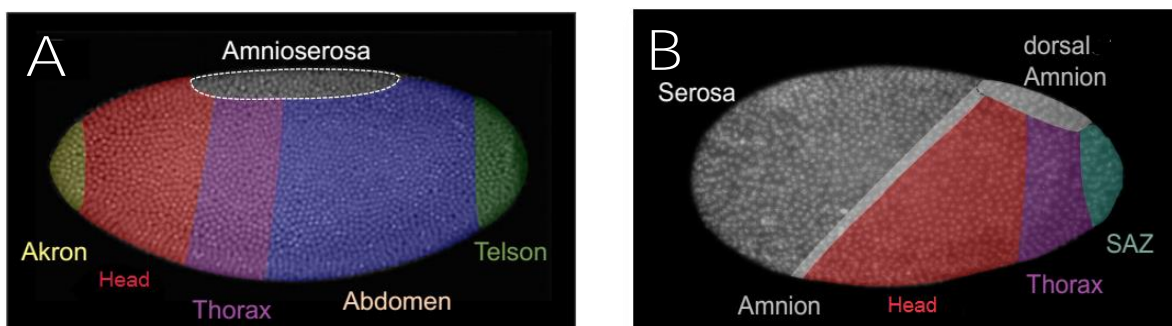


Figure 2.2 Long vs short germ band comparison. (A) Long germ band in *Drosophila*. (B) Short germ band in *Tribolium*. Taken from Nicole Troelenberg PhD thesis 2014.

2.6 A-P axis specification and patterning in *Tribolium castaneum*

Drosophila served as a reference model for the identification of A-P patterning gene sets in other organisms. This has been great to compare the function of *Drosophila* orthologs in the segmentation of short germ embryo, *Tribolium*. This candidate gene approach has been successful in gaining important insights into A-P axis formation and symmetry breaking during oogenesis (Kotkamp et al., 2010; Pridöhl et al., 2017a; Schröder, 2003). *Tribolium* has telotrophic meroistic ovarioles where nurse cells stay in the distal tropharium (transformed germarium) and connect to the developing oocytes in the follicle chamber via nutritive cords (Trauner and Büning, 2007). These nurse cells provide maternal factors as well as the cellular machinery for developing oocytes via the nutritive cords. The symmetry of *Tribolium* eggs is broken during oogenesis possibly by EGF signalling like in *Drosophila*. Both sequence and expression of EGFR in somatic cells are highly conserved in insects. However, the TGF α ligand-Grk is a newly evolved gene which is limited to the Diptera. *Tribolium* possesses a single gene which encodes a TGF α like protein. *Tc*-EGFR and the putative *Tc*-TGF α ligand seem to play some role in axis specification. Knockdown of the putative TGF α ligand leads to reduced egg production (possibly due to defects in follicle cells), normally cortical medially localized oocyte nucleus moved towards the posterior and anteriorly localized *Tc-eagle* mRNA was found at both anterior and posterior pole (Lynch et al., 2010).

Drosophila Bcd, which serves both instructive (activates head gap genes) and permissive (represses posterior structures) functions, was able to repress the *Tc-cad* translation suggesting the presence of Bicoid like molecules in *Tribolium* (Wolff et al., 1998). The gene sets that have been discovered for A-P axis formation in *Tribolium*, are suggested to compensate the instructive and permissive activity of Bcd. Permissive activity of anterior patterning is achieved by following two mechanisms. First, repression of Wnt signalling is required for proper anterior formation which is accomplished by conserved negative regulator of Wnt signalling, *Tc-axin*. *Tc-axin* mRNAs are maternally localized at the

anterior pole in freshly laid eggs (Fig. 2.3). Zygotic *Tc-axin* mRNAs are appearing from early cleavage stage onwards and become ubiquitously distributed by the end of late blastoderm. Knockdown of *Tc-axin* causes anterior shift of the blastoderm fate map and the graded loss of anterior segments at cuticle level (Fu et al., 2012a). Secondly, the posterior patterning function of Cad is highly conserved throughout the Bilateria. Even, *C. elegans* and mammals use Cad orthologs to pattern their posterior but use different mechanism to repress translation at the anterior pole. In case of *Tribolium*, *Tc-cad* is repressed at the anterior by the action of both *Tc-zen2* and *Tc-mex3* (Fig. 2.3) (Copf et al., 2004; Schoppmeier et al., 2009a). Instructive activity of anterior patterning has been suggested to provide by maternally ubiquitously distributed mRNAs of *Tc-hb* and *Tc-otd1* (Schröder, 2003). However, in the meanwhile it has been shown that *Tc-hb* is involved in giving identity to the anterior segments instead of a role in segmentation and is involved in the maintenance of abdominal segments. Moreover, *Tc-otd1* is involved in serosa formation and D-V patterning via *Tc-sog*. Therefore, it appears that neither *Tc-hb* nor *Tc-otd1* provide concentration dependent positional information for anterior patterning (Kotkamp et al., 2010; Marques-Souza et al., 2008a). Therefore, loss of anterior structures is a secondary effects of D-V patterning rather than a defect of instructive input.

In *Drosophila*, posterior patterning is done by permissive action of Nos and instructive function of Cad (Driever and Nüsslein-Volhard, 1988b; Dubnau and Struhl, 1996; Hülskamp et al., 1990; Irish et al., 1989a; Rivera-Pomar et al., 1996). *Tc-Nos* and *Tc-Pumillo* are involved in *Tc-hb* mRNA translational repression by binding to nanos responsive element (NRE) in the *Tc-hb* UTR. Mutation in *Drosophila* Nos and Pum result in the loss of all abdominal segments. Knockdown of *Tc-nos* and *Tc-pum* result in loss of 6-7 posterior abdominal segments, irregular cuticle structure and remnants of terminal structure. In addition, knockdown of *Tc-nos* and *Tc-pum* lead to deletion and transformation of head segments (Schmitt-Engel et al., 2012a). Tc-Cad is involved in posterior patterning by activating posterior gap genes (Copf et al., 2004; Schoppmeier et al., 2009).

Terminal patterning: In *Drosophila*, the terminal patterning starts at both termini through the receptor tyrosine kinase pathway via interaction of Torso receptor and its Trunk ligand. The localized Torso activation activates the zygotic expression of *tll* and *huckebein* (Lu et al., 1993; Martin et al., 1994). In *Tribolium*, *Tc-ts/* is expressed at both poles in follicle cells of ovaries. *Tc-tor* mRNA is maternally ubiquitously distributed in freshly laid eggs and later expression is present in embryonic anlagen. In summary, activation of *Tc-torso* signalling at both termini by localized *Tc-ts/* is a conserved mechanism between *Drosophila* and *Tribolium*. However, zygotic expression of *Tc-tll* is found only at the posterior terminal in *Tribolium* unlike expression at both termini of *Drosophila tll*. *Tc-tor* is involved in the formation of the serosa at the anterior end and setting up the growth zone at posterior end. *Tc-tor* exerts this dual function by regulating *Tc-zen1* in the anterior and *Tc-wnt* and *Tc-cad* in the posterior. Recently, a novel target of terminal system - *Tc-maelstrom* - was found to be involved in both anterior and posterior function of the *Tribolium* terminal system (Pridöhl et al., 2017a; Schoppmeier and Schröder, 2005; Schroder et al., 2000; Van der Zee et al., 2005). It appears that only the terminal system (not anterior-Bicoid and posterior-Nanos systems) are conserved between *Drosophila* and *Tribolium* to some extent.

2.6.1 Zygotic genes

Gap genes are involved in the segmentation of *Tribolium* embryo but their function is not similar to *Drosophila*. Knockdown of the gap gene orthologs often cause the homeotic transformations and deletion of posterior segments but without creating gaps due to loss of adjacent segments like in *Drosophila* larvae. This appears to be due to breakdown of the segmentation clock rather than direct regulation of pair rule genes.

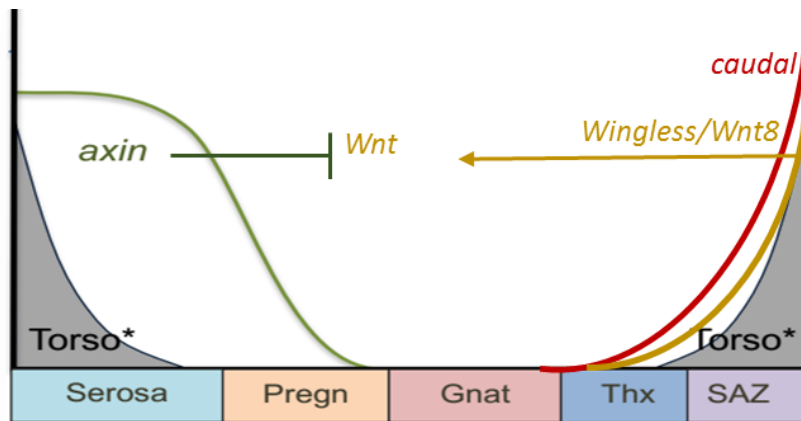


Figure 2.3 Genetic interaction during A-P axis formation in *Tribolium*. At the anterior pole, *Tc-axin* and *Tc-zen2* plus *Tc-mex3* (not shown) repress *Tc-Wnt* and *Tc-Cad*, respectively, for proper anterior development. At the posterior pole, *Tc-Torso* activate *Tc-Wnt* and *Tc-Cad* expression for proper posterior patterning. Taken from Nicole Troelenberg PhD thesis 2014 and modified.

For example, knockdown of *Tc-Kr* results in transformation of thoracic segments into gnathal segments and loss of abdominal segments. However, the expression of gap gene orthologs are more similar than their function. For example, *Tc-gt*, *Tc-kni* and *Tc-hb* have two domains of expression like their orthologs in *Drosophila*, one in gnathal segments (anterior domain) and another near the posterior pole (posterior domain). Exceptionally, *Tc-Kr* is expressed only in posterior domain (Bucher and Klingler, 2004; Cerny et al., 2005, 2008; Marques-Souza et al., 2008a). *Tc-millepattes*, a novel gap gene, encodes a polycistronic mRNA and has both anterior and posterior domain expression. In summary, *Tribolium* gap gene orthologs do not directly regulate pair-rule genes like the *Drosophila* gap genes and show neither the classical gap genes function nor the classical expression pattern of gap genes. (Savard et al., 2006).

Similar to *Drosophila* the pair rule genes- *Tc-eve*, *Tc-hairy*, *Tc-ftz*, *Tc-odd*, *Tc-slp*, *Tc-run* and *Tc-prd* are expressed in alternating segments. However, the simultaneous formation of all pair rule stripes does not happen due to the short germ mode of development of *Tribolium*. Rather, posterior stripes are added one after the other during the elongation of the germ band from the growth zone. Knockdown of *Tc-prd* and *Tc-slp* results in the loss

of alternating segments like *Drosophila* pair rule mutants. But knockdown of *Tc-eve*, *Tc-runt* and *Tc-odd* leads to loss of almost all gnathal and trunk segments, indicating the breakdown of the segmentation clock (Choe et al., 2006). *Tc-eve*, *Tc-runt* and *Tc-odd* are the primary pair rule genes which activate the secondary pair rule genes- *Tc-prd* and *Tc-slp* (Choe and Brown, 2007; Sarrazin et al., 2012).

en and both signalling pathway - *wnt* and *hh* - are highly conserved and also act as segment polarity genes in *Tribolium* (Brown et al., 1994; Nagy and Carroll, 1994). Expression pattern and function of the homeotic genes are conserved as well between *Drosophila* and *Tribolium* (Brown et al., 1999; Nie et al., 2001; Shippy et al., 2008).

In summary, early patterning genes are much more diverse than downstream events which use similar factors during the segmentation in *Drosophila* and *Tribolium*.

2.7 *germ cell-less*

The divergence of upstream events has the consequence that the involved components could not be identified by candidate gene approach. In the search of novel anterior patterning genes we mined the iBeetle Base, which stores the phenotypes recovered by the ongoing genome-wide RNAi screen iBeetle. The iBeetle screeners discovered two novel genes - *Tc-germ cell-less* (*Tc-gcl*) and *Tc-homeobrain* (*Tc-hbr*) - which are involved in A-P axis formation and whose knockdown results in a bicaudal phenotype.

Primordial germ cells (PGCs) are specified during the tenth nuclear cycle of *Drosophila* embryogenesis and serve as germ line stem cells for the next generation. The germ plasm is maternally posteriorly localized and contains the determinants for the formation of the germ line cells and posterior axis (Jongens et al., 1992). *Gcl* is one of the components of the germ plasm and is synthesized by nurse cells and then deposited to the developing oocytes. During embryogenesis, *gcl* mRNA is localized in precursors of germ cells. *Gcl* is localized at the interior surface of nuclear envelope of nurse cells and developing oocytes (Jongens et

al., 1992, 1994; Robertson et al., 1999). Moreover, weak Gcl protein expression is present in the cytoplasm of oocytes which later gets more pronounced at the anterior and posterior cortex of the oocyte. Bruno (*arrest*), a translational repressor of maternal RNA, restricts the *gcl*/mRNA translation to the germline via an RNA recognition motif (Moore et al., 2009). *gcl^A* embryos (embryos from homozygous *gcl* mutant females) lack all the maternal contribution of *gcl*/which results in no or fewer pole cells. *gcl^A* mutant do not show any other phenotype. Loss of zygotic Gcl function does not affect ovaries, testis, and egg laying rate of female or any obvious phenotype. Therefore, maternal *gcl* is required for the PGCs formation but not zygotic *gcl* expression (Robertson et al., 1999). Overexpression of maternal *gcl*/mRNA results in an increase number of PGCs. However, ectopic expression of maternal *gcl*/mRNA at anterior pole results in acquisition of PGC features in somatic cells and loss of anterior structure (Jongens et al., 1992, 1994). In summary, Gcl is one of the components of germ plasm which is involved in the pole bud formation, PGC formation and PGC survival. Nuclear lamina localization of Gcl is required for PGC formation but not for pole bud formation.

These are different models which propose the molecular mechanism behind the semi-fertile phenotype of *gcl^A* embryos. Gcl was suggested to act in transcriptional silencing during the development of germ cell precursor due to following reasons. First, loss of maternal *gcl*/and failure to establish transcriptional quiescence are tightly correlated with loss of PGCs. Second, ectopic expression of *gcl*/was able to repress the expression of genes at the anterior. Third, expression of the somatic markers *sisterless A* and *sisterless B* in PGCs of *gcl^A* embryos. Forth, the localization of Gcl at the inner surface of the nuclear envelope may be able to repress the transcription. Ectopic expression of *gcl* has indicated that transcriptional quiescence activity is not global but limited to few number of genes (Leatherman et al., 2002a). This hypothesis was further supported by mGcl (Mouse homolog of Gcl) that interacts with the DP3 α subunit of the E2F transcription factor and that leads to transcriptional repression of E2F factor responding genes (de la Luna et al., 1999). Another model was presented by Cinalli et al. (2015). They stated that PGCs formation requires

two constriction events. First, “the bud neck constriction” refers to separation of the pole bud via bud furrow constriction. Second, “Cytokinesis furrows” refers to separation of the dividing pole into two cells via anaphase furrow constriction. Gcl unexpectedly instructed the bud neck constriction event via spindle independent bud furrow cleavage. Here, the amount of Gcl is the rate limiting component for bud neck constriction (Cinalli and Lehmann, 2013a). Lerit et al. (2017) suggested another mechanism behind the semi-fertile phenotype of *gc^A* embryos. The formation of PGCs needs the proper segregation of germlasm determinant. Spatial distribution of germlasm determinants is ensured by the centrosome. Activity of the centrosome is regulated by Gcl. *gc^A* embryos show a disrupted centrosome separation and inefficient separation of germlasm content and as a consequence a semi-fertile phenotype. Disruption of the centrosome alone was able to phenocopy the *gc^A* phenotype (Lerit et al., 2017). Pae et al. (2017) suggested that Gcl is not directly involved in transcriptional silencing, bud furrow constriction, or centrosome separation but function as substrate-specific adapter of Cullin3-RING ubiquitin ligase (CRL3). According to Pae et al. (2017), Gcl is released upon nuclear envelope breakdown during the mitosis of emerging PGCs and localizes to the plasma membrane of PGC buds. Gcl then recruits the CRL3 complex and targets the Torso receptor (a somatic cell fate determinant) for degradation (Pae et al., 2017).

Gcl possess a BTB (Bric-a-brac, Tramtrack and Broad complex) domain also known as POZ (Pox virus and Zinc finger) domain which plays an important role in many biological process (e.g. transcriptional regulation, cytoskeleton dynamics and ubiquitination). Several known BTB proteins are part of the CRL3s (a major class of E3 ubiquitin ligases) which lead to the degradation of targeted proteins by ubiquitination. CRL3s are composed of a substrate adapters BTB-domain protein, the scaffold protein Cullin3 and the catalytic RING finger domain protein. (Genschik et al., 2013; Perez-Torrado et al., 2006; Stogios et al., 2005; Zollman et al., 1994). Gcl of *Drosophila* contains only a BTB domain but Gcl of *Danio rerio*, *Xenopus laevis*, *Mus musculus* and *Homo sapiens* contains an additional BACK (BTB-And-C-terminal-Kelch) domain. The BACK domain of BTB proteins act as

substrate recognition domain to the CRL3s. However, the GCL domain is a newly characterized domain of Dm-Gcl which provide the substrate specificity to CRL3s (Pae et al., 2017). Gcl protein from both fly and mouse contain a nuclear localization signal (NLS) that transports Gcl into the nucleus and an N terminal myristoylation sequence which is critical for localization to the inner surface of the nuclear envelope. The mGcl (mouse homolog of Gcl) show 36% identity and 56% similarities with Dm-Gcl. *mgcl* was able to rescue the *gcA* phenotype. *mgcl* is highly expressed in spermatocytes and PGCs of male and female (Kimura et al., 1999, 2003; Moore et al., 2009). Lap2 β , a nuclear membrane protein, regulates the transcriptional repression with or without *mgcl* through binding with the E2F-DP transcription factor (Nili et al., 2001). mGcl plays an essential role in the architecture of the nuclear-lamina. Loss of *mgcl* causes deformation of nuclear morphologies in testis, liver and pancreas. *mgclA* male sperms show insufficient chromatin condensation and an abnormal acrosome structure that leads to sterility (Kimura et al., 1999, 2003). Furthermore, mGcl shows the interaction with the *tumor susceptibility gene 101* (*tsg 101*) which inhibits the degradation of the oncoprotein MDM2 (Masuhara et al., 2003). Human *gcl* is expressed highly in testis and pancreas and weakly in kidney, heart and placenta. *Hs-gcl* is associated with spermatogenesis and mutations in *Hs-gcl* result in sterility like in respective mouse mutant *mgclA* male (Kleiman et al., 2003).

2.8 *homeobrain*

Drosophila homeobrain (*hbn*), a homeodomain containing gene, forms a homeobox gene cluster with *Drx* and *orthopedia*. All members of this cluster have specific expression patterns in the embryonic brain. The *hbn* transcripts appear during the blastoderm stage at the anterior dorsal region. A new expression domain arises at the anterior lateral region during the gastrulation stage. At the germ band stage, *hbn* transcripts are present in subregions of brain and ventral nerve cord. The Homeodomain of Hbn is located at the N-terminus. Hbn probably acts as transcription factor by binding to a specific DNA sequence.

However, neither phenotypic information for *hbn* nor information for its target genes is known.(Mazza et al., 2010; Walldorf et al., 2000a).

3 Material and Methods

3.1 Model organism

Tribolium castaneum, the red flour beetle, has been used as model organism in this work. The beetles were reared under standard conditions (Brown et al., 2009a). The transgenic line pBA19 (also known as pig 19) was used for injection during the second phase of the iBeetle screening (Schmitt-Engel et al., 2015a). pBa19 transgenic animals express the enhanced green fluorescent protein (EGFP) in larval muscle which allows us to analyze larval musculature defects. Adult males of the Black strain (black adult cuticle, (Sokoloff, 1974) were used for mating. The black adult cuticle allowed easy scoring of surviving injected female during further analyses.

The genetic background of males can affect the phenotype in terms of egg productivity and nature of the cuticle background. To be consistent with the iBeetle screening procedure, black adult males were used for mating with injected SB and pBA19 females during rescreening. L1 larvae from the first egg collection were analyzed in detail for head specific cuticle phenotype. The San Bernadino (SB) wild-type (WT) strain was used for inspection of strain specific phenotypes and for further *in situ* hybridization experiments during rescreening.

The Gcl project

For the validation of *Tc-gcl* and *Tc-hbn* phenotype, we followed the iBeetle screening protocol as mentioned in Schmitt-Engel et al. (2015). After validation of phenotypes, both males and females from *pBA19* strain were used for all experiments. VSR line (#254) ubiquitously expressing the inhibitor, viral suppressor of RNAi (VSR) CrPV1a, was used

to overcome the hypomorphic state of *Tc-axin* RNAi (Nayak et al., 2010; J. Ulrich, unpublished.)

3.2 The iBeetle screening procedure

The iBeetle screening is a single pass screening procedure to maximize the productivity. Four screeners participated in the second phase of “only pupa” iBeetle screening. Procedure for pupal screening was as previously described with the following modification (Schmitt-Engel et al., 2015a). Here, I would briefly describe the pupal screening phase in which I was involved as screener.

All screeners followed the pupa injection screening schedule as described below to achieve continuity (Fig. 3.1).

	Monday	Tuesday	Wednesday	Thursday	Friday	Saturday	Sunday
week 1		d0 Injection (10h)		d0 Injection (10h)	d3 Transfer (1,5h) Cuticle anal. (2h)		d3 Transfer (1,5h)
week 2	d0 Injection (10h)	Cuticle analysis (8h)	d0 Injection (10h)	d3 Transfer (1,5h) d9 Sieving (0,75h)	d0 Injection (10h)	d3 Transfer (1,5h) d9 Sieving (0,75h) d11 Sieving (0,75h)	
week 3	d13 Sieving Ovaries (4h) d13 Cuticle Prep (3h) d3 Transfer (1,5h) d11 Sieving (0,75h)	d14 Fresh Prep Muscle analysis (8h)	d9 Sieving (0,75h) d13 Sieving Ovaries (4h) d13 Cuticle Prep (3h)	d14 Fresh Prep Muscle analysis (8h)	d9 Sieving (0,75h) d11 Sieving (0,75h) Cuticle analysis (6h)		d13 Sieving Ovaries (4h) d13 Cuticle Prep (3h) d9 Sieving (0,75h) d11 Sieving (0,75h)
week 4	d14 Fresh Prep Muscle analysis (8h)	d21 Stinkgld.(1,5h) d13 Sieving Ovaries (4h) d13 Cuticle Prep (3h) d11 Sieving (0,75h)	d14 Fresh Prep Muscle analysis (8h)	d13 Sieving Ovaries (4h) d13 Cuticle Prep (3h) d21 Stinkgld.(1,5h)	d14 Fresh Prep Muscle analysis (8h)		
week 5	Cuticle analysis (8h)		Cuticle analysis (8h)	d21 Stinkgld.(1,5h) d21 Stinkgld.(1,5h) d21 Stinkgld.(1,5h)	Cuticle analysis (8h)		
week 6		d0 Injection (10h)		d0 Injection (10h)	Cuticle anal. (2h) d3 Transfer (1,5h)		d3 Transfer (1,5h)
week 7	d0 Injection (10h)	Cuticle analysis (8h)	d0 Injection (10h)	d3 Transfer (1,5h) d9 Sieving (0,75h)	d0 Injection (10h)	d3 Transfer (1,5h) d9 Sieving (0,75h) d11 Sieving (0,75h)	

Figure 3.1 Schedule for pupal injection screen. The schedule from week one to week 5 represent one bundle. One bundle contains five repetitions which are represented in five different colors.

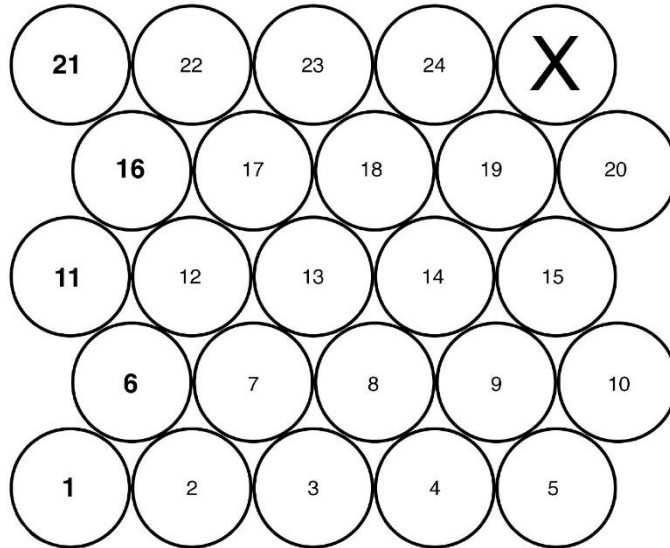
Each repetition contains different analyses, namely injection (at day 0), transfer (at day 3), sieving (at day 11), ovaries analysis and cuticle prep (at day 13), cuticle analysis (at day 15) and stink gland analysis (at day 21). One repetition includes 24 injections that consists of 21 iBeetle fragments, two buffer controls and one positive control. Positive controls represent those dsRNA which had been successfully reproduced previously. Each block represents time needed for the particular experiment. Analysis of one bundle ($21 \times 5 = 105$ genes) took five weeks. After six weeks, we started the injection for next bundle (Schmitt-Engel et al., 2015a).

screener:

repetition #:

injected at:

iB #s:



done		iB #s still to do	done		iB #s still to do
<input type="checkbox"/>	day 3: transfer date:		<input type="checkbox"/>	day 9: 1st egglay date:	
<input type="checkbox"/>	day 11: 2nd egglay date:		<input type="checkbox"/>	day 13: cuticle-prep date:	
<input type="checkbox"/>	day 13: ovary check date:		<input type="checkbox"/>	day 14: fresh prep & muscle analysis date:	
<input type="checkbox"/>	day 15+x: cuticle analysis date:		<input type="checkbox"/>	day 22: stink gland check date:	

comment:

Figure 3.2 25 vial system used as a route card for pupal screen. 24 out of 25 vials were used for every repetition. This asymmetry helped to identify the correct well. Each well was filled with approximately 10g of flour, ten injected female pBA19 pupa and 4 black male (Berghammer et al., 1999).

Day 0: Injection

Pupa sorting: Male and female pupae were sorted based on the genital pupilla which is located on the last abdominal segment. Using a flexible forceps, we sorted the pupae under transmitted-light illumination using a stereo-microscope. By using mandibles and wings as visual marker, we selected those pupa which were completed 70-90% pupal development (Dönitz et al., 2013).

10 female *pBA19* pupae were injected for each gene and controls. iBeetle dsRNA and positive control were provided by Eupheria Biotech GmbH, Dresden, Germany. Injected pupae were transferred to petri-dishes containing approximately 10g flour and incubated at 31°C with 40-60 percentage humidity in incubator.

Day 3: Transfer to block

After three days of injection (3dpi), injected beetles and flour were transferred to block system as mentioned in Fig. 3.2. In addition, we documented how many injected pupae eclosed into adult and mentioned lethality if any in our database. After that, we added four black adult males to each vial for mating. Males were added after female eclosion because black males can feed on pupae. We added male after eclosion of female pupae into adult because black male have tendency to feed on pupae.

Day 9: 1st egg lay

Eggs were sieved by using a semi-automated machine (Retsch GmbH) and then placed on 300 µm meshes with sunflower oil at bottom. This allow WT larvae to hatch and fall through meshes into oil. Irregularities in egg production compared to the buffer control and dead females were documented in our database.

Day 11: 2nd egg lay

As mentioned above, eggs were sieved and dead beetles documented in the database for second egg lay as well. However, eggs were kept on a 180 µm preparation block. This block was stored at 31°C incubator with flour for hatching larvae.

Day 13: Cuticle preparation

Eggs collected at day 9 were used for cuticle preparation. Oil collection blocks with hatched larvae were stored at 4 °C until cuticles were analyzed. Eggs were transferred from 300µm to the 180µm preparation block. Eggs were washed twice for 3 minutes in 50% bleach to **remove flour and the chorion. Cleaned eggs were embedded in a mixture of Hoyer's medium and lactic acid (ration 1:1)** Embedded slides were incubated at 65 °C overnight which allowed dissolution of any soft tissues but not the cuticle (Bucher and Klingler, 2004).

Day 13: Ovary analysis

If there was no or low egg production in injected beetles compared to buffer control then dissection of female beetles were performed in PBS. To do microscopic analysis, ovaries were cleaned of fat body and tracheas tissue. Cleaned ovaries were mounted in PBS using a coverslip with putty as spacers. Observation was documented in the database.

Day 14: Muscle analysis

Eggs were dechorionated and processed as mentioned identical to the cuticle preparation. **However, Voltalef oil was used for embedding instead of Hoyer's medium and lactic acid.** Muscle patterns were analyzed same day due to degradation of EGFP eggs/larvae under Zeiss axioplan 2 microscope. Phenotypes were documented in database.

Day 15: Cuticle analysis

Cuticle slides prepared on day thirteen were analyzed on day 15 or later because cuticles are quite stable for many months. For iBeetle screening, I used to take pictures with cy3 filter, 8bit mono and black/white setting of Zeiss Axioplan 2 microscope. All morphological phenotype and other were documented in database.

For detailed analysis, I used to take more than 30 slices using z stack setting of ImagePro v.6.2 software (Media Cybernetics, USA) then processed the image with Z-projection methods “Maximum Projection” of ImageJ software (Version 1.47, <http://rsbweb.nih.gov/ij/disclaimer.html>). For high quality pictures, I have also used ZEISS laser scanning microscope (LSM510) then processed using Fiji (Schindelin et al., 2012).

Day 21: Stink gland analysis

We analysed thoracic and abdominal stink glands for any abnormalities under the stereomicroscope. If we found any morphological or colors difference compare to WT glands then we dissected the ‘only abdomen stink gland’ for further analysis. All the observations were documented in database.

3.3 iBeetle Database annotation

All the observation and phenotype from day zero to day twenty one were annotated in an online database (Dönitz et al., 2013, 2015). Each screening day had a specific interface and had all inbuilt options to describe the phenotype. If needed comments were added to elaborate the phenotype. We followed the annotation EQM (entity, quality and modifier) system for the annotation of phenotypes. For example, ‘larvae (entity) completely (quantity) everted (modifier)’ phenotype was annotated by inbuilt dropdown menus from the iBeetle base vocabulary (Fig. 3.3). The EQM system was crucial to maintain the consistency in

documentation across the screener. The EQM system provide benefits like integration of the iBeetle database with other EQM based phenotype database in the future.

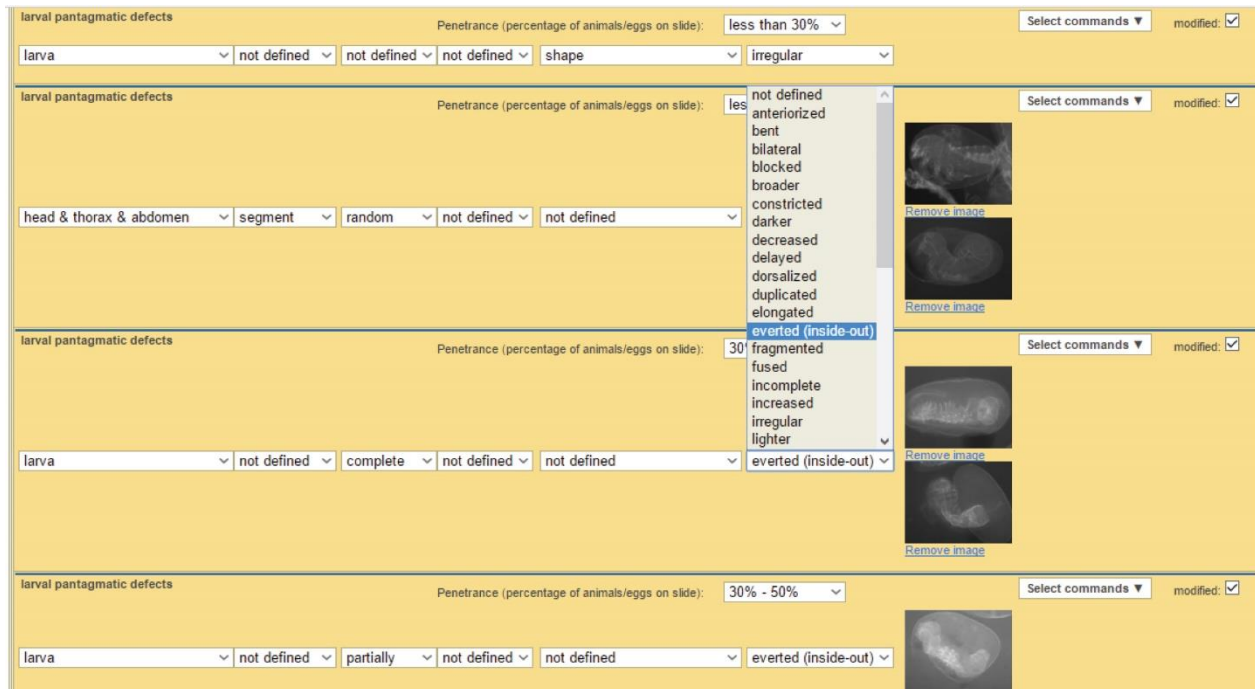
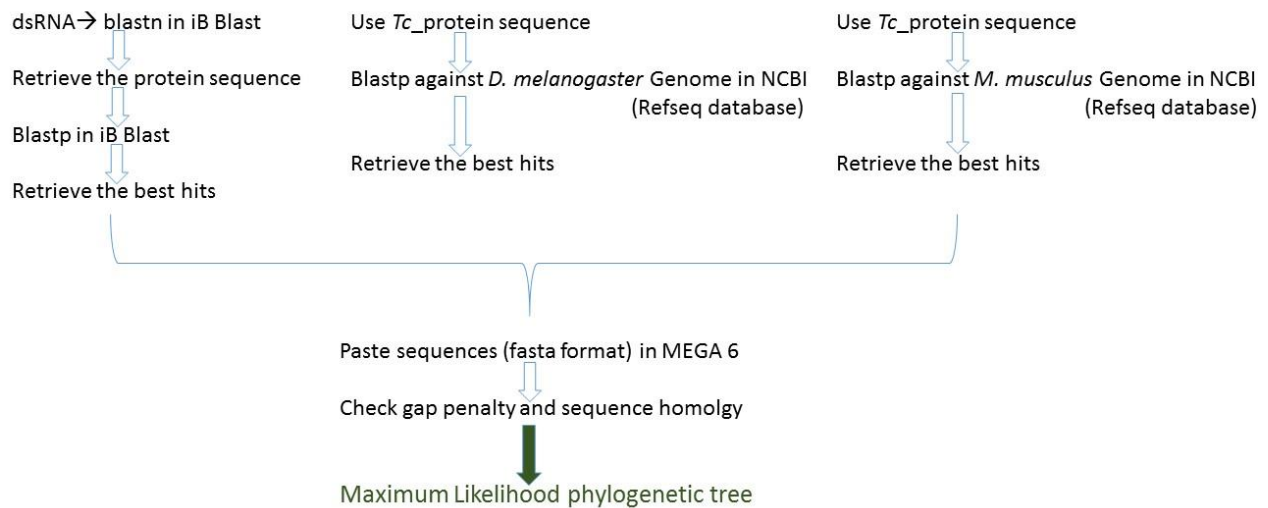


Figure 3.3. Database interface of day 15. This screenshot represent the overview of day 15 interface where we annotated the cuticle phenotype with the help of several dropdown menus based on EQM system. Respective pictures were uploaded that describe the annotated phenotype in visual form.

3.4 Phylogenetic analysis

Phylogenetic trees of selected iBeetle genes, *Tc-gcl* and *Tc-hbn* were made using MEGA 6 (Tamura et al., 2013) software. Protein sequences of the respective genes were retrieved from *Tribolium* BLAST (<http://bioinf.uni-greifswald.de/blast/tribolium/blast.php>) and NCBI and aligned in MEGA 6 with clustal W algorithm. I looked for effect of different gap penalties and trimmed sequences on phylogenetic trees. Phylogenetic trees were constructed based on the maximum likelihood method with JTT substitution model and 500 bootstrap tests (measure the support of nodes) (Fig. 3.4).



1

Figure 3.4. Workflow of Phylogenetic analysis. This chart showed the basic step which have been used for making the trees. dsRNA sequences (iBeetle fragments and NOFs) were used to extract the target protein sequences from iBeetle genome browser. This target protein sequences were used to blast against *Tribolium* genome, *Drosophila* genome and Mouse genome to find the respective paralogues and orthologs. ClustalW was used for multiple sequences amino acid alignment. Phylogenetic trees were constructed based on maximum likelihood method using MEGA 6.

3.5 Cloning

All genes required for making dsRNA and *in situ* probes were cloned into pJET1.2 vector (Thermo Fisher Scientific) by standard blunt end cloning method. cDNA (from 0-72hrs embryos) was made by Sebastian Kittelmann using the SMART PCR cDNA kit (ClonTech). All cloning procedure including primer design was done *in silico* using Geneious 9 software (<http://www.geneious.com>, Kearse et al., 2012). Cloning results were verified at nucleotide level by using ‘map to reference’ feature of Geneious with sequencing reports. All primer used in this study can be found in the appendix.

3.6 Fixation

Depending on experiment requirement, 'right age group' embryos were collected in 180 μ m sieves. For dechorionation, embryos were washed in 50% bleach twice for 3 minutes. Fixation protocol was performed as described Schinko et al. (2009) with following modifications. For blastoderm embryos 300 μ l formaldehyde (37 %) and 2 ml PEMS buffer (0.1 M PIPES, 2mM MgCl, 5 mM EGTA, pH 6.9) and 4 ml heptane were used. For germ band embryos the volume of formaldehyde (37%) was reduced from 300 μ l to 180 μ l. Fixed embryos were stored in methanol at -20°C and used for *in situ* hybridization and antibody staining (usually freshly fixed embryos because methanol can destroy the epitope).

3.7 Whole mount *in situ* hybridization

Whole mount *in situ* hybridization (WMISH) was performed using Nitro blue tetrazolium (NBT) and 5-Bromo-4-chloro-3-indolyl phosphate (BCIP) as described previously (Oberhofer et al., 2014a; Schinko et al., 2009; Siemanowski et al., 2015). After the colour development step, I incubated the embryos for 30 min in 1 μ g/ μ l DAPI in 1X PBT to stain the nuclei.

3.7.1 *In situ* probe

T7 RNA polymerase was used for making antisense *in situ* probe. It was synthesized by using Digoxegenin-UTP (DIG) or Fluorescin-UTP; (FLUO) labeling mix kit (Roche, Germany) according to the manufacturer's instructions. RNA pellets were dissolved in 100 μ l resuspension buffer (50% formamid, 0.1% tween 20, 5x SSC pH 4.5, and 20ug/ml heparin).

3.7.2 Mounting

Embryos were submerged in 100% Glycerol on a black hollow microscopic slide without coverslip. This allowed the free movement of embryos which enabled us to take different angle pictures and also reuse embryos if needed. However, yolk was needed to remove from germ band before embedding in 80% Glycerol on microscope slide with coverslip and spacers.

3.8 RNAi

Cloned genes in pJet 1.2 vector were used to make PCR template which served as template for *in vitro* transcription of dsRNA. We used the pJET 1.2 specific forward and reverse primers with T7 promoter overhang to generate the amplicon under standard PCR conditions. dsRNA synthesis was performed using the Ambion® T7 MEGAscript® kit (LifeTechnologies, USA) according to manufacturer's instructions.

After *in vitro* transcription, RNA was precipitated using isopropanol. The RNA pellet was dissolved in injection buffer (1.4 mM NaCl, 0.07 mM Na₂HPO₄, 0.03 mM KH₂PO₄, 4 mM KCl, pH 6.8). RNA was incubated for 3 min. at 98°C and cooled to room temperature to allow the annealing of RNA and to increase the percentage of double stranded RNA. dsRNA concentration was adjusted to the desire concentrations (1µg/µl, 1.5µg/µl or 3µg/µl depending on requirement) with the help of NanoDrop 1000 Spectrophotometer (constant 45 setting), Thermo Scientific™, USA.

Pupae, larvae and embryos were injected as described previously (Bucher et al., 2002; Posnien et al., 2009) using the FemtoJet® device (Eppendorf, Germany). Off target effect for *Tc-gcl* and *Tc-hbn* were tested by non-overlapping fragments. Strain specificity of phenotype was also analyzed using SB, WT strain. All other genes have been already tested and published. dsRNA of iBeetle fragments and NOFs was provided by Eupheria biotech GmbH during the iBeetle screening and rescreening phase. Generally, parental RNAi was

performed in late pupa stage if not otherwise mentioned. 1µg/µl of dsRNA concentration was used during the iBeetle screening and the rescreening phase if not otherwise mentioned.

3.8 Image processing

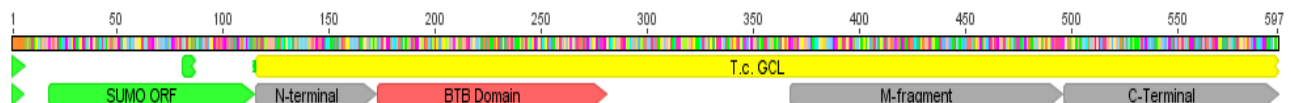
Image acquisition with cy3 filter, 8bit mono and black/white setting of Zeiss Axioplan 2 microscope and also ZEISS laser scanning microscope (LSM510). Stacks were processed with Z-projection method of ImageJ software (Version 1.47, <http://rsbweb.nih.gov/ij/disclaimer.html>). All figures were prepared using Adobe Photoshop (CS6) and Adobe Illustrator (CS6).

3.9 Generation of a Tc-Gcl polyclonal antibody

3.9.1 Cloning

I cloned the four different parts of *Tc-gcl* gene including a full length into the pET SUMO vector (Hanington et al., 2006); modified by Prof. R. Ficner lab and K. N Eckermann, Göttingen) to overexpress the protein. The N-terminal polypeptide of Tc-Gcl (57 amino acids) was overexpressed and was shown to be soluble (Table 3.1).

Table 3.1 Different part of *Tc-gcl* gene were cloned into pET SUMO vector and its overexpression



	Cloning	Over-expression	Soluble fraction	Insoluble fraction
Full length GCl	✓	✗		
BTB domain	✓	✓		✓
C-terminal	✓	✗		
M-fragment	✓	✓		✓
N-terminal	✓	✓	✓	

The pET SUMO vector has SUMO-to increase the solubility of protein and His-for purification and detection on western blots. (<https://www.thermofisher.com/order/catalog/product/K30001>).

The N-terminal part of *Tc-gcl* was amplified from cDNA pool using primer pairs-Gcl_GG_Linkers forward and reverse (Appendix 7.2). After amplification of N-terminal sequence, I performed golden gate cloning procedure which included restriction digestion (BsaI HF) and ligation (T7 ligase) simultaneously. pET-SUMO backbone and insert were used in 1:5 molar ratio. I added 1µL Cutsmart Buffer, 1µL BSA, 1µL ATP, 0.75µL BsaI HF and 0.25µL T7 Ligase. Final volume of 10 µl was adjusted with ddH₂O.

Program in Thermocycler:

1. 37°C 10 min
2. 27°C 10 min
3. Go to 1 repeat 25x
4. 70°C 20 min

Hold at 14°C

- Transformed into cells of the DH10b strain

- Positive clones were selected by Colony PCR and confirmed by sequencing.

3.9.2 Protein expression and purification

N terminal polypeptide fused with His-SUMO at N terminus was expressed in BL21-DE3 Rosetta cells at 16 °C. Cells were lysed in lysis buffer (50 mM TRIS-HCl pH=7.5, 150mM NaCl, 10mM Imidazole) using Fluidizer (mechanical lysis by high pressure-80 psi). Protein was purified via Ni²⁺-chelate affinity chromatography in gradient fashion with 200mM imidazole in lysis buffer. Dialysis (50mM Tris-HCl pH 7.5, 150mM NaCl) and cleavage of His-SUMO tag from His-SUMO-N terminal gcl polypeptide was done simultaneously overnight. The tag was separated from the polypeptide via Re-Ni²⁺-chelate affinity chromatography. Size exclusion chromatography (Superdex 30-GE Healthcare) was used to remove the remaining contaminations and stored the final purified polypeptide into Phosphate-buffered saline (PBS). All the steps for purification was done at 4°C (Monecke et al., 2009). Handling the instrument like fluidizer, Äkta, polyacrylamide gel electrophoresis, western blot etc. were done according to instructor manual.

3.9.3 Antibodies

Purified N-ter polypeptide of Gcl (57 amino acids) was sent to Eurogentec (Liège, Belgium) for speedy 28 days polyclonal immunization program in guinea pig. As quality control check, pre-immune sera of 5 guinea pigs were analyzed and best two guinea pigs were chosen to raise antibodies against Gcl polypeptide. The final serum was affinity purified against Gcl polypeptide to get rid of non-specific antibodies.

Embryos: 1:200 dilution of the npurified Gcl polyclonal antibody was used as primary antibody. 1:1000 dilution of HRP-coupled (for visible stainings) or 555 –coupled Alexa Fluor (for fluorescent staining) anti guinea pig antibodies were used as secondary antibodies.

Ovary: In case of ovaries tissue, dilution for Gcl antibodies was 1:1000 and for monoclonal anti-nuclear pore complex protein (against rat liver nuclei extract, clone 414, Sigma) was 1:2000.

3.9.4 Antibody staining of *Tribolium* embryos

Freshly fixed embryos were rehydrated in PBT (1x PBS with 0.1% Triton) then blocked with 3% BSA before overnight incubation with primary antibodies (diluted in 3% BSA) at 4 °C. After washing with PBT, secondary antibodies (diluted in PBT) were incubated for 90 minutes. The Diaminobenzidine (DAB) staining was performed if horseradish peroxidase (HRP) coupled secondary antibody was used (Shi et al., 1988). The DAB staining solution was prepared with 0.1M NaAcetate, DAB stock solution (20x), D-glucose stock solution (100x) and glucose-oxidase stock solution (500x). DAPI staining was also performed if needed to stain the nuclei.

3.10 Ovary analysis

3.10.1 Ovary WMISH

Ovary dissection was performed as described by (Trauner and Buning, 2007). WMISH was performed as described in (Bäumer et al., 2011). However, probe needed to be smaller in size (250-500bp) to increase the penetration efficiency into ovaries. Probe were carbonated to generate smaller fragments. Fast Red tablets from Roche were used for staining according to **manufacturer's instruction**.

3.10.2 Ovary antibody staining

Dissected, cleaned (removed muscle sheath) and fixed ovaries were rinsed in PBT then washed 3 times with PBT/BSA (1x PBS, 1% BSA, 0.5% Triton X-100) for 15 minutes on rotator at room temperature. After overnight incubation with primary antibody (diluted in PBT/BSA) at 4 °C, ovaries were washed again as mentioned above with PBT/BSA. Secondary antibody (diluted in PBT/BSA) was either incubated at room temperature for 4hrs or overnight at 4 °C. Ovaries were washed again with PBT/BSA as earlier then mounted on slide in 1:1 mixture of glycerol and 1x PBS with coverslip and putty as spacers (Bäumer et al., 2011; modified by M. Teuscher, Erlangen).

3.11 qRT PCR

3.11.1 RNA extraction

0-4hrs old RNAi and WT eggs; RNAi ovaries and WT ovaries were used for extraction of total RNA using Trizol (Ambion) according to (Schmittgen and Livak, 2008). Isolated RNA was treated with TURBO™ DNase to remove any DNA contamination. Later, DNase Inactivation Reagent used for removal of TURBO™ DNase and divalent cations as describe in 'TURBO DNA-free™ Kit, Ambion; AM1907' manual.

3.11.2 cDNA synthesis

The RNA concentration was measured using the NanoDrop 1000 Spectrophotometer (Thermo Scientific™, USA). 1µg for embryos and 500 ng for ovaries was used for the first strand cDNA synthesis according to the manufacturer's instructions. (SuperScript® III, Thermo Scientific™, USA).

3.11.3 Analysis

qRT PCR was performed in CFX96™ Real-Time PCR System (Bio-Rad Laboratories, Hercules, CA, USA) with HOT FIREpol® EvaGreen® qPCR Mix Plus (ROX) (Solis BioDyne, Tartu, Estland) according to manual. Three biological, three technical replicates and no-RT (without reverse transcriptase enzyme) and no template control were used. Primer efficiency and melting curve analysis were performed for all primers including internal control RPS3 and RPS18 gene primer. Relative gene expression between WT and RNAi tissues were calculated by double delta Ct method with RPS3 and RPS18 as reference gene (Livak and Schmittgen, 2001). Welch Two Sample t-test was performed to assess if difference in gene expression was significant or not.

4 Result

4.1 Part I: The iBeetle screen

To identify novel head patterning genes, I participated in the second phase of the genome-wide RNAi screen in *Tribolium castaneum*. This was consisted of three phases: Screening, Rescreening and functional analysis of selected genes (see chapter II).

4.1.1 Screening

Like in the first phase of the iBeetle screen pupal screening (Dönitz et al., 2015; Schmitt-Engel et al., 2015b), the second phase included injection of dsRNA and subsequent analysis of epidermal phenotypes from first egg collections, mesodermal (muscle) phenotypes from a second egg collections and ovary phenotypes in case of no or less egg production. In addition to the first phase, stink gland phenotypes were screened as well (Fig. 4.1). In total the four screeners of the second phase screened about 3,200 genes. I screened 865 genes myself. The observed phenotypes were annotated internally in the iBeetle annotation database. All the phenotypic information is publicly available at <http://ibeetle-base.uni-goettingen.de>. Detailed protocols of the iBeetle screening are described in Schmitt-Engel et al., 2015, ‘materials and methods’ sections and in the figure legends.

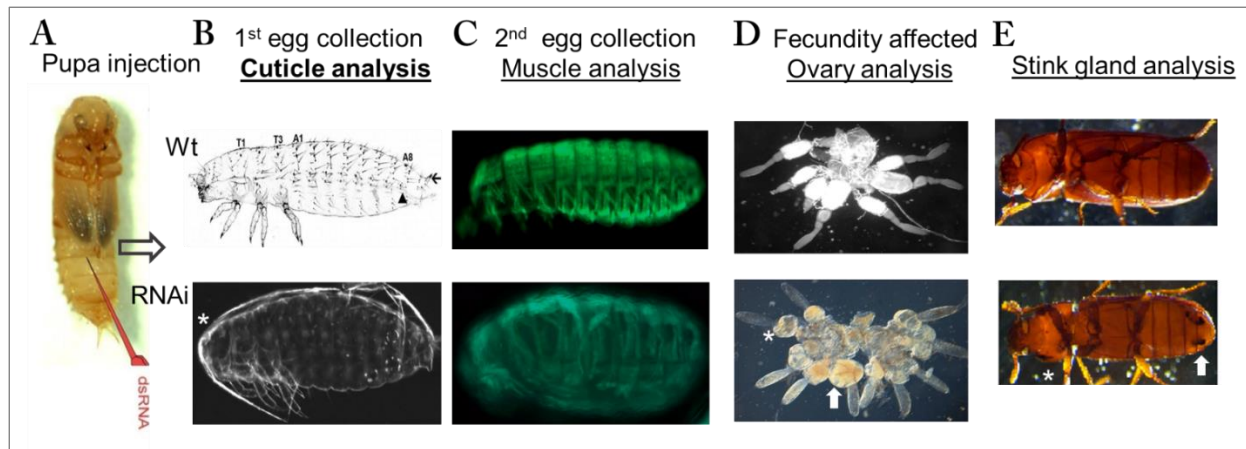


Figure 4.1 Overview of the second phase iBeetle screening. A. The iBeetle dsRNAs were injected into a lower abdominal segment of female pupae to knockdown the specific gene during the embryogenesis. B. For ectodermal phenotypes, cuticles were analysed from the first egg collection. In this example, after knockdown of the target gene, L1 larva lost the head capsule (*) compared to the wild type (WT) larva. C. For mesodermal phenotypes, muscles were analysed from the second egg collection. In this example, after RNAi muscle patterns are deformed and irregular compared to the WT muscle pattern. D. For ovary phenotypes, if there was no or less egg production in first and second egg collections, then usually four females were dissected for detailed ovary analysis. In this example, after RNAi the tropharium remained unchanged, but follicle chambers were absent (*) and the lateral oviduct was degenerated (arrow) compared to the WT ovary. E. For stink gland phenotype, females were analysed first without dissection. In case of abnormalities in thoracic and abdominal stink glands. Abdominal stink gland of four adult females were dissected and analysed. In this example, dsRNA injection led to darkening of both thoracic (*) and abdominal stink glands (arrow). Anterior is to the left in panels B, C and E. The upper panels from B to E show the WT and lower panels are examples of RNAi phenotypes.

Positive and negative controls were used to evaluate and monitor the sensitivity of iBeetle screening. Negative controls were provided by the injection of buffer twice in an injection day (see details in ‘materials and methods’). As positive controls, dsRNA which gives a defined phenotype were injected. More than 80% positive controls and more than 90% negative controls were successfully recognized (Fig. 4.2). These high numbers of successful recognition of controls indicate the reliability of the iBeetle screen.

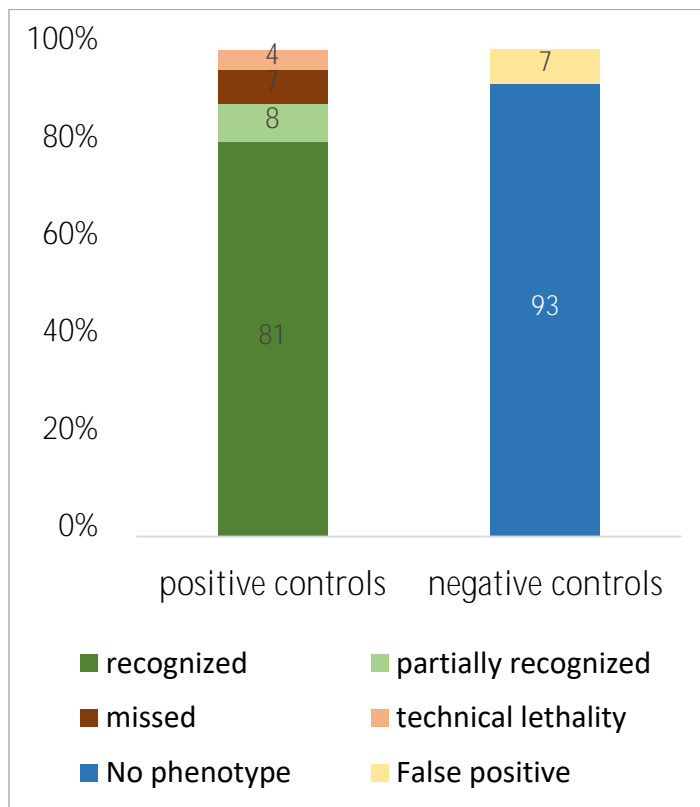


Figure 4.2 Recognition rate of positive and negative controls in the second phase of the iBeetle screening. Ninety percent (80% fully and 10% partially) of positive controls were recognized. Seven percent were missed. In case of negative controls, seven percent were false positive. Data for this figure was provided by screeners and processed by Dr. Daniela Grossmann. Prof Dr. Gregor Bucher kindly provided the figure. Positive controls $n= 178$; Negative controls $n= 99$.

4.1.2 Selection criteria for head phenotypes

After completion of the screening, I aimed to identify novel head patterning genes from all 3,200 genes. To do so, I mined the iBeetle annotation base (<http://ibeetle-base.uni-goettingen.de/ibAnno>) which stored the phenotypic data annotated by the screeners. Potential novel head patterning candidates identified during the first phase of screening were already studied. So, I looked for those which were screened after the first phase of screening (time period- from 2nd Feb 2012 until 17th Nov 2014). The following criteria were used to select novel genes potentially involved in head patterning from the iBeetle annotation base.

1. Head related phenotype: I choose the ‘larval head’ feature in the iBeetle annotation database which automatically collect all the head related phenotypes.
2. Penetrance: Penetrance is the percentage of animal showing a particular phenotype after knockdown. The higher the penetrance the higher is chance that a particular phenotype can be successfully reproduced. Initially, we planned to use a >50% penetrance search criterion because of past experience from previous screeners. However, in order not to miss any interesting phenotypes I lowered the penetrance percentage criteria to >30%. The >30% penetrance criterion allowed us to find all the head related phenotype above 30% penetrance (eg. 30-50%, 50-80% or >80%).
3. Head specificity: The phenotype should specifically affect the head. Moreover, they should have a low percentage of empty eggs (eggs without any cuticle) and pantagmatic effects (phenotypes that affect two or more than two tagma simultaneously).
4. Gene information: I used the ‘iBeetle’ dsRNA fragment (iB fragment) sequence to obtain the gene information from the iBeetle genome browser (<http://bioinf.uni-greifswald.de/blast/tribolium/blast.php>). The iBeetle genome browser also provide the information of *Drosophila* orthologs through the ‘reciprocal best BLAST’ algorithm. In parallel, by BLAST analysis at NCBI (<https://www.ncbi.nlm.nih.gov>), I obtained the orthologs and at FlyBase (<http://flybase.org>) I obtained information of these orthologs. This helped me to exclude those genes which had already been studied.

5. Hatch rate: The hatch rate is the portion of larvae that hatched after RNAi. Generally, wild type larvae manage to crawl through meshes but not larvae with knockdown of an essential gene. However, animals with mild phenotypes (e.g. only antenna specific phenotypes) can sometime hatch. Generally, a lower hatch rate indicates a stronger phenotype. Hatch rate was not used as a criterion to screen the candidates rather was used for classification.

Procedure: The search criteria used for candidate selection were 'larval head, >30% penetrance and time period' (to exclude the genes from the first screening phase). With these criteria (1 and 2), 340 hits were found out of ~3,500 genes. A detailed inspection of all the 340 hits was performed to assess criterion 3 'head specificity and no or few empty eggs and pantagmatic phenotype'. These criteria helped us to exclude the background phenotypes and resulted in total 105 candidates. Based on criterion 4 (gene information), I found that the role of 20 genes was previously studied concerning *Tribolium* head development. This reduced the novel genes number to 85 (105-20). A second round of close manual inspection of the selected 85 candidates based on annotated cuticle pictures and hatch rate (criterion 5) resulted in 32 candidates. The 32 candidates were classified into the higher penetrance (>50%) with lower hatch rate (<50%) and lower penetrance (30-50%) with 0-100% hatch rate groups which have 22 and 10 candidates respectively (Fig. 4.3).

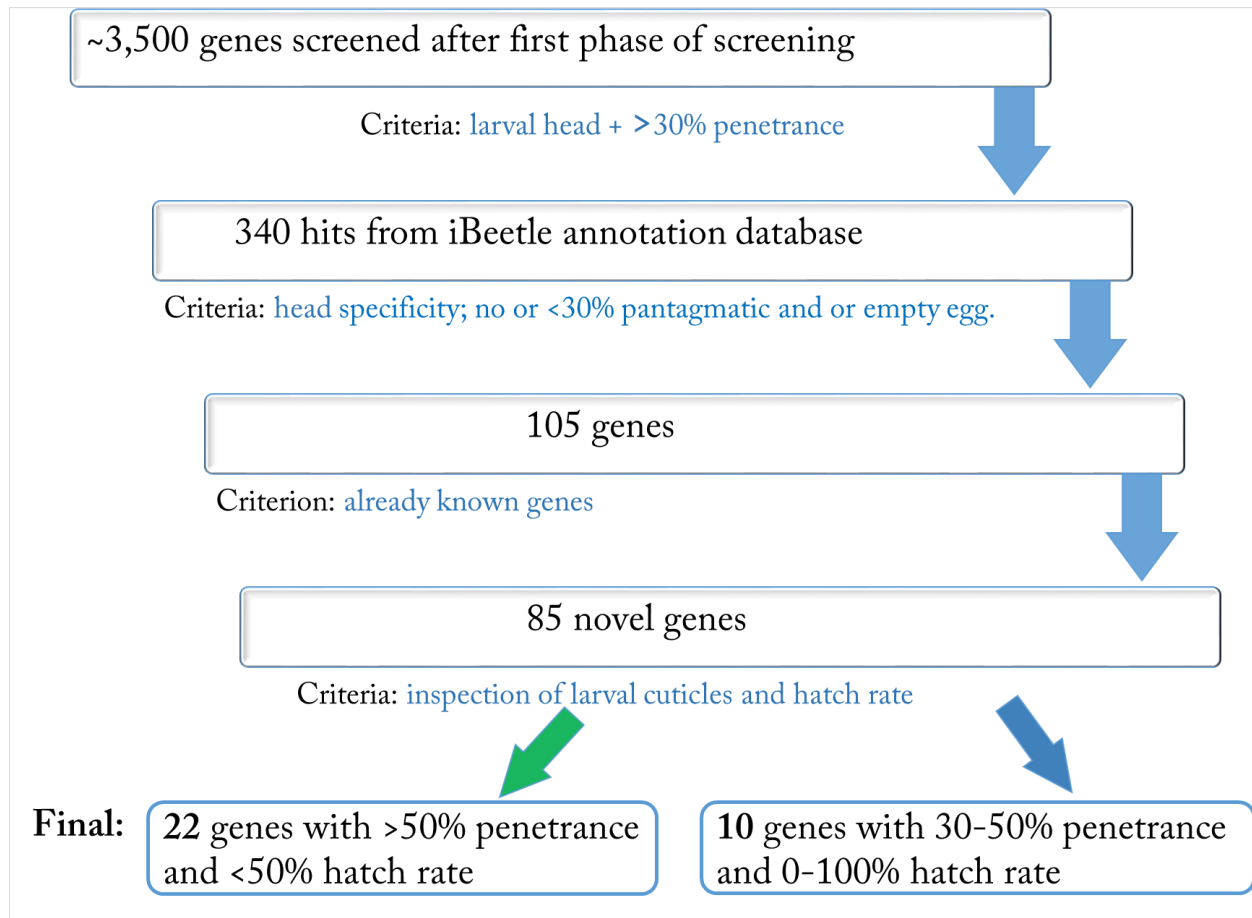


Figure 4.3 Overview of selection procedure for candidate genes. See previous paragraph for details.

4.1.3 Rescreening: I

The iBeetle project is a single pass screen. Hence, rescreening is a necessary step to confirm the observed phenotypes. Apart from the confirmation of the cuticle phenotype, rescreening also aimed to check for strain specificity of the phenotype and to exclude off-target effects. Strain specificity was checked by injection of the identical iBeetle dsRNA fragments into both the SB strain (which is a wild type strain of *Tribolium castaneum*) and the pBA19 strain (iBeetle screening strain). Off target effects were checked by injection of dsRNA of a non-overlapping fragment (NOF) targeting the same gene. Therefore, a minimum of four injections was performed during the rescreening. Procedure for injection, egg collection and cuticle preparation were same as during the iBeetle screening (See material and methods for details).

The total eight candidates (five fully reproduced and three fully reproduced with technical problems) were successfully confirmed from the '22 candidate list of >50% penetrance and <50% hatch rate group' (Table 2). One of the reasons of technical problems could be degraded dsRNA. There were two likely off-target phenotypes i.e. phenotypes were reproduced with the original dsRNA fragment but not with the NOF. In some cases, the experimental replicate worked but only with the iB fragment in the pBA19 strain. In summary, eight of the selected candidates were reproduced successfully (Table 4.1).

Table 4.1 Result of rescreening of 22 genes of >50% penetrance and <50% hatch rate group.

dsRNA ID shows the unique number of dsRNA fragments used in screen. iB fragment column represents whether the phenotypes were reproduced with dsRNA (iB fragment) or not in the pBA19 strain or the SB strain. The non-overlapping fragment column shows the same. Remark section denotes the status of reproducibility of the phenotypes. Phenotypes were called fully reproduced if similar larval cuticles were observed with iB fragment and non-overlapping fragment in the SB and the pBA19 strain. Technical problems were assumed if phenotypes were failed to reproduce with iB fragment in the pBA19 strain or the SB strain but reproduce successfully with non-overlapping fragments.

dsRNA_ID	iB fragment		Non overlapping fragment		Remarks
	pBA19	SB	pBA19	SB	
iB_00900	—	—	✓	✓	Fully reproduced + technical problem
iB_04393	✓	✓	✓	✓	Fully reproduced
iB_04730	✓	✓	✓	✓	Fully reproduced
iB_05677	✓	✓	✓	✓	Fully reproduced
iB_06600	✓	✓	✓	✓	Fully reproduced
iB_06673	✓	✓	✓	✓	Fully reproduced
iB_07145	—	—/✓	✓	✓	Fully reproduced + technical problem
iB_06244	✓	✓	✓	—	Fully reproduced + technical problem
iB_08646	✓	—/✓	—/✓	—	Partially reproduced
iB_09055	✓	—/✓	—/✓	—	Partially reproduced
iB_06391	✓	✓	—	—	Off target effect
iB_07647	✓	✓	—	—	Off target effect
iB_09103	✓	—	—	—	Experimental replicate
iB_06945	✓	—	—	—	Experimental replicate
iB_04939	—/✓	—	—	—	Partially experimental replicate
iB_03318	—	—	—	—	Not reproduced
iB_07057	—	—	—	—	Not reproduced
iB_08148	—	—	—	—	Not reproduced
iB_08916	—	—	—	—	Not reproduced
iB_09852	—	—	—	—	Not reproduced
iB_010545	—	—	—	—	Not reproduced
iB_010752	—	—	—	—	Not reproduced
— not reproduced, ✓ reproduced and —/✓ partially reproduced					

In case of the ten selected candidates of the ‘30-50% penetrance and 0-100% hatch rate group’ no candidate was successfully reproduced (Table 4.2). Five of selected candidates were not reproducible, three of selected candidates were reproduced only in the experimental replicate and two fell into the off-target category (Table 4.2). In summary, the rescreening reduced the number of potential candidates from 32 to 8.

Table 4.2 Result of rescreening of 10 genes of 30-50% penetrance and 0-100% hatch rate group. See legends of table 4.1 for details.

dsRNA_ID	iB fragment		Non overlapping fragment		Remarks
	pBA19	SB	pBA19	SB	
iB_00978	— / ✓	— / ✓	—	—	Partially off target effect
iB_06294	— / ✓	— / ✓	—	—	Partially off target effect
iB_01944	✓	—	—	—	Experimental replicate
iB_08185	✓	—	—	—	Experimental replicate
iB_07014	✓	—	—	—	Experimental replicate
iB_09566	—	—	—	—	Not reproduced
iB_04630	—	—	—	—	Not reproduced
iB_06554	—	—	—	—	Not reproduced
iB_06738	—	—	—	—	Not reproduced
iB_06364	—	—	—	—	Not reproduced

4.1.3 Rescreening: II

The expressivity and penetrance of RNAi knockdown phenotypes are variable depending on the degree of gene knockdown. Degree of knockdown is mostly correlated with injected dsRNA concentration in female beetles (Miller et al., 2012). We have used 1µg/µl concentration of dsRNA throughout screening and rescreening. However, I wanted to check whether the higher dsRNA concentration will result in stronger phenotypes and finally in higher reproducibility rate or not. Therefore, I selected the nine candidates from iBeetle database with relaxed criteria (head related phenotype with >30% penetrance and

some empty egg and pantagmatic defects) and performed the rescreening with two different concentrations-1 μ g/ μ l and 3 μ g/ μ l. Nevertheless, I got only one successfully reproduced gene after rescreening of nine candidates (Table 4.3).

Table 4.3 Result of rescreening of nine candidates.

iB fragment column represents either the phenotypes were reproduced with 1 μ g/ μ l and 3 μ g/ μ l dsRNA (iB fragment) or not in pBA19 strain and SB strain. Non overlapping fragment column shows either the phenotypes were reproduced with 1 μ g/ μ l and 3 μ g/ μ l dsRNA (NOF) or not in pBA19 strain and SB strain. See legends of table 4.1 for details.

dsRNA_ID	iB fragment				Non overlapping fragment				Remarks
	pBA19		SB		pBA19		SB		
	1 μ g/ μ l	3 μ g/ μ l	1 μ g/ μ l	3 μ g/ μ l	1 μ g/ μ l	3 μ g/ μ l	1 μ g/ μ l	3 μ g/ μ l	
iB_10029	✓	✓	✓	—	✓	✓	✓	—	Fully reproduced + technical problem
iB_10578	✓	✓	✓	✓	—	—	—	—	Off target effect
iB_10654	✓	✓	✓	✓	—	—	—	—	Off target effect
iB_06887	—	✓	—	—	—	—	—	—	Partial experimental replicate
iB_10577	—	—	—	—	—	—	—	—	Not reproduced
iB_10581	—	—	—	—	—	—	—	—	Not reproduced
iB_10594	—	—	—	—	—	—	—	—	Not reproduced
iB_10614	—	—	—	—	—	—	—	—	Not reproduced
iB_10619	—	—	—	—	—	—	—	—	Not reproduced

In summary, rescreening helped us to sort out the false positives, off targets or strain specific phenotype and resulted in nine candidates for further validation (Table 4.4).

Table 4.4 List of nine dsRNA IDs with its corresponding gene ID, phenotypes and their *Drosophila* orthologs and functions.

dsRNA_ID	Gene ID	Phenotype	Dm_orthologs	Dm_biological process
iB_04393/06244	TC032760	head bristle pattern, antenna irregular	fat	Cell morphogenesis, cell adhesion
iB_05677	TC031158	antenna, maxilla and mandible affected	CG7466	Multicellular organismal development
iB_04730	TC009940	head appendage shape, anterior muscle	protein Kinase D	Intracellular signal transduction
iB_010029	TC004152	labrum and antenna size shortened	CG8184	dsRNA transport, ubiquitination
iB_00900	TC005612	bell row, gena triplet absent	amun	Eye, wing and chaeta development
iB_06600	TC010832	head capsule absent	big brain	CNS, meso-ectoderm development
iB_06673	TC005276	tracheal opening at T1 and T2, ridge	suppressor of zeste 2	Chromatin silencing
iB_07145	TC007939	head, labrum, antenna size/shape,	Not found	

4.1.4 Initial analysis of novel head patterning genes.

Expression of a gene in a particular tissue generally indicates that this particular gene is involved in the development of that particular tissue. e.g. *Tc-six3* in head regions during embryonic development (Posnien et al., 2011). Therefore, we used the expression pattern of these selected candidates to further narrow down the number of candidates and to identify the most reliable and novel candidates for in depth analysis. To analyze the expression pattern of the eight candidates, *in situ* hybridization was performed on wild type SB *Tribolium* embryo with respective RNA probes. Semi-quantitative cuticle analysis of candidates were done with iBeetle fragments and NOF in both pBA19 strain and SB strain. Since, the penetrance of phenotypes varies with different fragments as well as different strains, here I will show the analysis result of 1µg/µl dsRNA NOF in pBA19 strain only. Moreover, phylogenetic trees using amino acids based on maximum likelihood method were made to validate the finding of respective orthologs in *Drosophila* and mouse.

Henceforth, all nine candidates will be described following with their phylogenetic analysis, cuticle phenotypes, and expression patterns.

4.1.4.1 Phylogenetic analysis, RNAi phenotype and expression pattern of *Tribolium fat*

The gene TC032760 was found to be target of iB_04393 and iB_06244 by the BLASTn analysis using nucleotide sequences of iBeetle fragments against the *Tribolium* genome in the iBeetle genome browser (<http://bioinf.uni-greifswald.de/blast/tribolium/blast.php>). The gene TC032760 was mistakenly considered to be two genes due to previous inaccurate annotation which led to knockdown by two different iBeetle fragments (iB_04393 and iB_06244). BLASTp analysis using protein sequences of TC032760 against reference proteins of *Tribolium*, *Drosophila* and mouse genome was performed to find out the potential paralogs and orthologs. Phylogenetic analysis using the protein sequences revealed *Dm-fat* as ortholog of TC032760 (Fig. 4.4). NCBI called this gene *Tc-cadherin-related tumor suppressor* (*Tc-fat* will be used from here onwards). Semi-quantitative analysis of *Tc-fat* knockdown with iB_04393 NOF in pBA19 strain revealed a swollen legs and decreased tibiotarsus with more than 80% penetrance. Further, gena triplet setae numbers were increased and antenna flagellum was missing with 50-80% penetrance (Fig. 4.5). No expression was detected for *Tc-fat* during blastoderm stages (not shown). *Tc-fat* was widely expressed from early germ band stages onward, but became enriched at the ventral midline, in the developing appendages and the segmental borders at later germ band stages (Fig. 4.6). Interestingly, *Dm-fat* expression appears only at later stages (stage 9/10; elongated germ band stage) but then shows a similar segmentally modulated expression. *Dm-fat* is a cadherin related tumor suppressor gene which is involved in biological processes like cell-cell adhesion and negative regulation of cell proliferation (Flybase: <http://flybase.org/reports/FBgn0001075.html>).

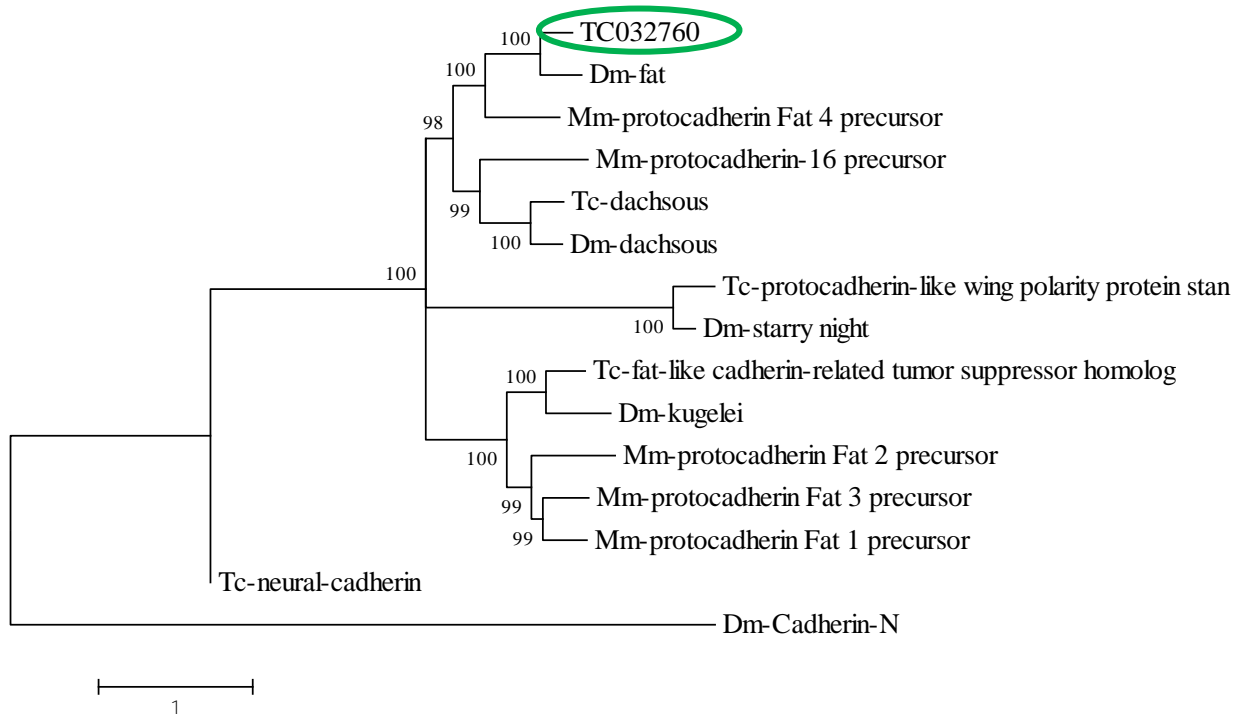


Figure 4.4 Phylogenetic analysis of TC032760 based on Maximum Likelihood method with bootstrap scores at the nodes. The evolutionary history was analyzed by using amino acid sequences. TC032760 (circled in green) is the ortholog of *Dm-fat*.

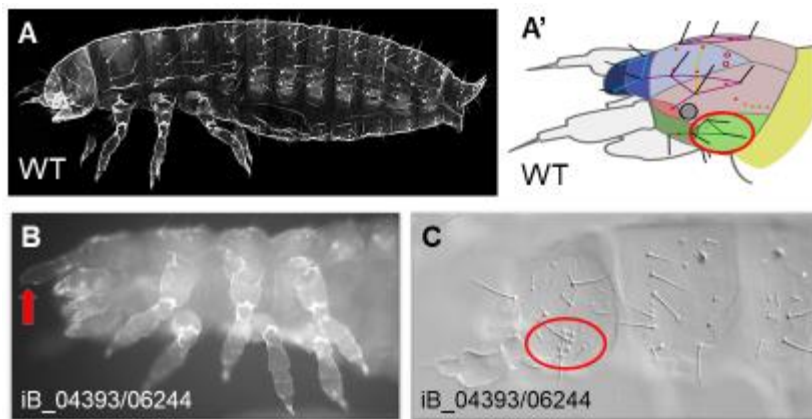


Figure 4.5 *Tc-fat* RNAi leads to defects in larval head cuticle and legs. (A) Lateral view of wildtype first instar larval cuticle and (A') schematic representations of head bristles patterns and segments. (B) *Tc-fat* RNAi led to loss of the flagellum (red arrow), swollen legs and (C) increased number of gena triplet setae (circled in red) in C and A'. The figure A' was kindly provided by Prof. Gregor Bucher.

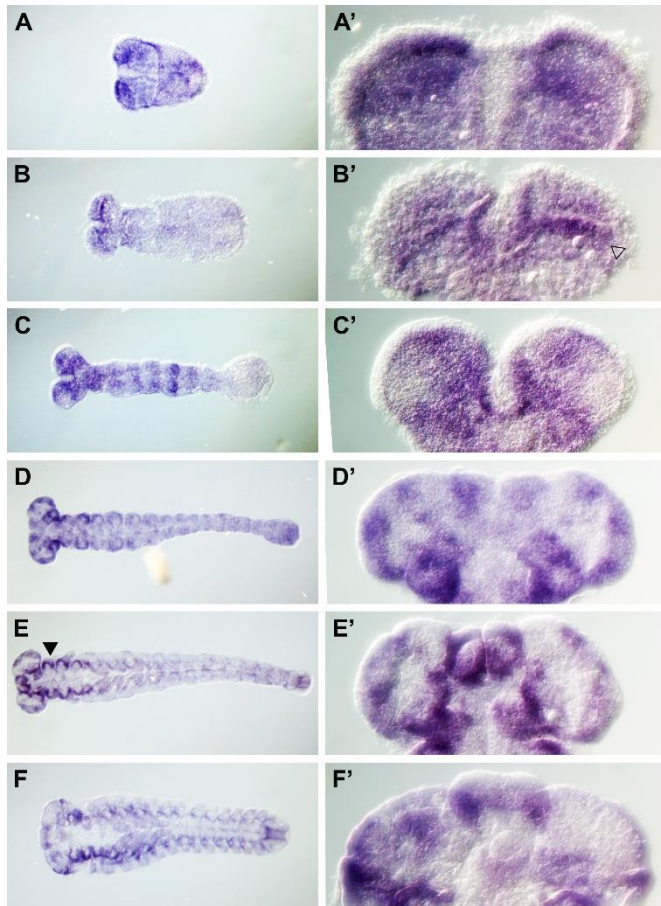


Figure 4.6 *Tc-fat* mRNA expression pattern during embryogenesis. A to F show 10x magnification figures with anterior to the left. A' to F' show close ups (40x magnification) with anterior to the top. (A and A') During the germ rudiment *Tc-fat* transcripts are widely distributed throughout the embryo. (B to C') At early germ band extension stage, there is wide expression, but increased level of expression is observed in stripes near the ocular regions (B', open arrowhead) and in the trunk (C). (D and D') In elongated germ band stages, transcripts were started to confine towards lateral regions. (E and E') During late elongating germ band stages, expression is found mainly in growing appendages (arrowhead). (F and F') During retracted germ band stages, the lateral rim of head lobes, the anterior lateral part of the labrum buds, the antenna region, the stomodeum region and some cells of each segment expressed *Tc-fat*.

4.1.4.2 Phylogenetic analysis, RNAi phenotype and expression pattern of *Tribolium multiple epidermal growth factor-like domain protein 8*

iB_05677 targets the gene TC031158. Phylogenetic analysis using the protein sequences revealed *Dm*-CG7466 and *Mm*-multiple epidermal growth factor-like domain protein 8 (*Mm*-*megf8*) as respective *Drosophila* and mouse orthologs (Fig. 4.7). NCBI called this gene *Tc*-multiple epidermal growth factor-like domains protein 8 (*Tc*-*megf8*) based on the ortholog found in the mouse. *Tc*-*megf8* knockdown led to shortened antenna pedicellus and swollen maxilla, labium and mandible with more than 80% penetrance (Fig. 4.8). In addition, shape of head appendages was irregular and labrum was decreased with less than 30% penetrance. *Tc*-*megf8* mRNAs were not detected during blastoderm stages (not shown). *Tc*-*megf8* was widely expressed during early germ band stages. *Tc*-*megf8* transcripts remained widely expressed at later stages with relatively high expression in the head lobes (Fig. 4.9). There are neither biological, molecular nor phenotypic data available for the *Dm*-CG7466 ortholog (Flybase: <http://flybase.org/reports/FBgn0031981.html>). However, *Mm*-*megf8* encodes a 2845 amino acid long protein (compare to 1361 amino acids long *Tc*-MEGF protein) involved in left-right patterning. *Mm*-*megf8* orthologs can be found from human to fruit fly, and expression is similar to *Tc*-*megf8* expression (Zhang et al., 2009).

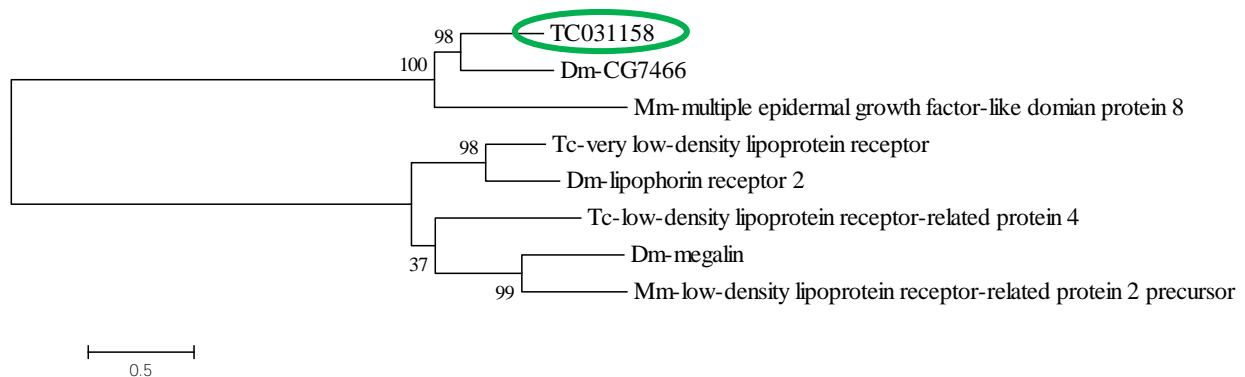


Figure 4.7 Phylogenetic analysis of TC014696 based on Maximum Likelihood method with bootstrap scores at the nodes. The evolutionary history was analyzed by using amino acid sequences. TC031158 (circled in green) is the ortholog of *Dm*-CG7466 and *Mm*-*megf8*.

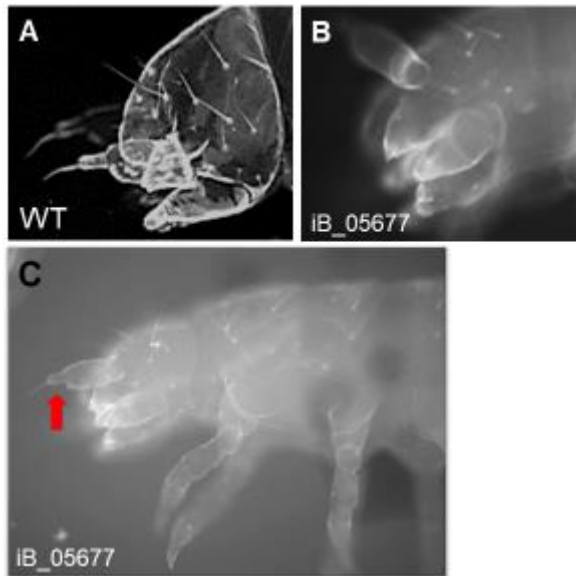


Figure 4.8 *Tc-megf8RNAi* shows head related phenotype. (A) Lateral view of wildtype larval head (B) *Tc-megf8RNAi* resulted in swollen maxilla and the labium and (C) decreased antenna size (red arrow).

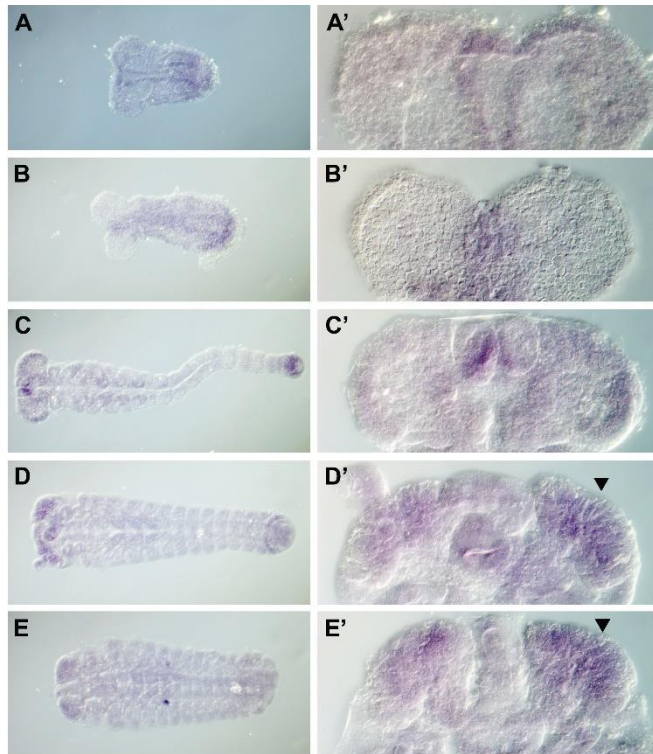


Figure 4.9 *Tc-megf8* mRNA expression pattern during embryogenesis. A to E show 10x magnification figures with anterior to the left. A' to E' show close ups (40x magnification) with anterior to the top. (A and A') In germ rudiment stages, *Tc-megf8* transcripts are widely expressed. (B and B') At early germ band extension stages, transcripts are present widely with the exception of head lobes. (C and C') At elongated germ band, expression is broadly present. (D to E') During elongating germ band and retracting germ band stages, mRNAs are widely distributed with increased expression at the rim of the head lobes (arrowhead).

4.1.4.3 Phylogenetic analysis, RNAi phenotype and expression pattern of *Tribolium protein kinase D3*

The gene TC009940 was found to be target of iB_04730. Phylogenetic analysis using the amino acid sequences revealed *Dm-protein kinase D* and *Mm-protein kinase D3* as closest ortholog of TC009940 (Fig. 4.10). NCBI named this gene *Tc-protein kinase D3* based on the orthologs found in *Drosophila* and mouse. *Tc-protein kinase D3* RNAi caused broadening of the maxillary palp, a swollen labium and a decreased size of the antenna flagellum and pedicellus with more than 80% penetrance (Fig. 4.11). No expression of *Tc-protein kinase* was detected during the blastoderm stage. Transcripts of *Tc-protein kinase D3* were first detected in the growth zone of germ rudiment stage embryos but became widely expressed at later stages (Fig. 4.12). *Dm-protein kinase D* is a kinase of the PKC family and putatively involved in protein kinase D signaling and protein phosphorylation. However, no phenotypic data for *Dm-protein kinase D* is available (Flybase: <http://flybase.org/reports/FBgn0038603.html>).

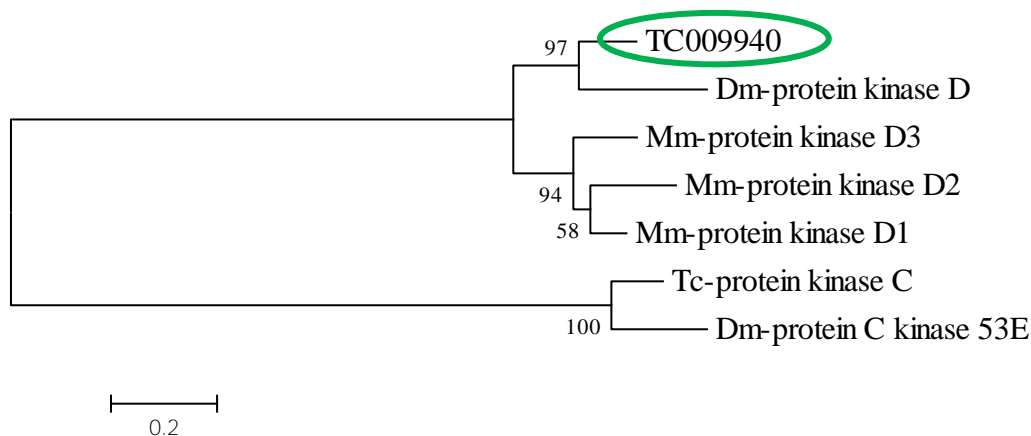


Figure 4.10 Phylogenetic analysis of TC009940 based on Maximum Likelihood method and JTT matrix with bootstrap scores at the nodes. TC009940 (circled in green) is the orthologs of *Dm-protein kinase D*.

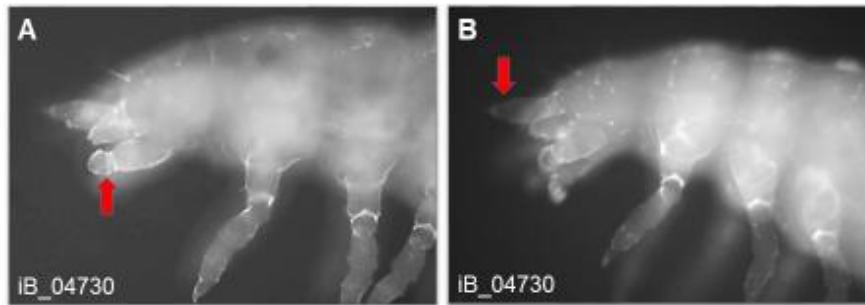


Figure 4.11 RNAi phenotype of TC009940. (A) *Tc-protein kinase D3* knockdown led to broader maxillary palp (red arrow) and (B) decreased antenna size (red arrow).

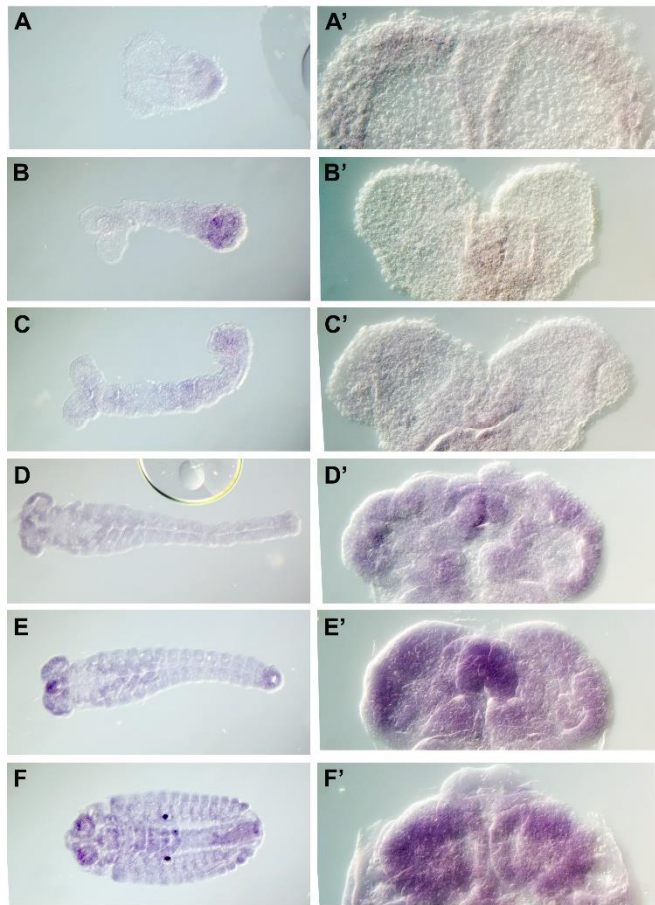


Figure 4.12 Expression pattern of *Tc-protein kinase D3* during embryogenesis. A to F show 10x magnification figures with anterior to the left. A' to F' show close ups (40x magnification) with anterior to the top. (A and A') *Tc-protein kinase D* expressed at the posterior part of germ rudiment embryos with very weak expression in the anterior region. (B and B') At early germ band extension stages, weak expression extends towards anterior but the growth zone has relatively high expression. (C and C') In elongating germ band stages, transcripts are ubiquitously distributed. (D and D') In late elongated germ band stages, weak ubiquitous expression is present, but the rim of head lobes and rim of developing appendages have elevated expression. (E to F') During the retraction and in late retracting embryos, transcripts are ubiquitously distributed throughout the embryo with relatively stronger expression in the head.

4.1.4.4 Phylogenetic analysis, RNAi phenotype and expression pattern of *Tribolium E3 ubiquitin protein ligase HUWE1*

iB_10029 dsRNA targets the gene TC004152. Phylogenetic analysis predicted the *Mm-E3 ubiquitin-protein ligase HUWE1* and *Dm-CG8184* as orthologs of TC004152 gene (Fig. 4.13). NCBI named this gene *Tc-E3 ubiquitin-protein ligase HUWE1* based on the orthologs found in the mouse. Semi-quantitative analysis of *Tc-E3 ubiquitin-protein ligase HUWE1* knockdown in SB and pBA19 strains revealed a decreased labrum (more than 80% penetrance) and antenna size (30-50% penetrance) as well as an irregular shape of the posterior terminus (30-50% penetrance) (Fig. 4.14). Further, head appendages shape was irregular and their appendages partially missing with 30-50% penetrance. The labrum, vertex triplet setae, posterior abdomen segments and posterior terminus was missing with less than 30% penetrance. *Tc-E3 ubiquitin-protein ligase HUWE1* expression started at the blastoderm stage. Mostly, it was widely expressed from early germ band stages to retracted germ band embryos (Fig. 4.15). *Dm-CG8184* is involved in dsRNA transport. Based on structural similarities, *Dm-CG8184* is predicted to involve protein ubiquitination process (Flybase: <http://flybase.org/reports/FBgn0030674.html>).

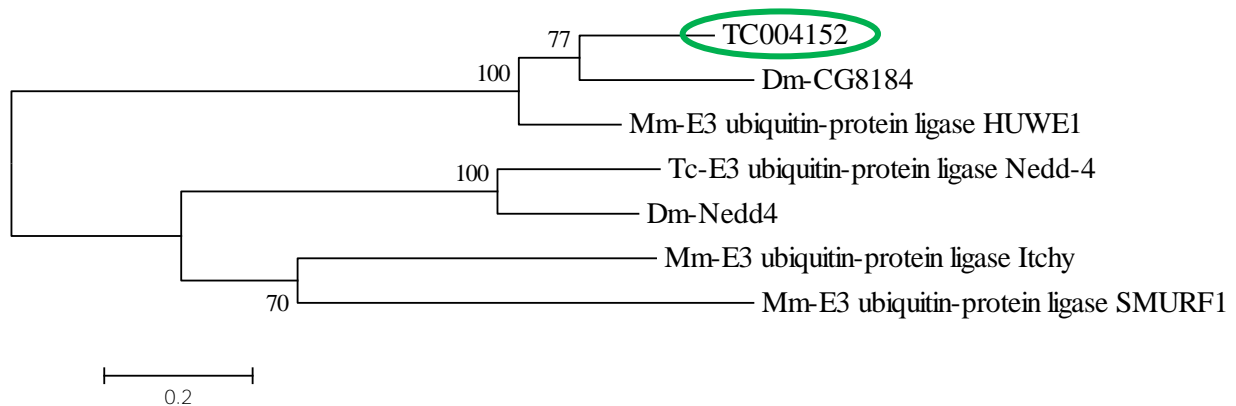


Figure 4.13 Phylogenetic analysis of TC004152 based on Maximum Likelihood method with bootstrap scores at the nodes. TC004152 (circled in green) is the ortholog of *Dm-CG8184* and *Mm-E3 ubiquitin-protein ligase HUWE1*.

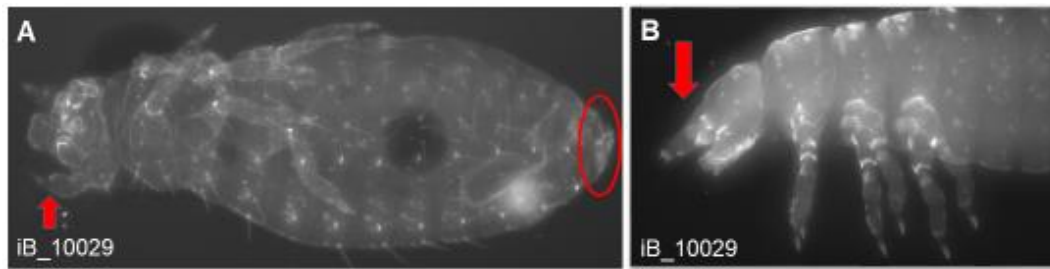


Figure 4.14 *Tc-E3 ubiquitin-protein ligase HUWE1* RNAi exhibits defects in larval cuticle. (A) *Tc-E3 ubiquitin-protein ligase HUWE1* RNAi resulted in partial loss and irregular shape of head appendages (red arrow) as well as loss of posterior terminus (circled in red) and (B) decreased antenna and labrum size (red arrow).

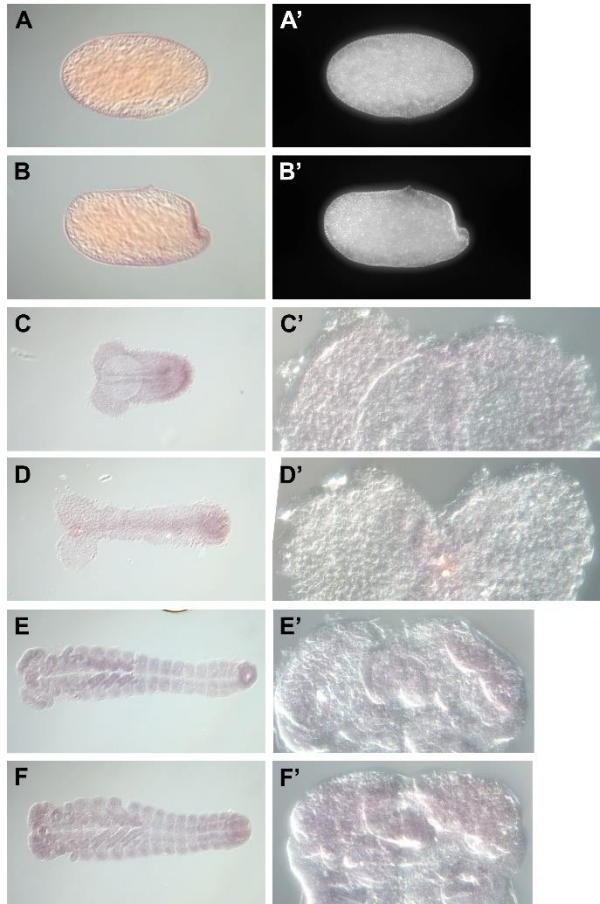


Figure 4.15 *Tc-E3 ubiquitin-protein ligase HUWE1* mRNA expression pattern during embryogenesis. A to F as well as A' and B' show 10x magnification figures with anterior to the left. A' and B' are DAPI staining of respective embryos. C' to F' show close ups (40x magnification) with anterior to the top. (A) *Tc-E3 ubiquitin-protein ligase HUWE1* was expressed during blastoderm stages and (B) with increased intensity in the posterior pit during the differentiated blastoderm stages. (C and C') It is expressed widely in germ rudiment stages. (D and D') mRNAs are present ubiquitously with exception of head lobes during early germ band stages. (E to F') It is ubiquitously distributed in elongating germ band and retracting germ band stages.

4.1.4.5 Phylogenetic analysis, RNAi phenotype and expression pattern of *Tribolium amun*

Injection of the iB_00900 dsRNA caused knockdown of the gene TC005612. Phylogenetic analysis and reciprocal BLAST revealed neither *Tribolium* paralogs nor related genes in mouse. However, *Dm-amun* is the only gene in *Drosophila melanogaster* which is predicted to be ortholog of TC005612 based on phylogenetic analysis and reciprocal BLAST. Other beetles' species such as Asian long-horned beetle (*Anoplophora glabripennis*), burying beetle (*Nicrophorus vespilloides*) have TC005612 orthologs. Moreover, Other *Drosophila* species such as *Drosophila navajoa* also have TC005612 orthologs. The zebrafish (*Danio rerio*) gene-LOC541336 have significant similarities to the TC005612 (Fig. 4.16). NCBI characterized TC005612 as uncharacterized protein but I will refer to this gene as *Tc-amun* due to *Dm-amun* orthology. The *Tc-amun* knockdown phenotype includes loss of bell row (more than 80% penetrance) and posterior gena triplet setae (50-80% penetrance) and the shape of the head (less than 30%) and thoracic appendages (30-50% penetrance) was irregular and the posterior vertex setae was missing with less than 30% penetrance (Fig. 4.17). *Tc-amun* expression started at the anterior of early blastoderm stages and showed ubiquitous expression from germ rudiments stages onwards with relatively higher expression in ventral midline at early germ band stages (Fig. 4.18). *Dm-amun* is involved in the development of the compound eye, wing disc and chaeta. *Dm-Amun* is a nuclear factor of Notch signaling that act as transcriptional regulator of *Dm-achaete* (Shalaby et al., 2009).

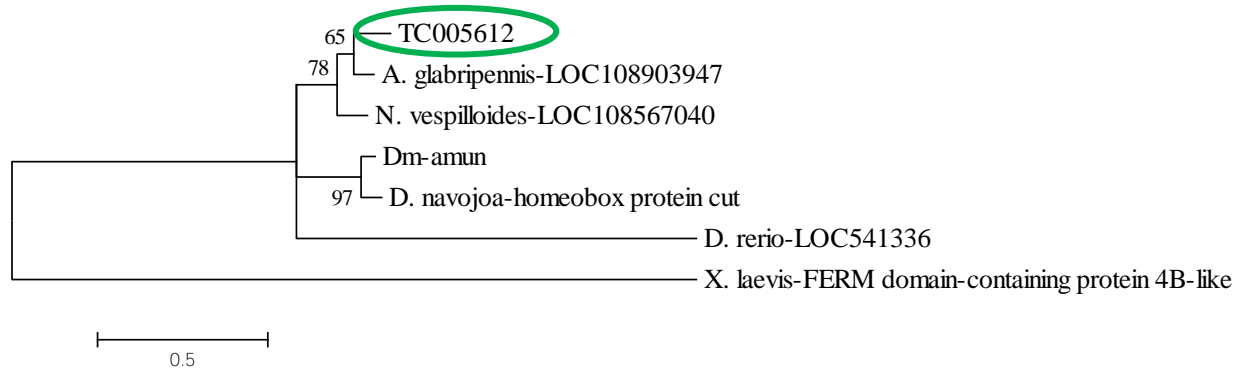


Figure 4.16 Phylogenetic analysis of TC005612 based on Maximum Likelihood method and JTT matrix with bootstrap scores at the nodes. TC005612 (circled in green) shows high similarity to the uncharacterized protein-LOC108903947 of *A. glabripennis* with high bootstraps value. The lack of significant similarities in mouse suggests that TC005612 may not be present in mammals.

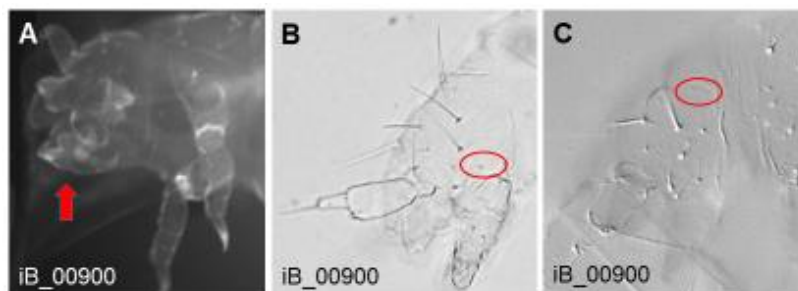


Figure 4.17 RNAi phenotype of *Tc-amun*. (A) Knockdown of *Tc-amun* caused irregular head appendages (red arrow) and (B) loss of the posterior gene triplet setae (circled in red) and (C) loss of bristles of the bell row (circled in red).

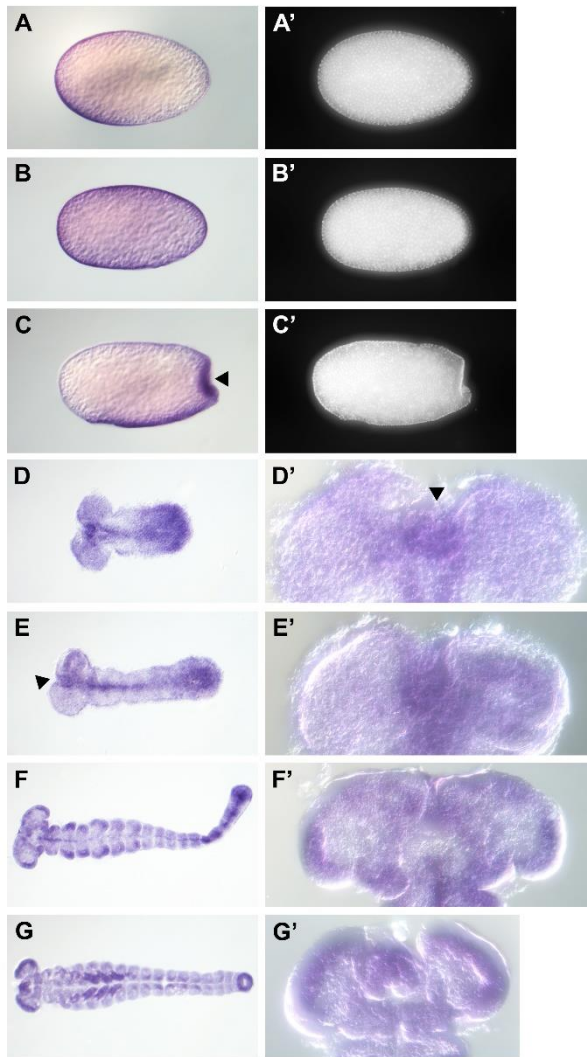


Figure 4.18 *Tc-amun* mRNA expression pattern during embryogenesis. **A** to **G** as well as **A'** to **C'** show 10x magnification figures with anterior to the left. **A'** to **C'** are DAPI staining of respective embryos. **D'** to **G'** show close ups (40x magnification) with anterior to the top. (**A**) *Tc-amun* expression was first observed during the early blastoderm stages at the anterior region but (**B**) became ubiquitously distributed at blastoderm stages and (**C**) expressed in the posterior pit during the differentiated blastoderm stages (arrowhead). (**D** to **E'**) It is expressed widely in germ rudiment and early germ band stages with increased expression at the ventral midline. (**F** to **G'**) It is broadly distributed in elongating germ band and retracting germ band stages.

4.1.4.6 Phylogenetic analysis, RNAi phenotype and expression pattern of *Tribolium neurogenic protein big brain*

Injection of the iB_06600 dsRNA caused knockdown of the gene TC010832 and its phenotype was a shape of irregular larvae, swollen and irregular shape of head appendages as well as a reduced head capsule size with more than 80% penetrance. Further, cervix cuticle (cuticle between the head capsule and prothoracic segment-cephalic region) was partially absent with 50-80% penetrance (Fig. 4.20). Phylogenetic analysis predicted *Dm-big brain (bib)* and *Mm-aquaporin-1* as orthologs of TC010832 (Fig. 4.19). NCBI named this gene *Tc-neurogenic protein big brain (Tc-bib)* based on the ortholog found in *Drosophila*. *Tc-bib* is expressed early in the germ anlagen of blastoderm stages. Later the expression decreased but becomes very strong in the neuroectoderm at germ elongation stages (Fig. 4.21D). In late stages, *Tc-bib* expressed in segmental cell clusters (Fig. 4.21E-F). *Dm-bib* transcripts are ubiquitously present in early and late germ elongation stages which is similar to *Tc-bib*. *Dm-bib* is a zygotic neurogenic gene that encodes an aquaporin transport protein and is involved in nervous system development, ectoderm development, Notch signaling (Flybase: <http://flybase.org/reports/FBgn0000180.html>).

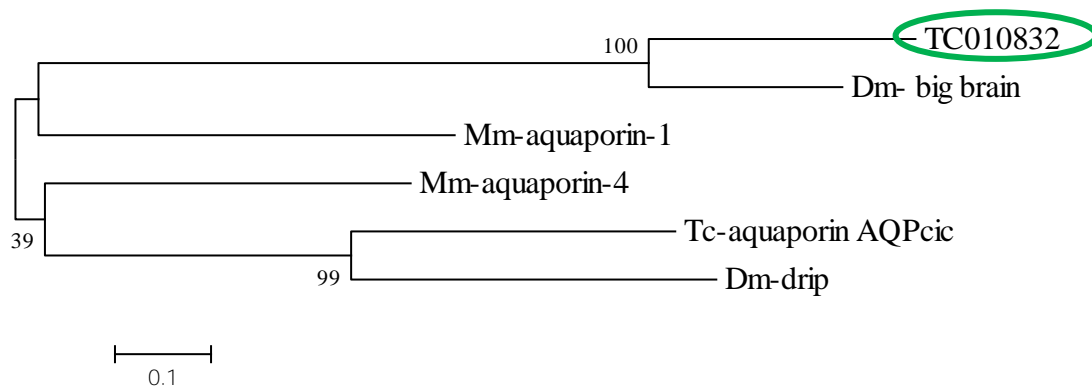


Figure 4.19 Phylogenetic analysis of TC010832 based on Maximum Likelihood method and JTT matrix with bootstrap scores at the nodes. The evolutionary history was analyzed by using amino acid sequences. TC010832 (circled in green) is the ortholog of *Dm-big brain* with high bootstraps value.

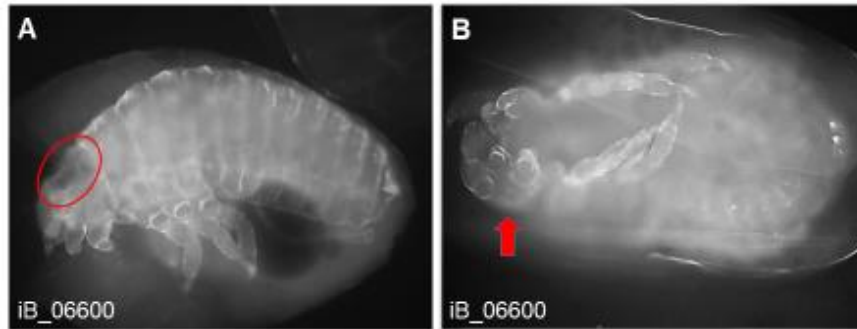


Figure 4.20 Larval cuticle of *Tc-bib* RNAi. (A) *Tc-bib* knockdown caused the irregular shape of the larvae and partial loss of the cervix cuticle (circled in red) and (B) swollen and irregular head appendages (red arrow).

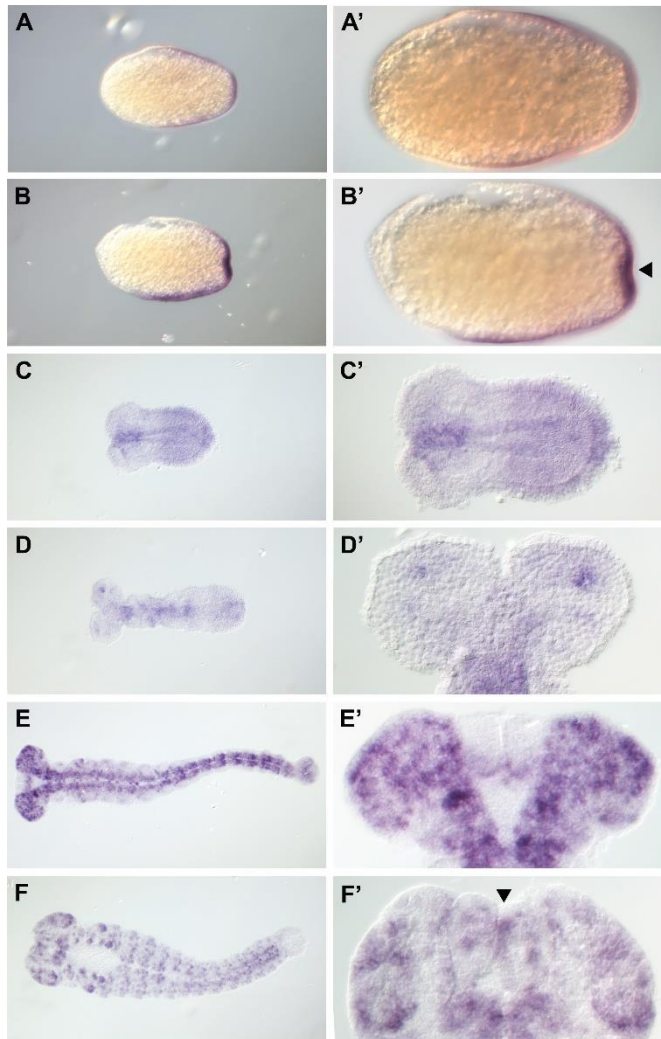


Figure 4.21 *Tc-bib* mRNA expression pattern during embryogenesis. A to F show 10x magnification figures with anterior to the left. A' to C' are 20x magnification figures of respective embryos. D' to F' show close ups (40x magnification) with anterior to the top. (A and A') During the blastoderm stage, *Tc-bib* expression was detected in the posterior half. (B and B') During the differentiated blastoderm stages, *Tc-bib* transcripts were present in extraembryonic anlagen and posterior pit (arrowhead). (C and C') In germ rudiment stages, expression is widely observed with increased expression in the anterior median tissue and growth zone. (D and D') During early germ band extension stages, transcripts were in the median tissues. In addition, transcripts were present in the anterior head lobes. (E and E') At elongated germ band stages, mRNAs were present in all clusters of the putative nervous system. Moreover, the posterior region of the labral buds show

expression. (F and **F'**) During retracting germ band stages, expression was in cells clustered throughout the embryos except in the posterior terminus (arrowhead).

4.1.4.7 Phylogenetic analysis, RNAi phenotype and expression pattern of *Tribolium polycomb group protein Psc*

The gene TC005276 was found to be target of iB_06673. Phylogenetic analysis predicted the *Dm-suppressor of zeste 2 (su(z)2)* ortholog of TC005276 (Fig. 4.22). NCBI named this gene *Tc-polycomb group protein Psc*. *Tc-polycomb group protein Psc* RNAi led to formation of tracheal opening at prothoracic and mesothoracic segments, change of labium orientation as well as swollen of labium shape, broader proximal structure of maxilla and irregular antenna shape with more than 80% penetrance. Further, the dorsal ridge row was missing and labrum size was reduced with 50-80% penetrance (Fig. 4.23). *Tc-polycomb group protein Psc* mRNAs were ubiquitous at blastoderm. It was widely expressed in germ rudiment stage with relative high expression in the ventral region. Localized expression was observed in the CNS during retracting germ band embryos (Fig. 4.24). *Dm-su(z)2* share the sequence similarities with mammalian *bmi-1 proto-oncogene* and *Dm-Psc*. *Dm-su(z)2* is involved in chromatin silencing and phenotype manifest in arista, wing, macrochaeta etc. (Flybase: <http://flybase.org/reports/FBgn0265623.html>).

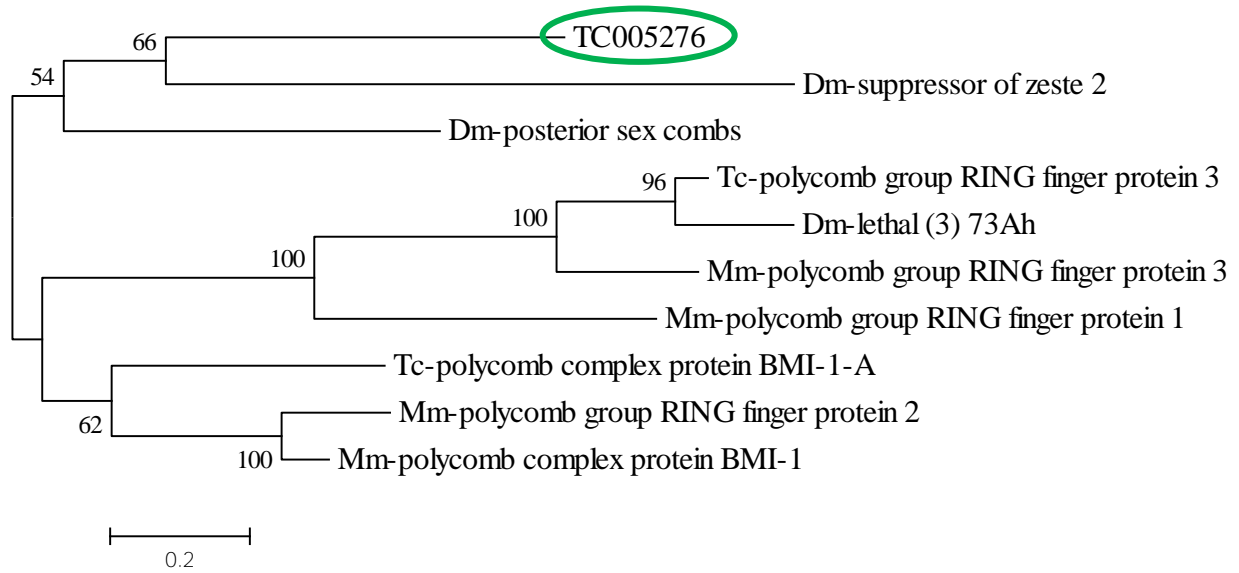


Figure 4.22 Phylogenetic analysis of TC005276 based on Maximum Likelihood method and JTT matrix with bootstrap scores at the nodes. The evolutionary history was analyzed by using amino acid sequences. *Dm-su(z)2* is the ortholog of TC005276 (circled in green). *Dm-posterior sex combs* is the paralog of *Dm-su(z)2* and have significant similarities to the TC005276.

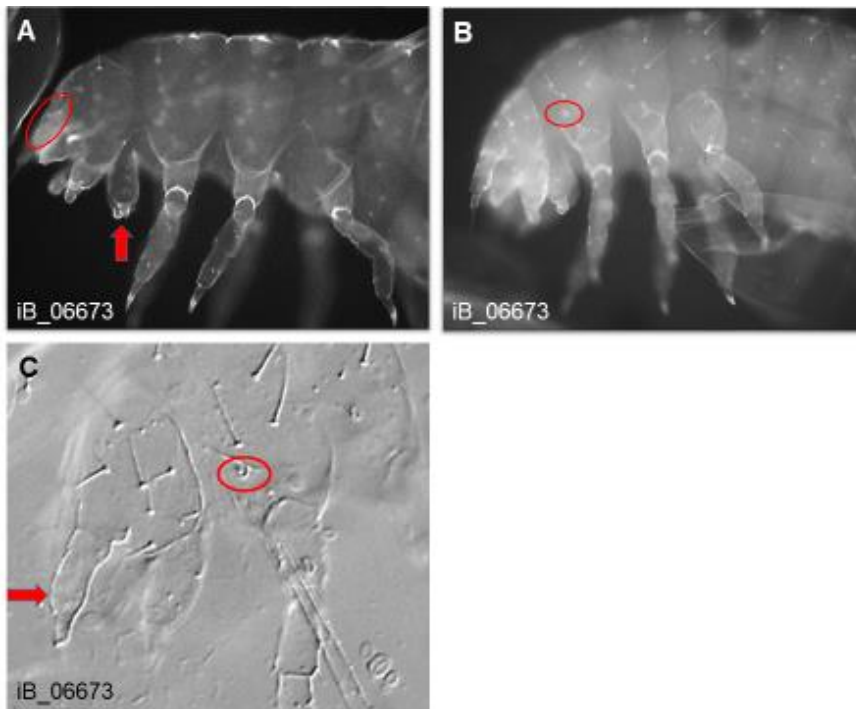


Figure 4.23 *Tc-polycomb group protein Psc* RNAi exhibits defects in larval cuticle. (A) *Tc-polycomb group protein Psc* RNAi led to irregular labium orientation (red arrow), reduced labrum size (circled in red) and (B and C) additional opening of tracheal at prothoracic segment (circled in red) and irregular shape of antenna (red arrow) (C).

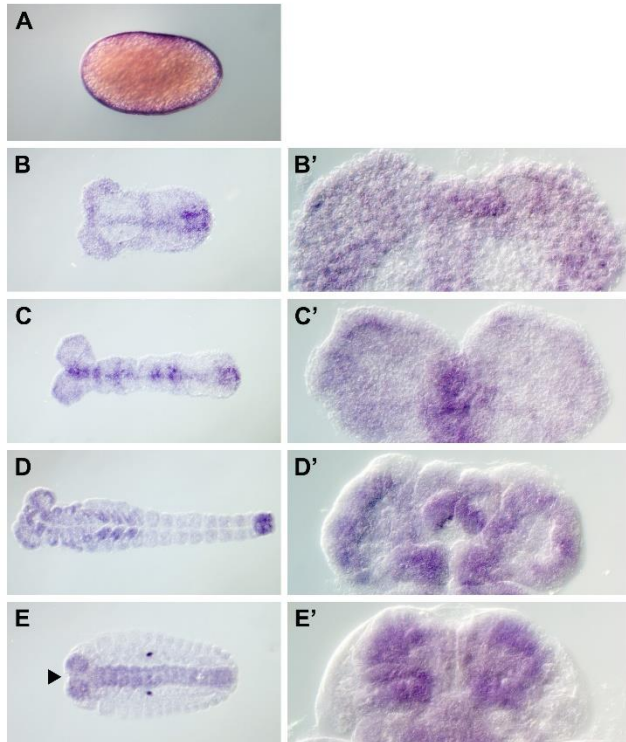


Figure 4.24 Expression pattern of *Tc-polycomb group protein Psc* during the embryogenesis. A to E show 10x magnification figures with anterior to the left. B' to E' show close ups (40x magnification) with anterior to the top. (A) During the blastoderm stage, expression was ubiquitous. (B and B') In germ rudiment embryos, expression was widely observed. (C and C') During early germ band extension stages, expression is broadly distributed but ventral cells show increased expression. (D and D') At elongated germ band stages, transcripts were widely distributed with increased expression at the posterior terminus. (E and E') At late retracting germ band stages, expression is confined to the CNS.

4.1.4.8 Phylogenetic analysis, RNAi phenotype and expression pattern of TC007939

iB_07145 dsRNA targets the gene TC007939. Semi-quantitative analysis of TC007939 knockdown in SB and pBA19 strains resulted in loss of the labrum, the antenna flagellum and the vertex triplet setae as well as irregular legs shape with 50-80% penetrance (Fig. 4.25). Both complete CDS and mRNA sequences were used as probe to detect the expression pattern of TC007939 but no staining was detected. Phylogenetic analysis and reciprocal BLAST revealed neither *Tribolium* paralogs nor orthologs in *Drosophila* and mouse. However, beetle species such as Asian long-horned beetle (*Anoplophora glabripennis*), small hive beetle (*Aethina tumida*), and mountain pine beetle (*Dendroctonus ponderosae*) have TC005612 orthologs (not shown). There was no protein homology found outside of beetle species. Therefore, TC007939 seems to be evolve specifically in beetle species.

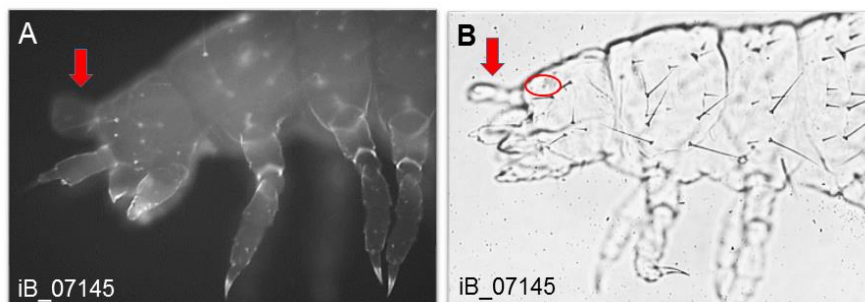


Figure 4.25 TC007939 RNAi exhibits defects in the larval head cuticle. (A) TC007939 RNAi led to a decreased size of the labrum (red arrow) or (B) loss of labrum, the antenna flagellum and the vertex triplet setae (circled in red).

4.1.5 Head patterning genes after genome-wide screen

The iBeetle community has covered 53% of the *Tribolium* genome after the second phase of screening, out of approximately 16,000 predicted genes. With this 53% genome coverage, we speculate the total number of anterior head patterning genes would be $n=42$ after genome-wide screen. Out of 42 anterior head patterning genes, nine were discovered through the iBeetle screening and four will be discovered in the screening of remaining 50% genome. Based on this estimation, we calculated that 31% head patterning genes are found through the iBeetle screening compared to 62% discovered through the candidate gene approach. This estimation uses only anterior head patterning genes but not gnathal genes (Fig. 4.26).

Data were provided by screeners and the figure was kindly provided by Prof. Gregor Bucher.

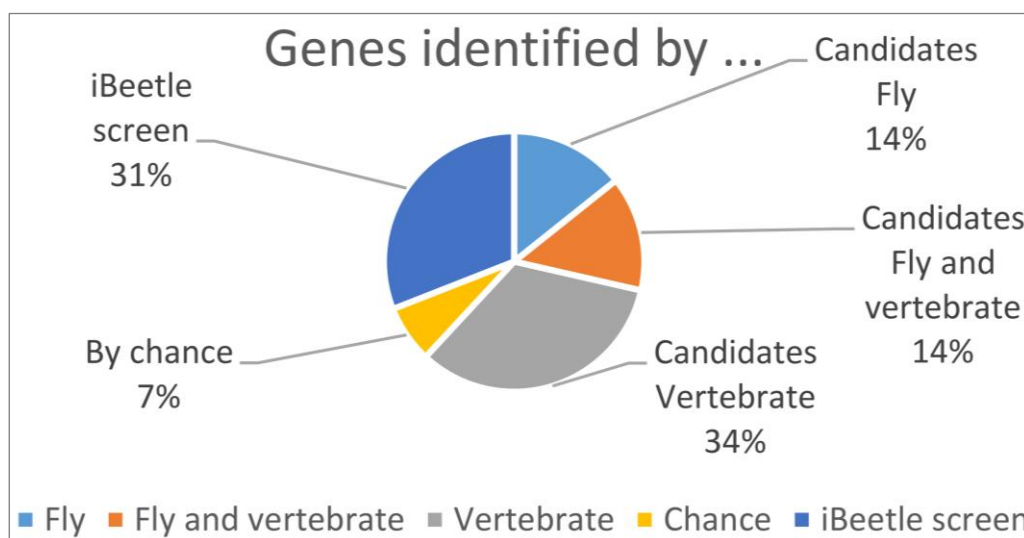


Figure 4.26 Head patterning genes identified by different methods. This chart shows the contribution of different approaches in the identification of head patterning genes.

4.2 Part II: The Gcl project

During the first phase of screening, screeners found two very interesting candidates that unexpectedly produced a double abdomen upon RNAi. This was the first case that a double abdomen phenotype was reported in any beetles. The analysis of these genes was started by Nicole Troelenberg and I continued as a part of my thesis. All data shown in this work were prepared and analyzed by me. The manuscript was written by me, Prof. Gregor Bucher and Prof. Martin Klingler.

Authors contributions to the experiments:

Salim Ansari: All experiments except for:

Nicole Troelenberg: Initial validation of phenotypes and analysis of marker genes expression in *Tc-gcl* and *Tc-hbn* RNAi embryos.

Julia Ulrich: Generation of VSR transgenic line (RNAi inhibitor technique).

Van Anh Dao: Found the *Tc-gcl* phenotype during the iBeetle screening.

Tobias Richter: Found the *Tc-hbn* phenotype during the iBeetle screening.

Status: In submission process.

Research article

Title

Maternal *germ cell-less* and zygotic *homeobrain* and *zen1* in axis formation

One Sentence Summary

We show how a short germ insect lacking *bicoid* distinguishes head vs. abdomen. The system is fundamentally different from the one in the fly.

Authors:

Salim Ansari*, Nicole Troelenberg*, Julia Ulrich*, Van Anh Dao, Tobias Richter, Gregor Bucher#, Martin Klingler

* These authors contributed equally to this work

corresponding author: gbucher1@uni-goettingen.de

Abstract

The distinction of anterior versus posterior is a crucial step in animal embryogenesis. In the fly *Drosophila*, this axis is established by morphogenetic gradients contributed by the mother that regulate zygotic target genes. This principle was considered to hold true for all insects but is fundamentally different from vertebrates. We investigated symmetry breaking in the beetle *Tribolium*, which represents the more ancestral short germ embryogenesis. We found that maternal *Tc-germ cell-less* is required for anterior localization of maternal *Tc-axin*, which represses Wnt signaling. *Tc-germ cell-less* inactivation leads to a duplicated abdomen.

Interestingly, also double-knockdown of the zygotic genes *Tc-homeobrain* and *Tc-zen1* results in such a phenotype. Conversely, interfering with two posterior factors, *Tc-caudal* and Wnt, causes double anterior phenotypes. Hence, anterior repression of Wnt and regulation among zygotic genes is essential for axis formation in this more basal insect, bridging the different systems found in flies and vertebrates.

Main text

One of the most important first steps in animal embryogenesis is the establishment of anterior-posterior polarity (AP-polarity), distinguishing head from tail. If this process fails, **mirror image duplications of embryonic structures may develop like the “double abdomen”** embryos induced by classical manipulations of insect embryos by ligation or UV-irradiation experiments (Yajima, 1960; Sander, 1961; Kalthoff and Sander, 1968). Based on such experiments, autonomous patterning mechanisms were proposed for the insect egg (Meinhardt, 1977).

In the fly *Drosophila melanogaster*, mRNA of the *bicoid* gene is localized to the anterior pole from where the Bicoid protein diffuses to form an anterior to posterior gradient. An opposing gradient of Nanos protein forms from posterior to regulate Hunchback translation, which thus forms another anterior gradient. In addition, the graded activity of the Torso pathway directs patterning near both poles of the *Drosophila* embryo. Together, these maternal morphogenetic gradients provide positional information and initiate zygotic segmentation gene expression in a concentration dependent manner (Nüsslein-Volhard et al., 1987; Driever and Nüsslein-Volhard, 1988). Mutations in *bicoid* result in duplication of some posterior structures at the anterior, while symmetric larvae with "double abdomen" form after double inactivation of both, Bicoid and Hunchback (Hülskamp et al., 1990) and a number of other genotypes (Nüsslein-Volhard, 1977; Mohler and Wieschaus, 1986) where *bicoid* and *nanos* localization is impeded in more subtle ways. Mutations in zygotic genes do not phenocopy the axis duplication events seen for mutants affecting maternal factors. However, axis formation in *Drosophila* is derived. First, *bicoid* is not present outside

higher dipterans (Stauber et al., 1999) and axis formation in another long germ fly relies on a different maternal factor (Klomp et al., 2015). In the wasp *Nasonia*, a more distantly related long germ insect, *orthodenticle* (*otd*) provides maternal morphogenetic gradients – intriguingly at both poles. *giant* substitutes for the permissive role of *bicoid* at the anterior (Brent et al., 2007; Lynch et al., 2006).

However, all these long germ embryos lack the predicted autonomous posterior patterning mechanism. In contrast, typical short germ insect embryos form posterior segments sequentially from a "growth zone" or segment addition zone (SAZ), which is specified at the posterior pole of the blastoderm. Further, in short germ insects, extraembryonic tissue is formed at the anterior blastoderm, rather than head structures as in *Drosophila*. The red flour beetle *Tribolium* is a model for short germ embryogenesis where the formation of abdominal segments requires *Tc-caudal* expression as well as Wnt and Torso signaling at the posterior pole. Torso signaling appears to be the only conserved maternal signal. It had been suggested that *Tc-otd* and *Tc-hunchback* substitute for the anterior morphogen in the beetle *Tribolium* (Lynch et al., 2006; Schröder, 2003). However, more recent data do not support a morphogenetic role of these genes in anterior patterning (Kotkamp et al., 2010; Marques-Souza et al., 2008b). Instead, anterior localization of maternal *Tc-axin* mRNA represses Wnt signaling, providing a permissive environment for anterior development, similar as in vertebrate embryos (Copf et al., 2004; Fu et al., 2012b; Petersen and Reddien, 2009; Schoppmeier and Schröder, 2005). Ubiquitously distributed *Tc-caudal* mRNA is translationally repressed by anterior Tc-Mex-3 and Tc-Zen2 but their knockdown does not lead to double abdomen phenotypes (Schoppmeier et al., 2009b). In summary, the mechanism of symmetry breaking and subsequent AP-patterning in short germ embryos is predicted to be different but has remained obscure. Notably, genetically induced mirror image phenotypes have not been observed so far. Likewise, the predicted autonomy of SAZ patterning has not been demonstrated.

New genes in AP-axis formation

In an ongoing genome-wide RNAi screen we searched for cuticle phenotypes affecting the anterior-posterior body axis (Dönitz et al., 2015; Schmitt-Engel et al., 2015a). We found two dsRNAs whose knockdown led to double abdomen phenotypes. One of these, iB_02693, targeted the ortholog of the *Drosophila germ cell-less* gene (*gcl*), which in the fly is required at the posterior pole for germ cell development. It encodes a BTB domain protein localized at the nuclear lamina in both, *Drosophila* and vertebrates, where it appears to be involved in transcriptional regulation (Jongens et al., 1994; Leatherman et al., 2002b; de la Luna et al., 1999) or cytoskeleton organization (Cinalli and Lehmann, 2013a; Lerit et al., 2017). Knockdown of *Tribolium germ cell-less* (*Tc-gcl*) results in double abdomen phenotypes with high penetrance (>95%) where head and thorax are replaced by a mirror image abdomen (Fig. 1B-C and Extended Data Fig. 1). Interestingly, in some specimen the total number of segments of these two abdomina (2x10 abdominal segments) exceeds the normal number of segmentation clock derived segments (16 segments), demonstrating the autonomy of the duplicated SAZ. Some segmentation and dorsal closure defects occur as well.

We found maternal *Tc-gcl* transcripts to be localized to the anterior half of the developing oocyte and the freshly laid egg (Fig. 1G-I). We generated an antibody detecting Tc-Gcl. As in *Drosophila*, we found the protein at the nuclear lamina, colocalized with nuclear pore proteins (Fig. 1M and N). Later, a posterior domain with similarity to *Tc-vasa* expression developed *de novo* (Fig. 1I and Extended Data Fig. 2C-H). However, neither dsRNA injected into embryos, nor into L5 larvae, resulted in strongly reduced egg production, suggesting that in *Tribolium*, *gcl* may be dispensable for germ cell development.

The second dsRNA (iB_04564) causing double-abdomina targeted the ortholog of *homeobrain*, which is a homeodomain transcription factor expressed in the head and brain primordium of *Drosophila* but for which a function has not been described (Walldorf et al., 2000a). Knockdown of *Tribolium homeobrain* (*Tc-hbn*) resulted in anterior deletions or

double abdomen phenotypes (Fig. 1D-F). Both, penetrance and expressivity of double abdomina were lower compared to *Tc-gcl* knockdown (Extended Data Fig. 1 O-P), and thoracic segments remained present even in the strongest phenotypes (Extended Data Fig. 1). *Tc-hbn* is expressed as one of the earliest zygotic genes in an anterior cap of the blastoderm, which later retracts from the pole and eventually forms bilateral domains in the head anlagen (Fig. 1J-L and Extended Data Fig. 2). Both phenotypes were reproduced by RNAi using non-overlapping dsRNA fragments in the same genetic background. It was unexpected to find axis duplication upon knockdown of a zygotic gene since the current insect paradigm holds that maternal morphogens establish the axes, while zygotic genes then interpret them.

In order to characterize the mechanism of axis duplication we scrutinized the expression of SAZ markers in RNAi embryos (Fig. 2). *Tc-gcl*/RNAi induced a mirror image duplication of *Tc-even-skipped* (*Tc-eve*) and *Tc-vasa* expression from early blastoderm stages onwards while *Tc-caudal* (*Tc-cad*) was expressed ubiquitously (Fig. 2B,E,Q). *Tc-wingless* (*Tc-wg*) expression in the SAZ was duplicated as well while its segmental pattern prefigured the duplication seen in the cuticles (Extended Data Fig. 3). In *Tc-hbn* knockdown blastoderm embryos, in contrast, the anterior expression boundary of these genes was only shifted anteriorly during blastoderm stages (Fig. 2C,F) while *Tc-vasa* expression was not altered (not shown). Later, in germ band embryos, duplicated expression domains of *Tc-cad* and *Tc-wg* arose in the head, which developed into a mirror image SAZ (Extended Data Fig. 4A-I).

Time and location of ectopic SAZ formation in *Tc-gcl*/knockdown embryos corresponds to a region with active Torso signaling, in line with the notion that Torso signalling is required for SAZ formation (Schröder et al., 2000). The fact that a functional SAZ can form at both poles of the blastoderm as well as later in the head of postblastodermal embryos strongly supports the idea of autonomy of SAZ patterning, i.e. the SAZ has self-organizing capabilities.

Tc-gcl acts upstream in anterior patterning

Next, we sought to establish the genetic interactions involved in ectopic SAZ formation. The maternal expression of the anteriorly localized morphogen *Tc-axin* (Fu et al., 2012b), a negative regulator of Wnt signaling, was strongly reduced or absent upon *Tc-gcl* knockdown (Fig. 2G-H). This was not a general effect on maternally localized mRNAs because *Tc-pangolin* (*Tc-pan*) remained properly localized at the anterior pole (not shown). Both, the expression of *Tc-zen1*, a marker for extraembryonic serosa (Fig. 2J-K), and of *Tc-hbn* was abolished (Fig. 2M-N). Conversely, *Tc-gcl* expression was not altered in *Tc-axin*, *Tc-pan* or *Tc-hbn* knockdown (not shown). These results place *Tc-gcl* upstream of both, maternally localized *Tc-axin* and of the earliest known zygotic anterior markers, *Tc-zen1* and *Tc-hbn*.

The lack of anterior localized *Tc-axin* could be due to reduction of transcription in the nurse cells, wanting transport of *Tc-axin* mRNA to the oocyte, or due to lack of anterior localization within the oocyte. In order to distinguish between these possibilities, we performed *in situ* hybridization in wildtype and *Tc-gcl* RNAi ovaries. We found that in RNAi ovaries, the signal in oocytes was reduced compared to the one in nurse cells (Fig. 3 J-M). qPCR confirmed that the *Tc-axin* message was significantly reduced 3.5 fold in both freshly laid eggs and in ovaries, which included late oocytes (Extended Data Fig. 7). Hence, Tc-Gcl appeared to act in transport either by a non-transcriptional role in cytoskeletal regulation or by transcriptional regulation of another factor required for mRNA transport (Cinalli and Lehmann, 2013a; Lerit et al., 2017).

Tc-Gcl may not act via Wnt signaling alone

We wondered, how much of the *Tc-gcl* phenotype was due to alteration of early Wnt signaling via *Tc-axin* reduction. By knocking down the Wnt pathway components *Tc-axin*, *Tc-arrow* and *Tc-pan* we found that the expression boundaries of *Tc-hbn* and *Tc-zen1* were shifted posteriorly in Wnt low and anteriorly in Wnt high situations (Extended Data Fig.

5). However, none of the treatments completely abolished their expression. Further, the shift of *Tc-hbn* was small in early blastoderm embryos but became prominent subsequently (Extended Data Fig. 5B-D and T-V). Hence, interference with early Wnt signaling alone does not phenocopy the *Tc-gcl* phenotype.

Of note, *Tc-axin* RNAi leads to sterility and lethality of the injected animal. Hence, a reduced dose of dsRNA was used in this and previous studies (Fu et al., 2012b; Oberhofer et al., 2014b), potentially leading to a hypomorphic situation. In order to increase effective *Tc-axin* downregulation, we developed a method to protect the injected mother from the RNAi effect. We generated the *ubiVSR-2* transgenic line which ubiquitously expresses the viral suppressor of RNAi CrPV1A (Nayak et al., 2010). Indeed, in transgenic females injected with 1 µg/µl instead of 250 ng/µl *Tc-axin* dsRNA, both sterility and lethality were rescued (Extended Data Fig. 6A,B). However, the embryonic phenotype remained comparable both at the cuticle and *Tc-caudal* and *Tc-vasa* expression level (Extended Data Fig. 6C-H). Together, these results indicate that *Tc-gcl* did probably not act via *Tc-axin* alone. We note that this method will in the future allow studying a number of genes where maternal lethality or sterility has so far impeded RNAi analysis of the offspring (e.g. *Tc-Notch* and *Tc-cactus*).

We next tested whether *Tc-axin* might cooperate with some other factor to repress anterior SAZ formation. However, double RNAi treatments of *Tc-axin* combined with either *Tc-zen1*, *Tc-zen2*, *Tc-hbn*, *Tc-tll* or *Tc-pan* did not produce double abdomina. Only in very few *Tc-axin/Tc-zen1* double RNAi embryos did we observed a small ectopic *Tc-cad* domain in the head anlagen of posterior pit stage embryos (not shown). Likewise, double knockdown of *Tc-pan* with either *Tc-zen1* or *Tc-hbn* did not lead to double abdomen on the cuticle level.

Zygotic genes contribute to axis formation

It was unexpected that RNAi targeting zygotic *Tc-hbn* resulted in axis duplication. However, this phenotype was weaker and less penetrant than the one of maternal *Tc-gcl*, suggesting *Tc-hbn* might be only one of several zygotic effectors. Indeed, combining *Tc-hbn* with *Tc-zen1* (but not *Tc-zen2*) resulted in a substantially more penetrant and stronger double abdomen phenotype (Extended Data Fig. 1 Q), including some additional segmentation defects and dorsal closure defects similar to *Tc-gcl* RNAi (not shown). Moreover, we observed near-homogeneous expression of *Tc-cad* and an increased anterior shift of *Tc-eve* expression in blastoderm embryos (Fig. 3 A-D), while *Tc-vasa* displayed mirror image expression at both poles (Fig. 3 E-F). Further, we found mutual activation of *Tc-hbn* and *Tc-zen1* RNAi (Fig. 2L and not shown). In summary, the zygotic genes *Tc-hbn* and *Tc-zen1* act synergistically in suppressing an anterior SAZ, thereby preventing axis duplication.

We wondered whether zygotic genes might likewise be involved in specifying the posterior pole. In *Tribolium*, both posterior *Tc-cad* expression and Wnt signaling are required for SAZ formation (Bolognesi et al., 2008; Copf et al., 2004; Schoppmeier et al., 2009b). Hence, we hypothesized that *Tc-cad* activity at the posterior pole cooperates with Wnt signaling to repress anterior patterning. Indeed, in the double knockdown of *Tc-cad* and *Tc-pan*, we found *Tc-hbn* and *Tc-zen1* to become ectopically expressed at the posterior pole of the blastoderm, indicating the ectopic specification of anterior tissues. (Fig. 3G,I). In germ rudiment embryos, both, *Tc-hbn* expression and embryo morphology indicated that a second head anlage had developed at the posterior (Fig. 3H and Extended Data Fig. 4 J-O; these embryos did not produce cuticles).

A model for axis formation in short germ embryos

Formation of the serosa at the anterior pole and the SAZ at the posterior pole both depend on Torso activity (Pridöhl et al., 2017b; Schoppmeier and Schröder, 2005), a conserved symmetric maternal signal in beetles and flies (Klomp et al., 2015; Lehmann and Frohnhofer, 1989). Symmetry breaking is initiated by maternal Tc-Gcl, which acts to establish *Tc-axin* mRNA at the anterior pole of the oocyte to repress Wnt signaling (Fig. 4 and Extended Data Fig. 8). In the absence of Wnt signaling, Torso signaling determines serosa by activating *Tc-zen1* expression (Pridöhl et al., 2017b), and allows for zygotic *Tc-hbn* at the anterior pole. Once activated, *Tc-hbn* and *Tc-zen1* form a zygotic feedback loop and cooperate to repress *Tc-cad*. Initially, *Tc-zen1* activates *Tc-zen2*, which translationally represses maternal *Tc-caudal* mRNA (Schoppmeier et al., 2009b; van der Zee et al., 2005). Subsequently, they repress the zygotic *Tc-cad* promoter while at the same time specifying extraembryonic tissues.

At the posterior pole, Wnt and Torso signaling together with maternal *Tc-cad* initiate another zygotic feedback loop between Wnt signaling and *Tc-cad* to form a signaling center that specifies the SAZ. Indeed, Wnt activates *Tc-cad* (Oberhofer et al., 2014b) but it remains unclear, whether *Tc-cad* activates the expression of Wnt ligands like it does in spiders (Schönauer et al., 2016) but not in *Gryllus* (Shinmyo et al., 2005).

Removing localized *Tc-axin* from the system results in derepression of Wnt signaling and *Tc-cad* translation at the anterior, which together with Torso signaling initiate a SAZ at the anterior pole using the same mechanisms known from the posterior pole (Bolognesi et al., 2008; El-Sherif et al., 2014; Oberhofer et al., 2014b; Pridöhl et al., 2017b). All three components are required for specifying the SAZ, while Wnt signaling and *Tc-cad* cooperate in suppressing the expression of *Tc-hbn* and *Tc-zen1* in the posterior Torso domain.

It has recently been shown that *Drosophila* Gcl acts via Cullin3 to target the Torso receptor for degradation (Lehmann, accepted *Dev Cell*). A similar interaction of zygotic Tc-Gcl in

the anterior half of the blastoderm could be at work in *Tribolium*, but it would not shut down Torso signaling completely: In wildtype embryos, activated Map-Kinase is present at the anterior pole and in RNAi embryos with reduced Torso signaling, anterior structures and gene expressions are altered indicating an essential role (Pridöhl et al., 2017b; Schoppmeier and Schröder, 2005). However, zygotic *Tribolium* Gcl might modulate Torso signaling to ensure that different target gene sets are activated at the anterior and posterior poles.

Zygotic regulation instead of gradients

In the long germ embryos of both, *Drosophila* and *Nasonia*, maternal morphogenetic gradients of transcription factors regulate zygotic genes in a concentration dependent manner (Driever and Nüsslein-Volhard, 1988; Lynch et al., 2006; St Johnston and Nüsslein-Volhard, 1992). In such a system, zygotic genes are not involved in axis specification and respective mutants lead to loss of body regions but not to axis duplications. Our data suggest that this paradigm does not hold true for short germ insects. Here, initial asymmetry provided by maternal signals needs to be reinforced by two zygotic signaling centers located at both poles, respectively. Hence, in contrast to long germ embryos, knockdown of zygotic genes (*zen1* and *hbn* or Wnt and *cad*) do lead to posterior or anterior axis duplications, respectively.

Apparently, insects possess a more regulative embryogenesis than the one represented by the *Drosophila* system. Actually, the principle is more similar to what is found in vertebrates. Here, the initial symmetry breaking is based on maternal molecules but subsequent zygotic interactions are required to establish the posterior organizer (Cho et al., 1991; De Robertis, 2009). This signaling center then governs gastrulation thereby defining the posterior of the embryo from where subsequently the somites emerge (Dubrulle and Pourquié, 2004). At the anterior, zygotic genes are involved in repressing Wnt signaling in vertebrate (Lewis et al., 2008; Niehrs, 1999) and ancestral animal embryos (Guder et al., 2006) but not *Drosophila*. Intriguingly, *Tribolium* uses a *Drosophila* like mechanism (anterior localization

of maternal mRNAs) to realize a vertebrate like situation (i.e. anterior repression of Wnt signalling).

Supplementary Information is linked to the online version of this appear at www.nature.com/nature

Acknowledgements:

We thank Deutsche Forschungsgemeinschaft (DFG) for funding the iBeetle RNAi screen (FOR1234) and this analysis (KL 656/7-1; BU1443/8-2 and BU1443/11). We thank Claudia Hinnners and Elke Küster for technical assistance and Mathias Teuscher and Michael Schoppmeier for help with ovary *in situ* hybridization and Laurin Tomasek for preliminary work on the *hbn/zen1* synergism. Ronald Van Rij provided the clone with the CrPV1A protein. We thank Achim Dickmanns and Max Farnworth for help with expressing the protein for antibody production.

Main Figures

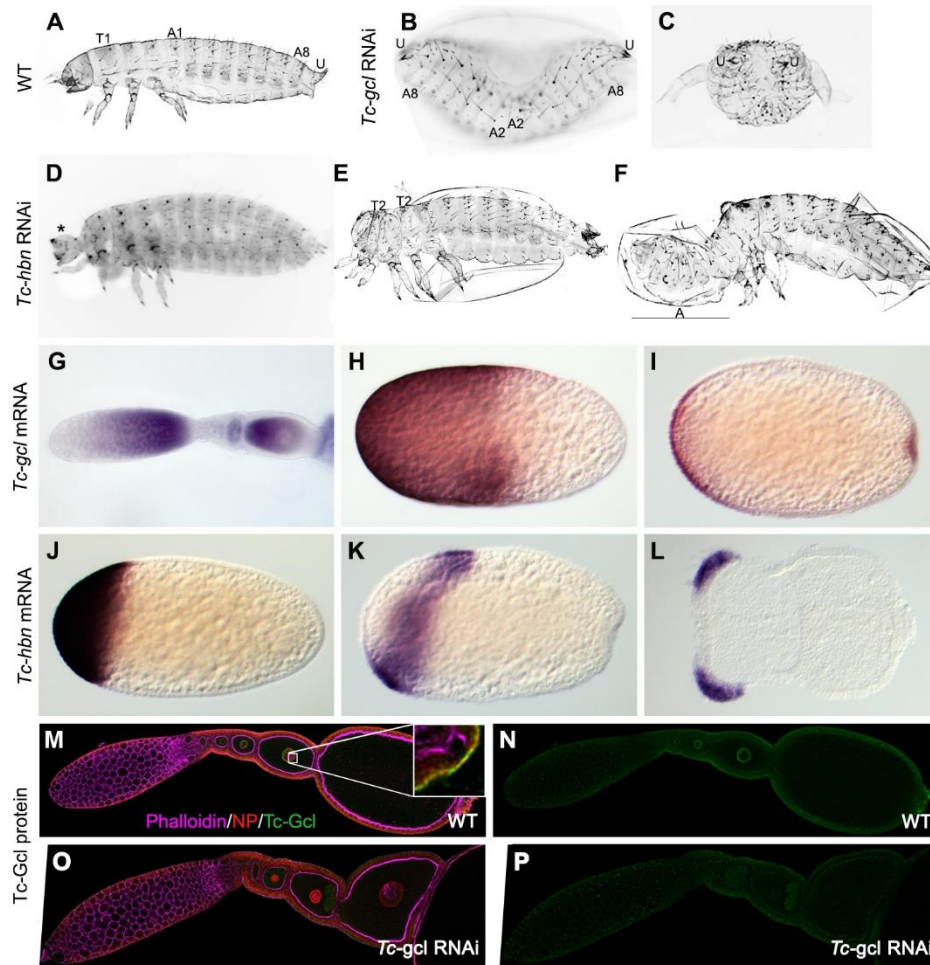


Fig. 1. *Tc-gcl* and *Tc-hbn* RNAi phenotype and expression. (A) Wildtype first instar larval cuticle with thoracic (T) and abdominal (A) segments and urogopmhi (U). (B and C) *Tc-gcl*/RNAi larvae lacking the thorax but displaying mirror image abdomina. (D to F) *Tc-hbn* RNAi phenotypes range from loss of the labrum and antennae (asterisk in D), to specimen with partially duplicated thorax (E) and incomplete double abdomen (F). (G to I) *Tc-gcl* mRNA is found in nurse cells and in the anterior of developing oocytes (G) and in the anterior half of freshly laid eggs (H). In differentiated blastoderm embryos, expression is found at the anterior and posterior poles (I). (J to L) Zygotic *Tc-hbn* mRNA is expressed in an anterior cap (J) but later retracts from the pole (K) to form domains in the head lobes of germ rudiments (L). (M and N) Tc-Gcl protein distribution in ovaries. Tc-Gcl (green signal) is found at the nuclear membrane co-localized with a nuclear

envelope protein (insert in M). (O and P) After *Tc-gcl* RNAi, the nuclear lamina staining is reduced. Anterior is to the left in panels A-L; panels A-F are not in the same scale.

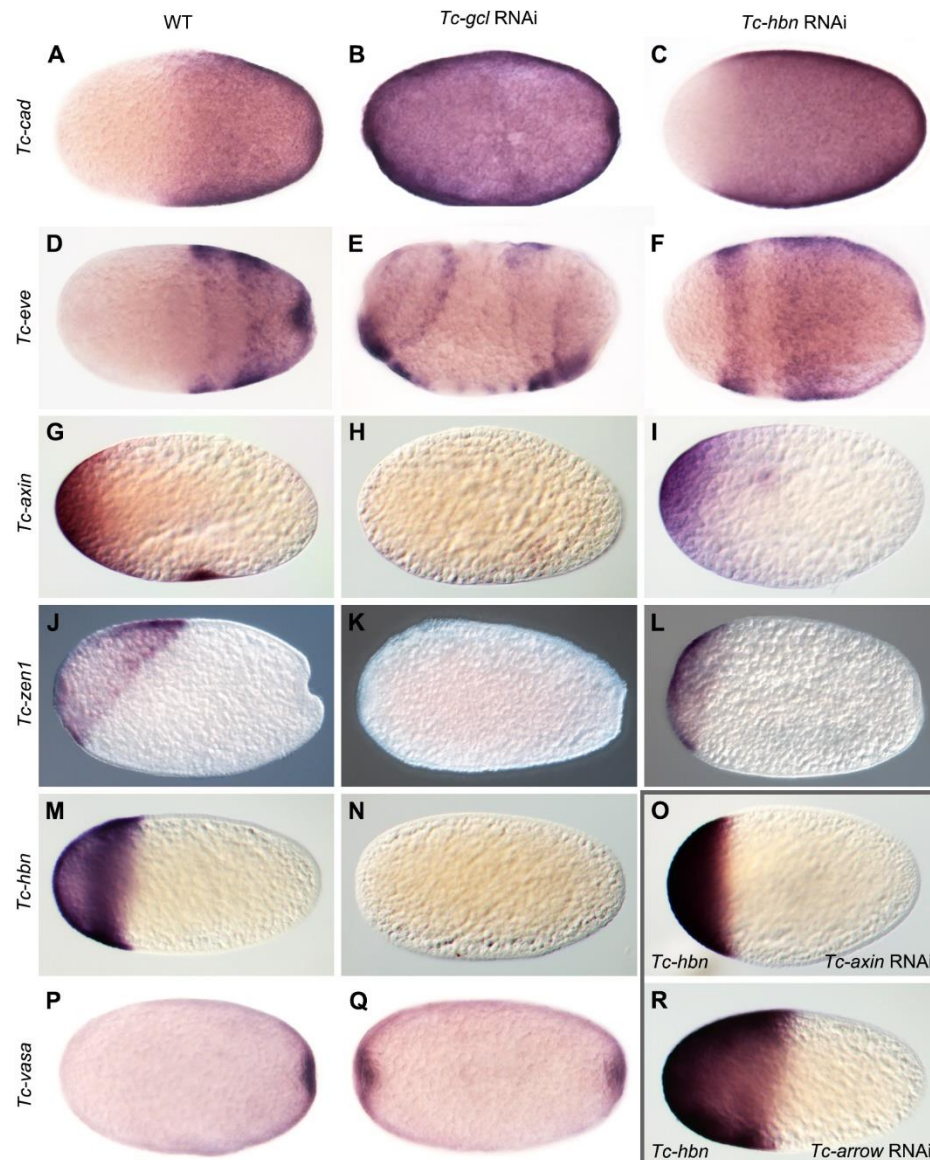


Fig 2. Change of embryo fate map after *Tc-gcl* and *Tc-hbn* RNAi. (A to C) *Tc-cad* mRNA is expressed in the posterior half of WT blastoderm embryos (A) but is ubiquitously distributed after *Tc-gcl* RNAi (B). It is shifted anteriorly after *Tc-hbn* RNAi (C). (D to F) Striped *Tc-eve* mRNA expression at late WT blastoderm embryos (D) is duplicated after *Tc-gcl* RNAi (E) but shifted anteriorly in *Tc-hbn* RNAi (F). (G to I) Maternal *Tc-axin* mRNA at the anterior pole (G) is lost after *Tc-gcl* RNAi (H) but not affected after *Tc-hbn* RNAi (I). (J to L) *Tc-zen1* expression in the serosa (J) is lost after *Tc-gcl* RNAi (K) and reduced upon *Tc-hbn* RNAi (L). (M to O and R) *Tc-hbn* expression at the anterior pole (M) is absent after *Tc-gcl* RNAi (N). In *Tc-axin* RNAi (Wnt derepression) the boundary is shifted towards anterior (O) while it is shifted posteriorly after *Tc-*

arrow RNAi (Wnt repression; R). (P and Q) *Tc-vasa* mRNA expression marking the posterior pit in WT (P) is duplicated after *Tc-gcl*/RNAi (Q).

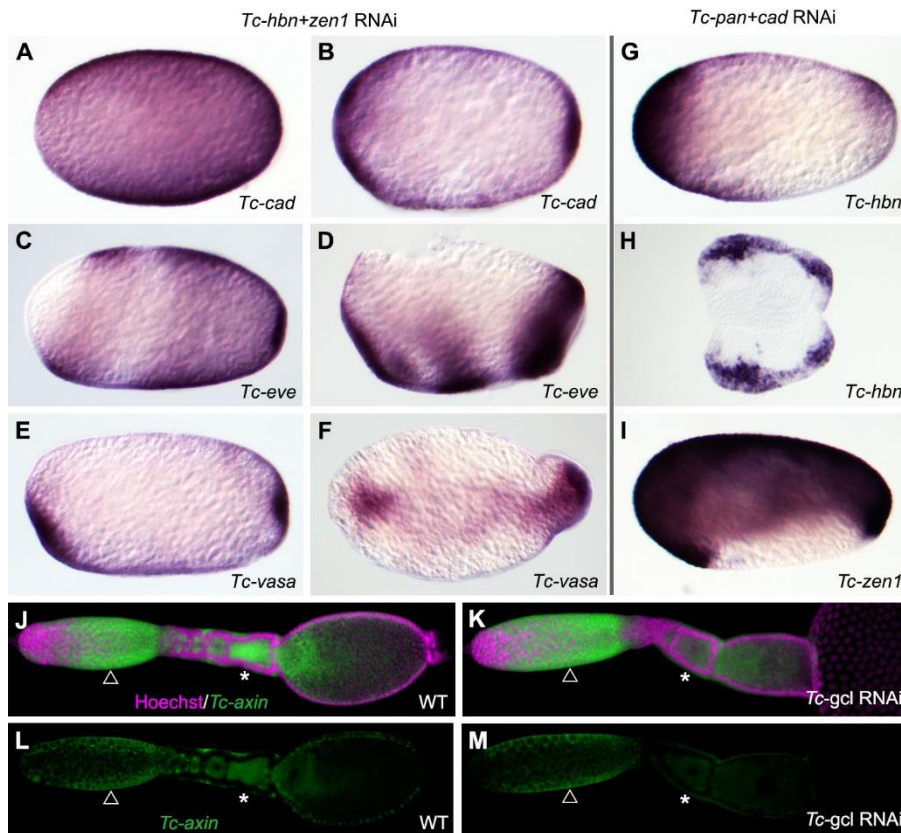


Fig 3. Zygotic genes required for anterior and posterior structures. (A to F) *Tc-hbn+ Tc-zen1* double RNAi leads to mirror image expression of SAZ markers like *Tc-cad* (A,B), *Tc-eve* (C,D) and *Tc-vasa* (E,F). (G to I) Upon *Tc-pan+ Tc-cad* double RNAi, anterior markers become expressed at the posterior pole. *Tc-hbn* mRNA develops an additional posterior domain (G) and marks duplicated posterior head lobes in germ rudiments (H). *Tc-zen1* expression covers both poles and dorsal tissue (I). (J to M) In *Tc-gcl*/RNAi ovaries, *Tc-axin* mRNA remains expressed in nurse cells (compare arrow in J,L with K,M) but is reduced in oocytes (compare stars in J,L with K,M). This indicates that *Tc-axin* transport is affected in *Tc-gcl*/RNAi. Respective WT embryos are shown in Fig1.

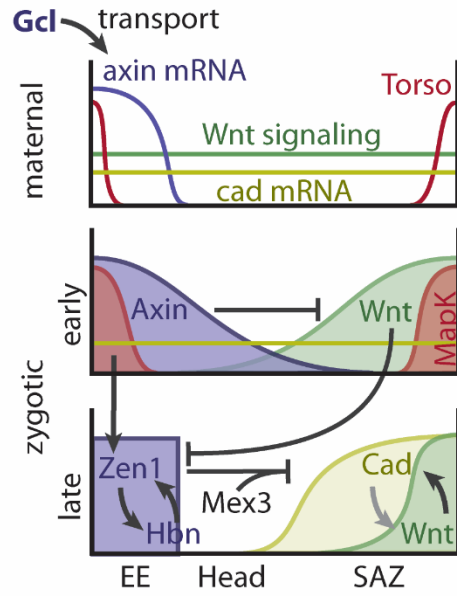


Fig 4. Model for axis formation *Tribolium castaneum*.

See text for details. EE: extraembryonic tissue.

Methods

Beetle strains and husbandry

Beetles were reared under standard conditions (Brown et al., 2009b). For initial validation, the same strains were used as in the iBeetle screen (Schmitt-Engel et al., 2015a). Females of the transgenic line *pig19* (alternative name: *pBA19*) were used for injection. *pig19* is an enhancer trap expressing EGFP in somatic muscles (Lorenzen et al., 2007). Males of the *black* strain (Sokoloff, 1974) were used for mating. For all further experiments, both *pig19* males and females were used. The *ubiVSR-9* line was generated in the *vermillion white* (v^w) genetic background.

Phylogenetic analysis

Phylogenetic tree analysis was performed using MEGA 6 (Tamura et al., 2013) software. Protein sequences of the respective genes were retrieved by Blast analysis from <http://bioinf.uni-greifswald.de/blast/tribolium/blast.php> (*Tribolium*) and NCBI (other species) and aligned in MEGA 6 using the clustalW algorithm. The phylogenetic trees were constructed based on the maximum likelihood method with JTT substitution model and 500 bootstrap tests (Felsenstein, 1985).

Cloning and generation of the *ubiVSR-9* line

All genes required for generating dsRNA and *in situ* probes were cloned into the pJET1.2 vector using cDNA (from 0-72hrs *San Bernadino* (*SB*), wild-type strain embryos). All primers used in this study are listed in Extended Data Table 1.

A plasmid containing the viral suppressor of RNAi (VSR) *CrPV1A* (from Cricket Paralysis virus), was provided by Ronald Van Rij (Radboud Institute for Molecular Life Sciences, Netherlands). The ubiquitously active *Tc-alpha-tubulin1 promoter* (843bp) (Siebert et al., 2008) was amplified via PCR using sequence primers with attached NheI and XhoI restriction sites and inserted together with the VSR coding sequence into the *piggyBac* transposon. *Tribolium* germline transformation was performed as described (Berghammer et al., 2009b) in the v^w genetic background using *Tc-vermillion* as marker.

RNAi

dsRNA synthesis was performed using the Ambion® T7 MEGAscript® kit (Life Technologies, USA) according to manufacturer's instructions. RNA was precipitated using isopropanol. The RNA pellet was dissolved in injection buffer (1.4 mM NaCl, 0.07 mM Na₂HPO₄, 0.03 mM KH₂PO₄, 4 mM KCl, pH 6.8). dsRNA samples were denatured and subsequently allowed to anneal to increase the portion of double stranded RNA.

Pupae, larvae and embryos were injected as described previously (Bucher et al., 2002; Posnien et al., 2009) using the FemtoJet® device (Eppendorf, Germany). Off target effects for *Tc-gcl* and *Tc-hbn* were tested by non-overlapping fragments (see Extended Data Fig. 1). Generally, parental RNAi was performed in late pupal stage if not stated otherwise. dsRNA concentrations used in this study are listed in Extended Data Table 2.

Generation of a Tc-Gcl polyclonal antibody

The N-terminus of Tc-Gcl (amino acids 1-57) was cloned into pET SUMO vector generating a fusion with a His-SUMO tag using the golden gate cloning procedure (Thermo Fischer). The protein was expressed in BL21-DE3 Rosetta cells at 16 °C. Cells were lysed (50 mM TRIS-HCl pH 7.5, 150mM NaCl, 10mM Imidazole) using Fluidizer (mechanical lysis by high pressure-80 psi). The protein was purified via Ni²⁺-chelate affinity chromatography using a gradient with 200mM imidazole in lysis buffer. Dialysis (50mM Tris-HCl pH 7.5, 150mM NaCl) and cleavage of the His-SUMO tag from the Gcl polypeptide was done simultaneously overnight. The His-SUMO tag was removed from the polypeptide via Re-Ni²⁺-chelate affinity chromatography. Size exclusion chromatography (Superdex 30-GE Healthcare) was used to remove the remaining contaminations and the purified polypeptide was stored in phosphate-buffered saline (PBS). All the steps for purification were performed at 4°C (Monecke et al., 2009).

Antibodies were produced in guinea pigs by Eurogentec (Liège, Belgium). The final serum was affinity purified with the Gcl polypeptide. Specificity was confirmed by staining ovaries of wildtype and *Tc-gcl* RNAi embryos. The specific staining at the nuclear lamina was strongly reduced or absent in RNAi embryos (see Fig. 1).

For embryonic stainings, a 1:200 dilution of the primary antibody was used. 1:1000 dilution of HRP-coupled (for bright field stainings) or 555-coupled Alexa Fluor (for fluorescent staining) anti guinea pig antibodies were used as secondary antibodies.

For ovaries stainings, a 1:1000 dilution of the primary antibody was used together with a 1:2000 diluted monoclonal anti-nuclear pore complex protein antibody (clone 414, Sigma) to analyze the localization.

Embryo whole mount *in situ* hybridization

For dechoriation, embryos were washed in 50% bleach twice for 3 minutes. Fixation protocol was performed as described in (Schinko et al., 2009) with the following modifications. For blastoderm embryos 300µl formaldehyde (37 %) and 2 ml PEMS buffer (0.1 M PIPES, 2mM MgCl, 5 mM EGTA, pH 6.9) and 4 ml heptane were used. For germ band embryos the volume of formaldehyde (37%) was reduced from 300µl to 180µl. Fixed embryos were stored in methanol at -20°C. Digoxigenin-UTP (DIG) or Fluorescein-UTP (FLUO) probes were produced according to the manufacturer's instructions (Roche, Germany). *In situ* hybridization (ISH) was performed using Nitro blue tetrazolium (NBT) and 5-Bromo-4-chloro-3-indolyl phosphate (BCIP) as described previously (Oberhofer et al., 2014b; Schinko et al., 2009; Siemanowski et al., 2015).

Ovary WMISH

Ovary dissection and WMISH were performed as described by (Trauner and Buning, 2007)(Bäumer et al., 2011). Probe size was reduced to 300bp using the carbonation method. Fast Red tablets from Roche were used for staining according to manufacturer's instruction.

Ovary antibody staining

Ovaries were dissected and the muscle sheath removed manually. Fixed ovaries were rinsed in PBT, then washed 3 times with PBT/BSA (1x PBS, 1% BSA, 0.5% Triton X-100) for 15 minutes on a rotator at room temperature. After overnight incubation with the primary antibody (diluted in PBT/BSA) at 4 °C, ovaries were washed with PBT/BSA. Secondary antibody (diluted in PBT/BSA) was either incubated at room temperature for 4hrs or overnight at 4 °C. Ovaries were washed with PBT/BSA and mounted on a slide in a 1:1 mixture of glycerol and 1x PBS with coverslip and putty as spacers (Bäumer et al., 2011).

Image processing

Image acquisition was performed with a Zeiss Axioplan 2 microscope with DIC filter, 24bit color and RGB setting, or with a ZEISS laser scanning microscope (LSM510). Stacks were processed with Z-projection method of ImageJ software (Version 1.47, rsbweb.nih.gov/ij/disclaimer.html). Figures were prepared using Adobe Photoshop (CS6) and Adobe Illustrator (CS6).

Real-time qPCR

RNA was extracted from 0-4hrs old RNAi and WT eggs; RNAi ovaries and WT ovaries were used for extraction of total RNA using Trizol (Ambion) according to (Schmittgen and Livak, 2008). Isolated RNA was treated with TURBO™ DNase to remove any DNA contamination. Later, DNase Inactivation Reagent was used to remove the TURBO™ DNase and divalent cations as described in the ‘TURBO DNA-free™ Kit (Ambion). ; AM1907’ manual.

The RNA concentration was measured using the NanoDrop 1000 Spectrophotometer (Thermo Scientific™, USA). 1µg for embryos and 500 ng for ovaries was used for the first strand cDNA synthesis according to the manufacturer’s instructions. (SuperScript® III, Thermo Scientific™, USA).

qRT PCR was performed in CFX96™ Real-Time PCR System (Bio-Rad Laboratories, Hercules, CA, USA) with HOT FIREpol® EvaGreen® qPCR Mix Plus (ROX) (Solis BioDyne, Tartu, Estland) according to the manual. Three biological, three technical replicates and no-RT (without reverse transcriptase) and no template control were performed. Primer efficiency and melting curve analysis were performed for all primers including the internal control for RPS3 and RPS18.3. Relative fold change expression between WT and RNAi tissues were calculated by double delta Ct method with RPS18.3 as reference genes (Livak and Schmittgen, 2001). Welch Two Sample t-test was performed to assess significance of differential gene expression.

Extended Data

Maternal *germ cell-less* and zygotic *homeobrain* and *zen1* in axis formation

Salim Ansari*, Nicole Troelenberg*, Julia Ulrich*, Van Anh Dao, Tobias Richter, Gregor Bucher#,
Martin Klingler

Figs. S1 to S8

Tables S1 to S2

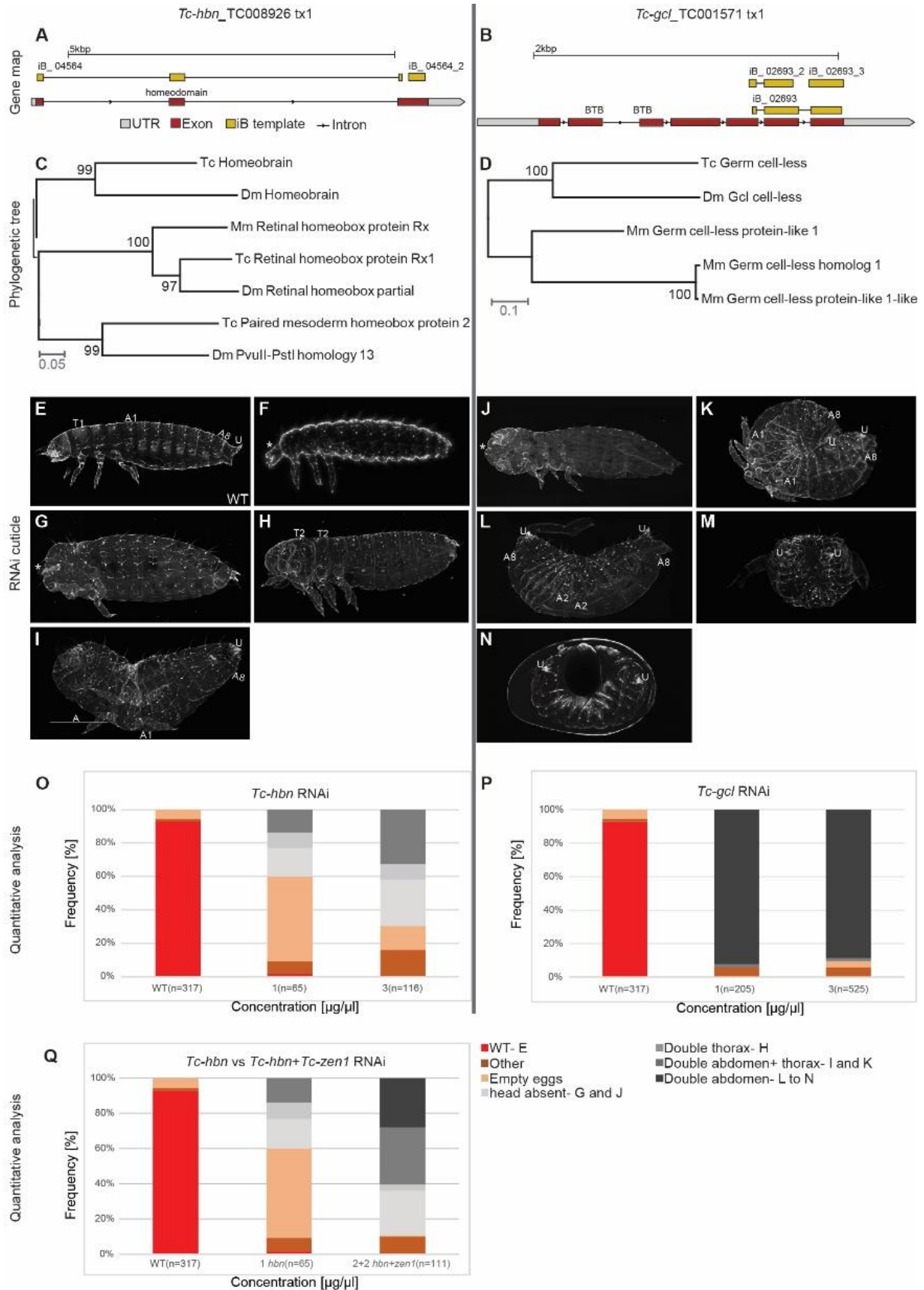


Fig. S1 *Tc-hbn* and *Tc-gcl*/sequence analysis and quantification of RNAi effects.

(A and B) *Tc-hbn* (A) and *Tc-gcl* (B) gene structures with iBeetle fragments used for RNAi experiments. (C and D) Phylogenetic trees of *Tc-hbn* (C) and *Tc-gcl* (D) based on maximum likelihood with bootstrap scores at the nodes. (E) Lateral view of WT L1 cuticle. (F to I) Phenotypic series of *Tc-hbn* RNAi cuticles from weak to strong: Anterior segments (*) are missing (F), the head (*) is fused with the thorax (G), partial duplication of thoracic segments (H) and fused thoracic segments with incomplete double abdomen (I). (J to N) Phenotypic series after *Tc-gcl*/RNAi from weak to strong: Head segments (*) disturbed (J), mirror symmetric double abdomen and urogomphi (U) with partial duplication of thoracic segments (K), two incomplete double abdomina (L), irregularly segmented incomplete double abdomen (M) and incomplete double abdomen with dorsal opening (N). (O to Q) Quantitation of RNAi phenotype classes using different concentrations of maternally injected dsRNA. *Tc-hbn* RNAi phenotype strength increased with concentration (O) but did not reach the penetrance and expressivity of *Tc-gcl*/RNAi (P). Double RNAi targeting *Tc-hbn*+ *Tc-zen1* increased both penetrance and expressivity (Q) but did not reach *Tc-gcl*/RNAi.

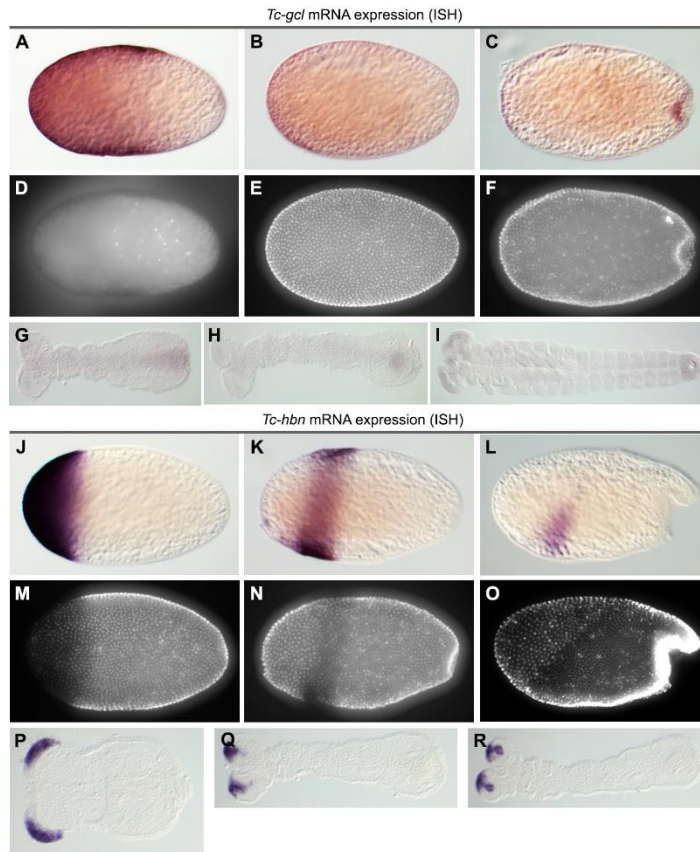


Fig. S2. *Tc-gcl* and *Tc-hbn* mRNA expression.

(A to C) RNA *in situ* hybridization of *Tc-gcl* in unfertilized/freshly laid eggs (A), uniform (B) and differentiated blastoderm (C) stages. (D to F) DAPI staining of respective embryos. (G to I) RNA *in situ* hybridization of *Tc-gcl* in early (G) and elongating (H) and fully elongated germ band embryos (I). The posterior expression is similar to *Tc-vasa* expression. (J to L) RNA *in situ* hybridization of *Tc-hbn* at uniform blastoderm (J), differentiated blastoderm (K) and gastrulation (L) stages. (M to O) DAPI staining of respective embryos. (P to R) *Tc-hbn* expression at germ rudiment (P), and elongating germ band stages (Q and R).

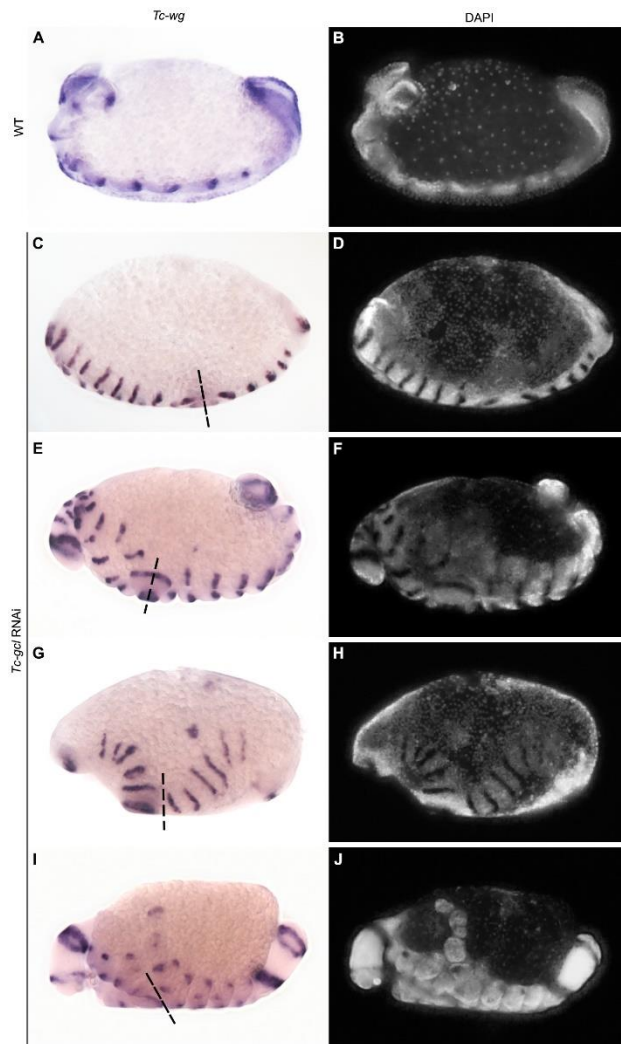


Fig. S3. *Tc-wg* expression in WT and *Tc-gcl*/RNAi embryos.

(A) *Tc-wg* expression in trunk and head segments in a WT germ band. Anterior is to the left. (C,E,G,I) Mirror image embryos that develop from two autonomous SAZ. The symmetry axis is indicated with a hatched bar. We do not know whether anterior is left or right. (B,D,F,H,J) DAPI stainings of the respective embryos. Morphogenetic movements of *gcl*/RNAi embryos are quite abnormal, probably due to missing extracellular membrane material (serosa is missing, amnion reduced to its dorsal component).

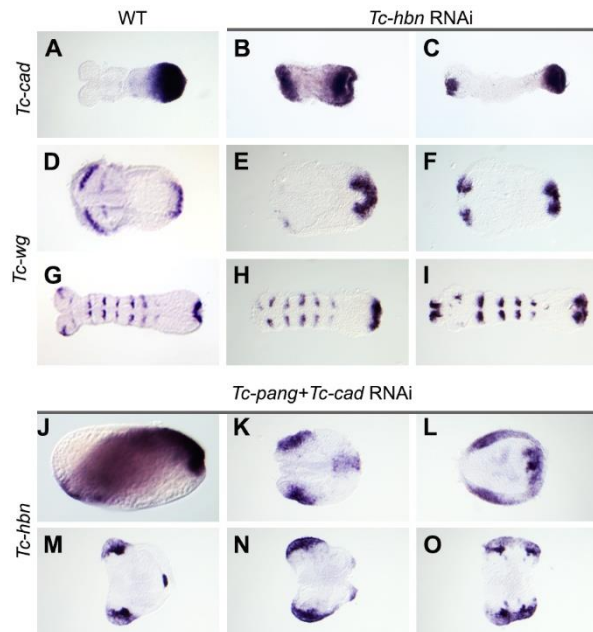


Fig. S4. Double abdomen in *Tc-hbn* embryos and double heads in *Tc-pang + Tc-cad* double RNAi

(A to C) *Tc-cad* expression in WT (A) and *Tc-hbn* RNAi embryos, where an anterior duplication of *Tc-cad* expression develops during early elongation (B,C). Anterior is to the left in all panels. (D to I) *Tc-wg* expression in WT (D and G) and *Tc-hbn* RNAi embryos, where the head domain is absent (E and H) or replaced with a putatively duplicated posterior domain (F and I). (J to O) *Tc-pang + Tc-cad* double RNAi leads to posterior duplication of *Tc-hbn* expression. A posterior domain develops in the blastoderm (J). Germ rudiments show the expected bilateral *Tc-hbn* expression in the anterior head lobes and additional expression at the posterior region (K to M) and duplicated head lobe anlagen (N,O). Anterior is to the left wherever discernible.

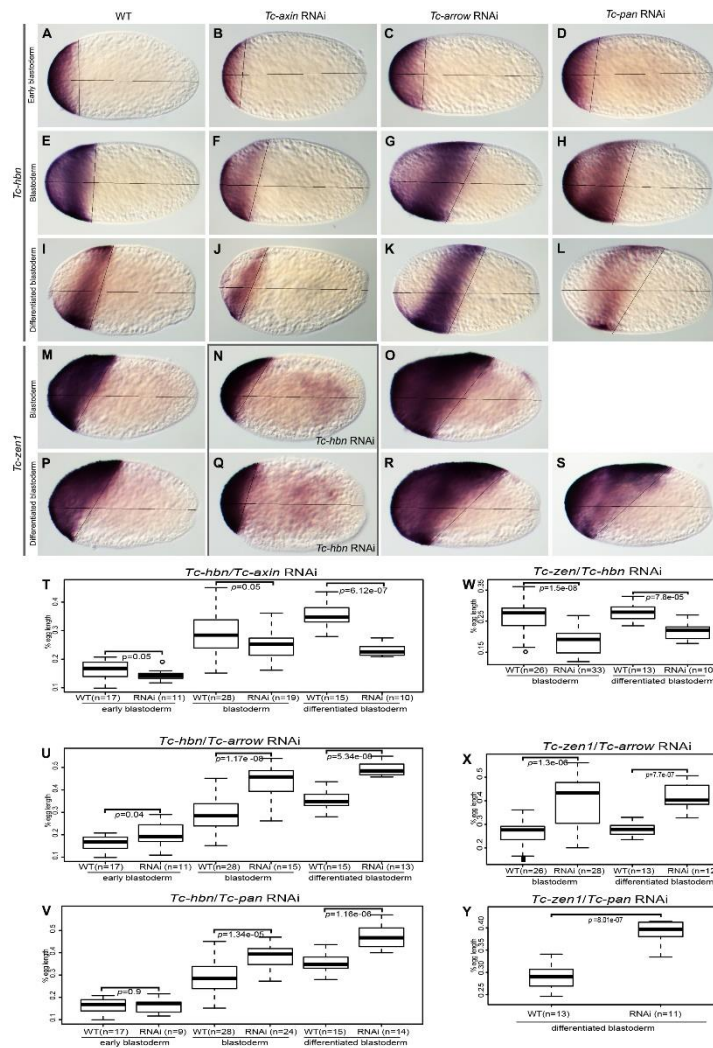


Fig. S5. Wnt signalling determines the boundary of *Tc-hbn* and *Tc-zen1* expression.

(A, E and I) Expression of *Tc-hbn* in WT embryos. Anterior is to the left in all panels. (B, F and J) *Tc-hbn* expression boundary is shifted anteriorly in Wnt derepression after *Tc-axin* RNAi. See quantitative analysis in (T). (C, G, H, K and L) *Tc-hbn* expression boundary is in most cases shifted posteriorly after Wnt repression in *Tc-arrow* (C, G and K) or *Tc-pan* RNAi embryos (H and L). An exception are early *Tc-pan* RNAi blastoderm embryos, where no shift was detected. The shifts were quantified (U and V). (M and P) *Tc-zen1* expression in WT. (N and Q) *Tc-zen1* expression was shifted anteriorly after *Tc-hbn* RNAi. See quantification in (W). (O, R and S) *Tc-zen1* expression was shifted posteriorly in *Tc-arrow* RNAi (O and R) and *Tc-pan* RNAi (S). See quantification in (X and Y). Due to the later onset of *Tc-zen1* expression, the early blastoderm

could not be scored. The intersection of the lines representing the ap-axis and the posterior expression boundary was used to calculate the position in % egg length.

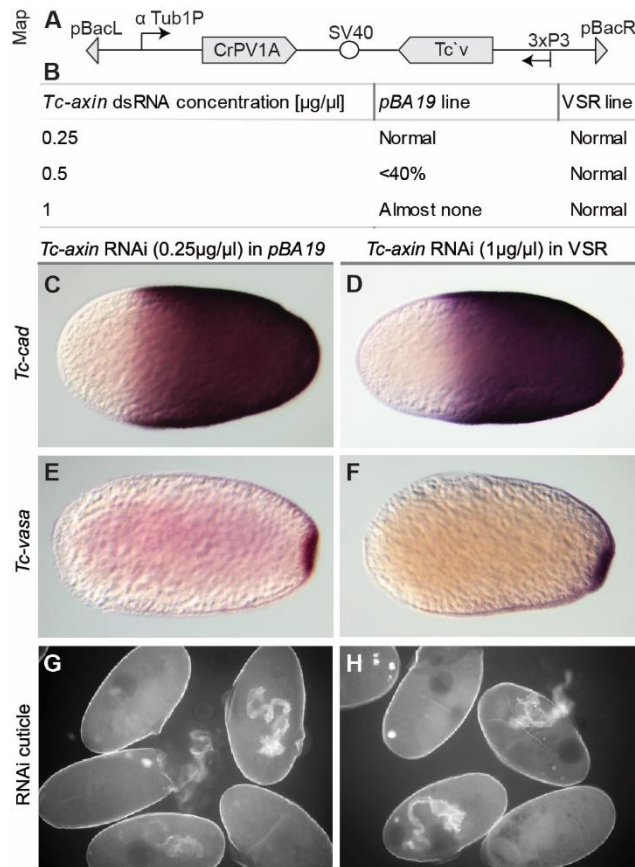


Fig. S6. Sterility of *Tc-axin* RNAi rescued in the *ubiVSR-9* line.

(A) Schematic of 8.1 kbp pBac transposon carrying the CrPV1A RNAi inhibitor under control of the *alpha-tubulin* promoter and *Tc-vermillion* under the control of the *3XP3* promoter. (B) Semi-quantitative analysis of fecundity of females after injection of different concentrations of *Tc-axin* dsRNA compared to buffer injection in both, the strain used in this work (*pig19*) and the *ubiVSR-9* line. (C and D) *Tc-cad* mRNA expression is affected in a similar way after *Tc-axin* RNAi in *pig19* and *ubiVSR-9* despite 4X higher dsRNA concentration. (E and F) Likewise, *Tc-vasa* mRNA expression remained unchanged after *Tc-axin* RNAi. (G and H) *Tc-axin* RNAi causes similar empty egg phenotypes in both strains.

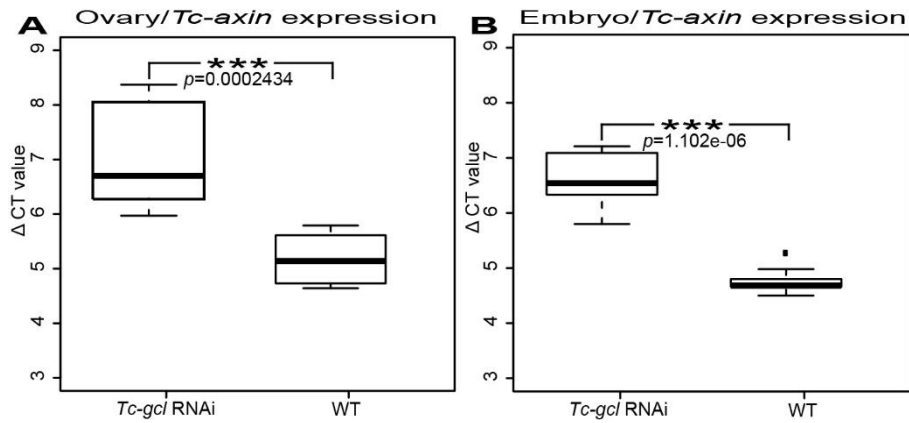


Fig. S7 *Tc-axin* expression is reduced 3.55 fold upon *Tc-gcl*/RNAi.

(A) Box plot shows that the Δ CT value (*Tc-axin*CT-RPS18.3 CT) is increased from 5.14 to 7 in ovary tissues. (B) Box plot shows that the Δ CT value (*Tc-axin*CT-RPS18.3 CT) is increased from 4.76 to 6.58 in embryonic tissues (0-4hrs). Hence, after *Tc-gcl*/RNAi the fold change expression was -3.6 ($-1/2^{-\Delta\Delta Ct} = -1/0.275$) for ovary and -3.5 ($-1/2^{-\Delta\Delta Ct} = -1/0.283$) for freshly laid eggs (0-4 h). Primer efficiency of *Tc-axin* was 103.2% and for ribosomal protein subunit 18.3 (RPS18.3) 90.1%. RPS18.3 was used as reference gene.

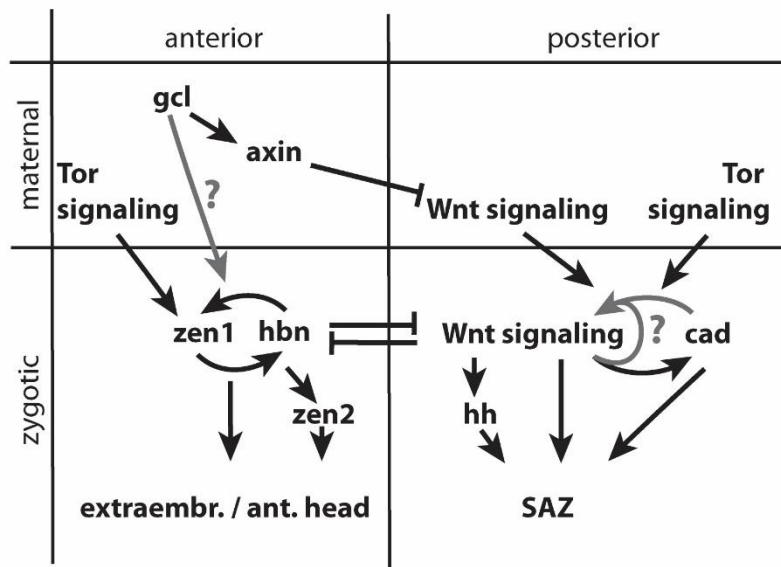


Fig. S8 Gene regulatory model of AP axis formation

Tc-germ cell-less (Tc-gcl) is required for transport of maternal *Tc-axin* into the oocyte, where *Tc-axin* is localized to represses anterior Wnt signalling (Fu et al., 2012b). *Tc-gcl* contributes to the expression of zygotic *Tc-zen1* and *Tc-homeobrain (Tc-hbn)* at the anterior pole. Torso signalling activates *Tc-zen1* but not *Tc-hbn* (data analyzed from 30) while Wnt signalling is determining their posterior boundaries (Fu et al., 2012b). *Tc-zen1* and *Tc-hbn* activate each other and target genes like *Tc-zen2*, contributing to the development of extraembryonic tissues and the head (van der Zee et al., 2005). In addition, they repress zygotic expression of *Tc-caudal (Tc-cad)*, whose activity is in addition translationally repressed by *Tc-zen2* and *Tc-mex3* (Schoppmeier et al., 2009b). Posterior *Tc-cad* activity delimits the region of sequential segment formation by the segment addition zone (SAZ) (Copf et al., 2004; El-Sherif et al., 2014).

Segmentation via the SAZ requires Torso and Wnt signalling and *Tc-cad* expression (Bolognesi et al., 2008; Copf et al., 2004; Schoppmeier and Schröder, 2005). Wnt signalling activates *Tc-cad* expression and Hh signalling in the SAZ (Oberhofer et al., 2014b). SAZ Wnt signalling is maintained by an autoregulatory loop, which could be direct or indirect via *Tc-cad* like in spiders (Oberhofer et al., 2014b; Schönauer et al., 2016).

Tables S1 and S2

Table S1: List of primers and dsRNA concentrations.

Supplementary Table 1: List of primers.

<i>Tc-gene</i> primer	Sequence	Purpose
<i>gcl</i> _Fw	ATGGGGCTGATTTACTCCAGTAG	full length <i>gcl</i>
<i>gcl</i> _Rv	TTAGGAGACAGTTTGCACGACC	full length <i>gcl</i>
<i>gcl</i> _N-ter_linker_Fw	CCAGGTCTCATGGTATGGGGCTGATTTACTCC	N-terminal <i>gcl</i>
<i>gcl</i> _N-ter_linker_Rv	GGGGGTCTCCTCGAGTCATGCAGTGCTCACTAG	N-terminal <i>gcl</i>
<i>gcl</i> _iB_02693_Fw	TCAACCAAACGACGATAAGG	dsRNA (iB fragment)
<i>gcl</i> _iB_02693_Rv	TGCACGACCTTTCCTGATT	dsRNA (iB fragment)
<i>hbn</i> _iB_04564_Fw	CGTCTACAGCATCGACCAGA	dsRNA (iB fragment)
<i>hbn</i> _iB_04564_Rv	CCTTTTCACGCTTTCTCCAC	dsRNA (iB fragment)
<i>pan</i> _iB_07007_Fw	TGTACGTGTACGCAGTGACG	dsRNA (iB fragment)
<i>pan</i> _iB_07007_Rv	CCCATGTTGAACGAAGAGGTG	dsRNA (iB fragment)
<i>axin</i> _qPCR_EE_Fw2	CAGCCAGTGCAGTACGG	qPCR Primer for <i>axin</i>
<i>axin</i> _qPCR_EE_Rv2	TGCTTCGGTATATCAAACCAGC	qPCR Primer for <i>axin</i>
RPS3.3_Fw	AGGGTGTGCTGGGAATTAAG	reference gene for qRT-PCR
RPS3.3_Rv	GGGTAGGCAGGCAAAATCTC	reference gene for qRT-PCR
RPS18.3_Fw	AACCCTCGCCAATACAAAATC	reference gene for qRT-PCR
RPS18.3_Rv	CTTCATGCGTTCCAAATCCTC	reference gene for qRT-PCR
CrPV_i_Fw	ACAGGTACCATGCTTTTTCAACAACAACAACAAC	CrPV1A with <i>Acc65</i> I
CrPV_i_Rv	ACAGCGCCGCTTGAAGGCTCTGCATTTCATTACT	CrPV1A with <i>Not</i> I
tubulin_Fw	CATCTCGAGACCTCACACTTGCCGTAATGGAG	α Tubulin1 with <i>Xho</i> I
tubulin_Rv	GTATCGCTAGCTTGGTAGTTGAGTTTACAAATTAC	α Tubulin1 with <i>Nhe</i> I

Table S2 List of dsRNA concentrations.

Pupal RNAi	
Single RNAi	
<i>Tc-gene</i>	dsRNA Concentration [$\mu\text{g}/\mu\text{l}$]
<i>gcl</i>	3
<i>hbn</i>	3
<i>zen1</i>	3
<i>arrow</i>	3
<i>pan</i>	3
<i>torso</i>	3
<i>axin</i>	0.25
Double RNAi	
<i>Tc-gene</i>	dsRNA Concentration [$\mu\text{g}/\mu\text{l}$]
<i>pan+hbn</i>	1.5+1.5
<i>pan+zen1</i>	1.5+1.5
<i>axin+hbn</i>	0.25+1.5
<i>axin+zen1</i>	0.25+1.5
<i>axin+pan</i>	0.25+1.5
<i>axin+zen1</i>	0.25+2
<i>axin+zen2</i>	0.25+2
<i>hbn+zen1</i>	2+2
<i>hbn+zen2</i>	2+2
<i>pan+cad</i>	3+3
<i>pan+torso</i>	3+3
<i>arrow+Tcad</i>	3+3
<i>arrow+torso</i>	3+3
Larval RNAi	<i>Tc-gcl</i> RNAi: 1 and $3\mu\text{g}/\mu\text{l}$, <i>Tc-hbn</i> RNAi: $3\mu\text{g}/\mu\text{l}$.
Embryonic RNAi	<i>Tc-gcl</i> RNAi with $1\mu\text{g}/\mu\text{l}$.

5 Discussion

5.1 Part I: The iBeetle screen

The classical genetic screen by Christiane Nüsslein-Volhard and Eric Wieschaus led to the discovery of the components required for early embryonic development of *Drosophila melanogaster*. Since then *Drosophila* serves as an excellent model organism to study insect development. However, *Drosophila* represent a derived situation e.g. an involuted larval head, reduced extra-embryonic tissues, as well as absence of some processes and tissues like stink glands. These drawbacks are planned to be addressed by a genome-wide RNAi screening in *Tribolium castaneum* (iBeetle screen) (Schmitt-Engel et al., 2015a). The aim of this project was to find, screen and confirm novel head patterning genes from the preliminary gene list of the second phase screening (of which I was a part).

5.1.1 The iBeetle screen- a new way to identify novel genes for many insect biological processes

The iBeetle screen serves as an efficient and reliable way to identify the genes which regulate biological processes. This has been demonstrated by successful completion of the first screening phase which led to identification of many interesting candidates which was not possible before (Schmitt-Engel et al., 2015c). For example, it revealed novel factors with important functions in the development of *Tribolium* as exemplified by *Tc-FoxQ2* (a gene discovered during the second phase) a novel component involved in the development of the labrum (Kitzmann et al., 2017 accepted in Development). However, a function for the *Drosophila* ortholog (*Dm-FoxQ*) have not been studied in the head development. Another example is the discovery of a new gene (TC010650) involved in cell adhesion. Knockdown

of this gene results in a wing blister (dissociation of the two epithelial sheets of the wing) phenotype. The *Drosophila* ortholog produced a similar wing blister phenotype when the ortholog was knocked down via transgenic RNAi (Schmitt-Engel et al., 2015). iBeetle is the only ongoing genome-wide RNAi screen in an insect species other than *Drosophila melanogaster*. Moreover, iBeetle base and Flybase both complement each other and provide phenotypic as well as genetic information that provides insight into the role of individual genes in insect biology (Dönitz et al., 2015).

iBeetle is an ongoing genome-wide RNAi screening and it is planned to cover the whole genome by the end of 2019. The selection of knockdown targets with iBeetle fragments (dsRNA) was almost random in the first screening phase (except some bias towards highly expressed genes and conserved genes) (Schmitt-Engel et al., 2015). However, in the second phase genes were pre-selected genes based on their GO terms (e.g. transcriptional factor, developmental genes etc.) to enrich for more promising genes. The main focus was to achieve the continuity in the technical performance and annotation across the screeners.

Success rates (successful recognition) of positive and negative controls were similar in both phase and were quite high- positive control 93% (in the first phase), 90% (in the second phase) and negative control 97% (in the first phase), 93% (in the second phase) except being the single pass screening project. This means that a maximum of 10% of phenotypes were missed during the annotation which demonstrates the efficient screening (from injection to annotation) by all screeners and we were able to achieve the continuity in technical performance and annotation. However, the rate of reproducibility varies depending on the phenotypic class and strength. For example, 95% of highly penetrant phenotypes with simple readout (e.g. lethality) were recognized but the reproducibility of embryonic defects was lower than 60%. In the case of my rescreening (to confirm the reproducibility and specificity of selected head patterning genes), 36% candidates were successfully reproduced from the '>50% penetrance and <50% hatch rate group'. However, not a single candidate

from 10 genes of '30-50% penetrance and 0-100% hatch rate group' was reproduced. Only 2.6 % of the candidate (9 from 340 hits) were finally confirmed which shows the high rate of unspecific head phenotypes. In summary, strong phenotypes with high penetrance have a higher success rate in the reproduction of the phenotype (Schmitt-Engel et al., 2015a).

5.1.1.1 Reasons for false positives

We annotated potentially unspecific phenotypes rather than risking to miss an interesting phenotype as a rule, in case of doubt. In this context, phenotypes in the low penetrance groups - less than 30% or 30-50% - reproduced much less frequently. Further, off-targets and strain specificity were main reasons that contributed in the low reproducibility. For example, during the rescreening of '>50% penetrance group', the off target score was 9% but this increased significantly to 20% during the rescreening of '30-50% penetrance group'. Another category that failed to reproduce was the experimental replicate. For example, 14% of '>50% penetrance group' and 30% of '30-50% penetrance group' failed to reproduce. This means that a large group of phenotypes were reproduced with same iBeetle fragments in same strain but neither with NOFs nor in the SB strain. Further, about 10.6% of all screened genes were annotated with head defects (340 out of 3,200) which is a high portion. This all suggest that head tagma was much more prone to show defects than other tagmas in the iBeetle screen. This could be because of the complex morphology of the head and sensitivity of the genetic background of strain. Indeed, the pBA19 (screening) strain has the tendency to produce unspecific head defects as a background. This indicates that we were screening in a sensitized background (Schmitt-Engel and Gregor Bucher personal communication). One of the molecular reasons could be that the knockdown of housekeeping genes produce pleiotropic defects (which shows the unspecific head defects with low penetrance) because of the abortion of embryogenesis at different stages. In summary, off-targets and strain specific effects were the main reasons for false positive and unspecific head related phenotypes.

5.1.1.2 Reasons for false negatives

It is difficult to assess how many genes were missed or will be missed in the iBeetle screen. In this regard, Dr. Janna Siemanowski reanalysed those cuticle slides which had larvae on the slides but were not annotated for phenotypes (because of less or no hatched animals). She found four genes out of 132 candidates which shows a head bristle patterns related phenotypes. This demonstrate that there are significant chances that screeners may have missed the subtle phenotypes (e.g. head bristle/setae patterns) which were difficult to analyse. In addition, there are more factors that could hamper the identification of head patterning genes. For example,

1. Redundant genes: When two or more genes contribute collectively to a phenotype and loss of one gene function would be compensated by other genes. The iBeetle fragments (dsRNA) generally target only a single gene. In some cases, the roles of redundant genes have been analysed (for example *Knirps* gene group in *Drosophila* (Chen et al., 1998). However, a systematic test of redundancy is not possible in a genome-wide screening analysis.

2. Genes which cause pleiotropic defects: A gene could have more than one function and be involved in more than one process. The overall phenotype of the knockdown animal might make it difficult to recognize a specific head defect among many other defects and will likely be considered as an unspecific head phenotype and could eventually be missed during screening.

3. A particular gene may be required at an earlier stage of development in an essential processes. When the knockdown of these genes have an early lethal phenotype or affect egg production that it makes it impossible to study the later function of these genes. For example, knockdown of *Tc-axin* with 1µg/µl dsRNA or higher concentration causes strong sterility and hence prevents the study of *Tc-axin* function in head development (Fu et al., 2012c).

4. The output of reverse genetic screens depends on the quality of the gene annotation. For example, splice variants can present a problem: AUGUSTUS (OGS3) predicts approximately 16,000 official genes for *Tribolium castaneum* based on its genome and RNA-seq data. However, it is possible that predictions of certain splice variants are inaccurate or that a gene codes for several transcripts that will be missed in the official gene list and hence will not be targeted for knockdown. For example, *Tc-chitin synthases 1* (*Tc-chs1*) gene is required for cuticular chitin and all moulting stages (larval-larval, larval-pupal and pupal-adult). Interestingly, the splice variant *8a* of *Tc-chs1* is involved in all moults but *8b* splice variant in only pupal-adult moult (Arakane et al., 2005).

5. Efficiency of the gene knockdown: Highly expressed genes may not be sufficiently knocked down with the standard concentration of dsRNA used in the screen. Indeed, 16% genes ($n=98$) exhibit the stronger phenotypes after RNAi with 3µg/µl compare to 1 µg/µl dsRNA in the first phase screen (Schmitt-Engel et al., 2015). Hence, it could be possible that we have missed the subtle phenotypes because of the incomplete knockdown. qPCR controls were not performed to measure the efficiency of knockdown since this would have required a lot time and labour.

5.1.1.3 Results of the iBeetle project posed the following new questions to be answered in the future

1. Lost orthologs: Around 13% of the screened genes of the first phase do not have orthologs in *Drosophila* (Schmitt-Engel et al., 2015). The role of these genes needs to be studied in detail and their importance in insect development investigated. As illustrated by TC007939 which does not have orthologs in *Drosophila* but potentially plays an important role in the head development.

2. Empty egg screen: Knockdown of 14% of the genes (450 out of 3,200) resulted in the empty eggs phenotype (penetrance >50%) during the second phase. This could be because

the loss of housekeeping genes or of genes specifically involved in early embryogenesis. For example, knockdown of the axis formation genes *T-axin*, *Tc-dorsal*, *Tc-dpp* or the segmentation genes *Tc-cad* and *Tc-otd* produce the empty egg phenotype. An “empty egg” rescreen of those candidates found during the second phase screening might reveal interesting phenotypes and provide insights into embryogenesis (by discovering new axis polarity or segmentation genes).

3. “No egg” phenotype: Knockdown of 19% of the genes (600 out of 3,200) caused the cessation of egg production during the second phase. This means that no eggs were recovered for further analysis. The ovary phenotype was divided into subclasses. For example, 9% of the ovary phenotype did not produce a morphologically identifiable phenotype (Personal communication with Prof. Gregor Bucher). It will be interesting to find out the molecular reasons behind the cessation of egg production for this subclass. 27% of ovary phenotypes were annotated as starvation phenotype which results in degeneration of fat body and ovaries and eventually death of adults (Personal communication with Prof. Gregor Bucher). This subclass of genes probably interferes with metabolic processes. It would be useful to rescue the maternal RNAi in order to study the embryonic defects. For that purpose, misexpression of an RNAi inhibitor can be used to overcome the sterility problem and reveal the phenotype. For example, a VSR transgenic line (made by Dr. Julia Ulrich) was able to successfully rescue the sterility problem after *Tc-axin* RNAi (See The Gcl project).

In summary, the iBeetle screen is the only Genome-wide screen of insect besides *Drosophila* and is expected to contribute to the identification of novel factors and bridging the knowledge gap of insect biology with respect to embryogenesis, metamorphosis and development. In addition it can also serve as a platform for performing mini-screens (for few hundreds genes) in *Tribolium* with respect to other processes. This is mainly because of the commercial availability of dsRNA and affordable prices (approximately 10€) for each

dsRNA fragment. For instance, screening of all *Tribolium castaneum*'s transcription factors which is predicted to be approximately 753 genes would cost 7,530€. This mini-screening can be achieved in 7.5 weeks for simple readout or 12.5 weeks in case of complex readout by a screener (Personal communication with Prof. Gregor Bucher).

5.1.2 Lesson from the rescreening

AUGUSTUS predicts approximately 16,000 genes in *Tribolium castaneum* and approximately 3,200 genes were screened during the second phase. During the selection phase of rescreening, I found twenty genes which were reported to be involved in the head development already (list of these genes is in Table 7.1 of the appendix). This shows the success of the iBeetle project as well as the right approach for selection of candidate genes. At the end of rescreening, I found eight candidate genes that were involved in head patterning. Rescreening of these putative candidates turned out to be essential to eliminate unspecific candidates. My approach of rescreening was not to miss any potential candidates. Therefore, I included the candidates from 'low penetrance group 30-50%' despite the fact that low penetrance phenotypes have low reproducibility (Schmitt-Engel et al., 2015c). However, at the end of rescreening, not a single 'final candidate' was from this 'low penetrance group'. When time and resources are limited these low penetrance candidates may be excluded from a rescreen as the probability of losing a valuable candidate appears to be low.

Similarly, there was also no impact of using two different concentrations (1µg/µl and 3µg/µl) during the rescreening on the final number of candidates. In some studies, over 80% knockdown efficiency has been achieved with use of 1µg/µl dsRNA injection (Miller et al., 2012; Oberhofer et al., 2014b). This indicates that injections of 1µg/µl dsRNA are efficient enough to knockdown any genes. However, injection with higher concentrations could increase the phenotypic strength in some cases (as mentioned above) but can also lead to

lethality or prevent the cuticle secretion for longer periods (which will make impossible to analyze the epidermal phenotype).

5.1.3 Prioritization of the final candidates for detailed analysis

The expression patterns of selected candidates were analysed to further narrow down the final number of candidates. Based on only the expression pattern, I would choose TC010832 and TC005276 because these genes have a specific expression in the central nervous system which corresponds to their phenotype as well. However, this is not really a strict criterion because there are genes which are expressed and work exclusively in the head (e.g. *Tc-six3*, *Tc-rx*, *Tc-cap-n-collar* (Kittelman, 2012; Posnien et al., 2011) while others do not show exclusively localized expression but still play role in the head development. Moreover, I looked for the degree of conservation of these final candidates with their orthologs in terms of the phenotypic information, the putative function and the expression pattern.

TC031158: The *Drosophila* ortholog *Dm-CG7466* is expressed predominantly in the CNS, the trachea and the carcass at the larval stage. However, functional and phenotypic data are not available (Flybase: <http://flybase.org/reports/FBgn0031981.html>). Interestingly, *Mm-megf8* (mouse ortholog) is involved in left-right patterning, which is a feature of vertebrates but not insects. However, no head related phenotypes were observed (Zhang et al., 2009). Moreover, mutation in the human ortholog caused carpenter syndrome 2 that is associated with left-right patterning (Twiggy et al., 2012). Absence of functional data in insects and the importance of orthologs in vertebrates make TC031158 a very interesting candidate for future study.

TC009940: Both TC009940 and its *Drosophila* ortholog *protein kinase D* are expressed ubiquitously during late stages of embryonic development. *Dm-protein kinase D* is involved in glucose metabolism and regulation of actin dynamics but no phenotypic information is

available (Flybase: <http://flybase.org/reports/FBgn0038603.html>). *Mm-protein kinase D3* is more closely related to TC009940 than *Mm-protein kinase D1* and *Mm-protein kinase D2* paralogs (Figure 4.10). *Mm-protein kinase D3* is expressed in heart, nasal process and limb buds in early development but later transcripts are ubiquitously distributed (Ellwanger et al., 2008). Mutations in *Mm-protein kinase D3* leads to modulation of microtubule dynamics that affects the cell cycle (Zhang et al., 2016). Since TC009940 and its *Drosophila* and mouse orthologs share the similar expression pattern, putative function of TC009940 could be also regulation of actin dynamics like its orthologs. TC009940 is an interesting candidate because neither *Dm-protein kinase D* nor *Mm-protein kinase D3* are reported to play any role in head development.

TC004152: *Dm*-CG8184 is expressed predominantly expressed in the CNS and trachea of larval stages. Mutation in *Dm*-CG8184 leads to defects in chaeta and mesothoracic tergum (Flybase: <http://flybase.org/reports/FBgn0030674.html>). *Mm-E3 ubiquitin-protein ligase HUWE1* (*Mm-HUWE1*) is a testis ubiquitin protein ligase which is widely expressed. *Mm-HUWE1* targets many proteins for degradation including histones, p53, MCL1 etc. It regulates the neuronal differentiation and proliferation by MYCN degradation (Uniprot: <http://www.uniprot.org/uniprot/Q7TMY8>). TC004152 does have similarities in terms of ubiquitous expression with *Mm-HUWE1*. Both *Dm*-CG8184 and *Mm-HUWE1* do not led to any head related phenotypes which make TC004152 a very interesting candidate.

TC007939: TC007939 apparently does not have orthologs in either *Drosophila melanogaster* or in the mouse. TC007939 encodes a 144 amino acids long uncharacterized protein and there was no conserved domain identified through the conserved domain-search tool of NCBI (<https://www.ncbi.nlm.nih.gov>). I was not able to determine the expression pattern of TC007939 after many attempts with varying concentrations of probes as well as different probes. There could be either a problem with the gene annotation or the expression level is beyond the limit of typical ISH to detect this low abundance of mRNA.

Indeed, in the RNAseq data it shows a comparably low read coverage (http://bioinf.uni_greifswald.de/gb2/gbrowse/tcas5/?name=TC007939). TC007939 is a very interesting candidate because of its strong RNAi phenotypes and appears to be a beetle species specific gene but the gene prediction in order to may be pass the expression pattern needs to be validated.

TC005612: TC005612 has an ortholog in *Drosophila* (*Dm-amun*) but not in mouse and both TC005612 and *Dm-amun* are involved in chaeta development (Shalaby et al., 2009). TC005612 and *Dm-amun* have similar phenotypes and expression pattern during embryogenesis. Hence, TC005612 is not an interesting candidate because of the likely conserved function between *Drosophila* and *Tribolium*. However, this could be an interesting candidate for evolutionary biologist who would be interested in comparing the degree of conservation of TC005612 among insects.

TC010832: TC010832 and its *Drosophila* (*Dm-bib*) and mouse (*Mm-aquaporin-1*) orthologs are aquaporins which are integral membrane proteins. Homozygous *Dm-bib* mutation lead to loss of ventral, lateral, and most of the cephalic epidermis and affect the CNS (Flybase: <http://flybase.org/reports/FBgn0000180.html>). Knockdown of TC010832 also caused the loss of similar structure (cervix cuticle) and larvae were not able to hatch which suggests neurological defects. Based on similar expression in the CNS and phenotypes it seems that TC010832 has conserved function like *Dm-bib* which make TC010832 not so interesting candidate.

TC005276: *Dm-suppressor of zeste 2*, the ortholog of TC005276 is a RING-finger DNA binding protein that regulates gene expression by chromatin silencing. *Dm-suppressor of zeste 2* and *Dm-Psc* are the paralogs and member of Polycomb group (PcG) genes of *Drosophila*. Polycomb group (PcG) genes are involved in regulation of homeotic gene activity. However, mutation in *Dm-suppressor of zeste 2* does not lead to homeotic phenotypes but affect the setae development (Flybase:

<http://flybase.org/reports/FBgn0265623.html>) (Pirrotta, 1997). *Dm-Psc* mutation, in contrast, cause a homeotic transformation and head defects (Flybase: <http://flybase.org/reports/FBgn0005624.html>). Similarly, knockdown of TC005276 results in an opening of additional tracheal at the prothoracic segment, which indicates the homeotic transformation of the prothoracic segment into a mesothoracic segment and it affects the head appendages. These phenotypes are more similar to *Dm-Psc* mutant than *Dm-suppressor of zeste 2* mutant which suggest that only *Dm-Psc* has retained the ancestral function of TC005276 or a role of *Dm-suppressor of zeste 2* in homeotic transformation still needs to be investigated. It appears that TC005276 is a member of Polycomb group (PcG) genes and involved in segment identity regulation via chromatin silencing in *Tribolium*. Hence, this will probably be not a novel finding which make this gene not so interesting. However, it will be interesting to see how far the function of TC005276 is conserved with respect to the *Dm-Psc* function in the regulation of segment identity.

TC032760: *Dm-fat* is involved in the epithelial planar cell polarity (PCP) and negative regulation of tissue growth via tumor suppressive Hippo signaling. The *Dm-fat* phenotype affects many structures including wing, eye, chaeta, abdomen etc. (Flybase: <http://flybase.org/reports/FBgn0001075.html>) (Zhao et al., 2013). The Mouse ortholog- *Mm-fat4* is also involved in PCP and tissues growth. Mutation in *Mm-fat4* causes a kidney disease and alter neuronal proliferation and migration (Kuta et al., 2016; Saburi et al., 2008). Based on conserved expression pattern and phenotypes, it seems that TC032760 has similar function to its *Drosophila* and mouse orthologs and is putatively involved in PCP and Hippo signaling. This suggest that detailed analysis of TC032760 might probably not reveal novel function which makes TC032760 not a very interesting candidates.

In the future, we should study how these eight candidates interact with other known head patterning genes and vice versa.

5.2 Part II: The Gcl project

Axis formation in *Drosophila* is highly derived and factors are either not present (e.g. Bicoid, Oskar) or have different functions (e.g. Nanos, Pumilio) outside of dipterans (Brown et al., 2001; Klomp et al., 2015; Lynch et al., 2011; Schmitt-Engel et al., 2012b; Stauber et al., 1999). In the absence of Bcd, insects achieve anterior patterning either by using structurally novel molecules or re-deploying genes from other processes. For instance, Panish, a structurally different anterior global patterning organizer, shares a similar permissive function with Bicoid but neither the molecular mechanism of this permissive activity nor any instructive activity has been identified in the midge *Chironomous riparius* (Klomp et al., 2015). On the contrary, *Nasonia* utilizes the genes *Nv-otd1* and *Nv-gt* to perform instructive and permissive functions of anterior patterning respectively. The *Drosophila* orthologs *otd* and *gt* are the zygotic trunk gap genes but both *Nv-otd1* and *Nv-gt* are maternally deposited to developing oocytes and establish the A-P axis in *Nasonia* (Brent et al., 2007; Lynch et al., 2006). *Drosophila melanogaster*, *Chironomous riparius* and *Nasonia vitripennis* show quite diverse mechanisms of the long germ mode development and there is no mechanism described for A-P axis formation in short germ insects.

5.2.1 Finding of *Tc-gcl* and *Tc-hbn*

Using the candidate gene approach, the underlying mechanisms of anterior patterning and an anterior global patterning organizer in the short germ development model organism, *Tribolium castaneum*, has remained elusive (note that the previously described model has been challenged by new data.) (Lynch et al., 2012; Schröder, 2003). One of the reasons is the functional divergence of upstream factors of the segmentation machinery (mainly maternal effector and gap genes) (Brown et al., 2001; Bucher and Klingler, 2004; Cerny et al., 2008; Stauber et al., 1999). To search for novel candidates for anterior patterning we mined the database of the ongoing genome-wide RNAi screen (iBeetle) which resulted in

the identification of two candidates: one maternal- *Tc-gcl* and one zygotic- *Tc-hbn*, whose knockdown caused a double abdomen phenotype. This bicaudal phenotype was similar to those phenotypes identified by knockdown of *panish* in *Chironomus riparius* and the double mutant of *bicoid* and *hunchback* in *Drosophila* (Bull, 1966; Driever et al., 1990; Klomp et al., 2015; Simpson-Brose et al., 1994). This shows the importance of *Tc-gcl* and *Tc-hbn* in the *Tribolium* axis determination and patterning and they could act as anterior global pattern organizers. Interestingly, the *Tc-hbn* RNAi has been reported previously to result in the loss of anterior and dorsal head (Sebastian Kittelmann PhD thesis). By contrast, *Tc-hbn* RNAi produced a double abdomen phenotype in the iBeetle screen. In order to test these different findings, I performed the knockdown experiment of *Tc-hbn* in SB and pBA19 strain independently with different non-overlapping fragments (dsRNA). I found that the *Tc-hbn* double abdomen phenotype is a strain specific phenotype and can be seen in pBA19 but not in SB strain. Strain specific phenotypes have been reported earlier for *Tribolium* (Kitzmann et al., 2013). This indicates that these closely related *Tribolium castaneum* strains (namely pBA19 and SB) might have genetic variations in the coding or non-coding region of *Tc-hbn* which in turn either affect the *Tc-hbn* expression or protein function and results in the strain specific phenotypes. It would be very interesting to study the molecular mechanisms behind this strain specific double abdomen phenotype.

5.2.2 Where and how does Tc-Gcl Work?

Gcl proteins from *Drosophila* to mammalian (including human, mouse, *Drosophila* and *Tribolium*) all share the conserved BTB domain and nuclear localization signal. Subcellular localization of Dm-Gcl and mGcl was identified to be at the inner nuclear membrane (Dearden et al., 2006; Kimura et al., 1999; Moore et al., 2009). I also found that Tc-Gcl was localized to the inner nuclear membrane of developing oocytes. The subcellular localization of Gcl is conserved but the tissue specific (spatial) distribution of Gcl varies among different organisms. For example, Dm-Gcl is localized to the posterior pole but we

found that *Tc-gcl* transcript is localized to the anterior pole (Kimura et al., 1999, 2003; Moore et al., 2009). Loss of *Dm-gcl*, *mgcl* (the mouse homolog of Gcl) and *Hs-gcl* all cause sterility (Kimura et al., 2003; Kleiman et al., 2003; Lerit et al., 2017). The expression of Gcl in different tissues among different organisms allows for different protein-protein interactions which might contribute in the different biological processes and in result different phenotypes.

The conserved BTB domain and subcellular location of Gcl among different organisms suggest that the molecular mechanisms (namely protein-protein interactions and engaging of CRL3) through which Gcl acts might also be conserved (Perez-Torrado et al., 2006; Stogios et al., 2005). Indeed, Pae et al. 2017 showed that Dm-Gcl forms a protein complex with CRL3 and targets the degradation of Tor receptor (a somatic cell fate determinant) by ubiquitination. Tc-Gcl, similar to Dm-Gcl, possess a newly characterized GCL domain which provides the substrate recognition of the CRL3 complex in the absence of a BACK domain (Genschik et al., 2013; Pae et al., 2017). This suggests that Tc-Gcl might have a similar function and act as substrate adapter of CRL3 like Dm-Gcl. However, different target proteins could be marked for degradation.

On the other hand, mGcl evidently acts via a transcriptional repression mechanism by recruiting the DP3 α subunit of the E2F transcription factor with the help of the protein binding domain-BTB (de la Luna et al., 1999). There have been many alternative hypotheses to explain the semi-fertile phenotype of *Dm-gcl^A* embryos. For instance, recently, it has been found that *Dm-gcl* regulates the activity of the centrosome thereby controlling the distribution of germ plasm determinants (Lerit et al., 2017). However, I found that *Tc-gcl* is not only localized to the anterior pole but is also involved in anterior patterning by transporting or localizing the maternal *Tc-axin* mRNAs and by activating the zygotic factors *Tc-hbn* and *Tc-zen1*. This indicates an instructive role for *Tc-gcl* in anterior patterning by activating maternal and zygotic factors. Moreover *Tc-gcl* directly or indirectly

represses the expression of posterior patterning genes (e.g. *Tc-cad* and *Tc-wg*) in the anterior, suggesting a permissive role for *Tc-gcl*. Tc-Gcl could be involved in a transcription repression mechanism similar to mGcl by targeting the activator for degradation.

5.2.2.1 How does Tc-Gcl control the maternal *Tc-axin* expression?

Asymmetric localization of maternal components provide the essential inputs required for A-P axis specification during insect embryogenesis. This asymmetry is established during oogenesis by nurse cells and transporter proteins as well as a specific cytoskeletal organization which facilitates the deposition of maternal information to the respective poles. For instance, Bcd is localized at the anterior pole and any disruption in its localization causes defects in anterior patterning (Frohnhofer and Nüsslein-Volhard, 1987). *Tc-pan* and *Tc-eagle* were the first anteriorly localized transcripts found in *Tribolium* unfertilized eggs but do not have any function in early A-P patterning (Bucher et al., 2005). This suggests that *Tc-pan* and *Tc-eagle* are not required for axis specification and anterior determination. Interestingly, I found that nurse cells produce *Tc-axin* mRNAs that are loaded into developing oocytes through the nutritive cord. In younger (developing) oocytes, *Tc-axin* mRNAs are ubiquitously distributed. But in older (mature) oocytes, *Tc-axin* mRNAs are localized in a small domain of the anterior mature eggs. I found that *Tc-gcl* either controls the transport and/or the localization of *Tc-axin* mRNAs because after *Tc-gcl* RNAi, synthesis of *Tc-axin* mRNAs by nurse cells was not affected but in younger oocytes, the *Tc-axin* mRNAs quantity was reduced and there was almost no localized *Tc-axin* mRNA in mature oocytes. Based on the *Drosophila* knowledge, I speculate that it could be cytoskeleton regulation which indirectly interferes with the transport and/or localization. However, *Tc-pan* is still localized after *Tc-gcl* RNAi. Alternatively, there might be post-transcriptional regulation of *Tc-axin* by Tc-Gcl. It could also be that Tc-Gcl stabilizes the *Tc-axin* expression by transcriptional silencing of a *Tc-axin* repressor in developing oocytes but not in nurse cells chambers during *Tc-axin* synthesis.

5.2.3 Hypothesis of anterior localization of maternal *Tc-axin* mRNA

Tribolium developing oocytes contain maternal mRNAs which will be localized either anteriorly (e.g. *Tc-axin*, *Tc-pan* and *Tc-eagle*) or distributed ubiquitously (e.g. *Tc-cad*, *Tc-vasa* and *Tc-otd1*) in the freshly laid eggs (Bucher et al., 2005; Fu et al., 2012b; Schröder, 2003, 2006; Schulz et al., 1998). However, so far posteriorly localized transcripts were not identified in the freshly laid eggs. Those mRNAs, which are localized anteriorly in the freshly laid eggs, start to localize anteriorly in the mature oocytes. Initially, ubiquitously distributed mRNAs (*Tc-cad*, *Tc-vasa* and *Tc-otd1*) undergo posttranscriptional regulation (presumably degradation) and thereby will localize to their respective poles. For example, *Tc-cad* and *Tc-vasa* remain ubiquitous in freshly laid eggs but are localized posteriorly during the blastoderm stage (Schröder, 2006; Schulz et al., 1998). In conclusion, it seems that the nutritive cords load all the maternal mRNAs into the oocyte. This is likely to be based on microtubules of the nutritive cord because they are contiguous with the anterior cortical microtubule network (CMN) of oocytes (Peel and Averof, 2010). Afterwards, either active transport or passive entrapment to the CMN or posttranscriptional regulation of mRNAs may lead to localization to the poles. Ubiquitous distribution of mRNAs happens in absence of localization. For example, anterior localization of *Tc-pan* but not *Tc-eagle* was disrupted by colcemid (a microtubule-depolymerizing agent) which suggests an active participation of CMN in the localization or anchoring of *Tc-pan* mRNA (Peel and Averof, 2010). On the other hand, *Tc-eagle* mRNA localization is independent of the CMN which indicates a passive entrapment or similar to the posterior entrapment of *Dm-nanos* mRNA (Bergsten and Gavis, 1999; Peel and Averof, 2010). I propose that Tc-Gcl is not required for the overall function of the CMN because *Tc-gcl* RNAi does not affect the anterior localization of *Tc-pan* mRNA. Instead, if Tc-Gcl is involved in the organization or the regulation of CMN, then the *Tc-axin* transcript should be distributed evenly but not

degraded like *Tc-pang* mRNAs after colcemid treatment. *Tc-gcl* appears to be more specifically required for the proper transport and/or localization of *Tc-axin* mRNA. Hence, the role of Tc-Gcl is probably either the stabilization of anterior *Tc-axin* mRNAs or the transport of *Tc-axin* mRNAs into the oocytes.

5.2.4 Tc-Gcl may not be involved in the germ cell development

The loss of maternal but not zygotic *Dm-gcl* resulted in a female semi-fertile phenotype (Robertson et al., 1999). Moreover, zygotic expression of *Tc-gcl* was found in the growth zone during early germ band stages. *Vasa* is believed to be a marker of PGCs in insects and *Tc-vasa* expression was also identified in a similar pattern in the growth zone during early germ band stages (Schröder, 2006). Surprisingly, a female semi-fertile phenotype was not observed after *Tc-gcl* knockdown in *Tribolium* embryos, larvae or pupae. I counted the number of eggs laid by knockdown females versus uninjected or buffer injected females. Therefore, any significant reduction would have been noticed. mGcl and *Hs-Gcl* show high expression in the testis and are involved in the spermatogenesis and *gcl* mutations lead to male sterility (Kimura et al., 1999, 2003; Kleiman et al., 2003). Therefore, there is a possibility that *Tc-gcl* is specifically involved in male fertility rather than female fertility. We have used females for injection of dsRNA in RNAi experiments but not males. Hence, the question of whether *Tc-gcl* plays a role in male PGCs should be tested in the future. In this context, loss of mouse *vasa* function affects only male germ cells and results in the loss of sperms in testis (Tanaka et al., 2000).

5.2.3 Role of Tc-Hbn in anterior patterning

The *hbn* mRNAs are localized anteriorly during blastoderm stages and later in the head of germ band stages in both *Drosophila* and *Tribolium*. But neither phenotypic information nor a validated molecular function of Dm-Hbn is available (Walldorf et al., 2000b). Surprisingly, *Tc-hbn* is the first reported zygotic gene whose knockdown caused double

abdomen phenotype. This is contradicting the long standing paradigm that maternal factors are sufficient for axis specification in insects. The Hbn protein possesses a homeodomain that is involved in transcriptional regulation by binding to specific DNA motifs. *Tc-hbn* is involved in the activation of *Tc-zen1* as instructive signal and in the repression of *Tc-cad* as permissive function. I believe that there may be additional downstream targets of *Tc-hbn* which could be involved in anterior patterning as head patterning is not yet fully understood (Schinko et al., 2008). Moreover, based on the expression pattern (first during the blastoderm and later in the head lobes in germ band stages) and the larval phenotype (double abdomen and lack of procephalic head segments), *Tc-hbn* seems to have dual functions- one during embryogenesis for axis patterning and later for development of the procephalic head.

We found that both *Tc-gcl* and *Tc-hbn* RNAi led to the formation of an autonomous segments addition zone (SAZ) at the anterior which are the first genes with this phenotype reported for short germ insects. However, *Tc-gcl*/RNAi resulted in the duplication of the SAZ at early blastoderm stages whereas the *Tc-hbn* RNAi phenotype became obvious after the blastoderm stage. In addition, the larval cuticle of *Tc-gcl*/RNAi showed a duplication of the hindgut and frequently a double abdomen without thoracic segments. But the larval cuticle of *Tc-hbn* RNAi did not show a duplication of the hindgut and a double abdomen mostly with thoracic segments. This explains the hierarchy of gene networks where *Tc-hbn* translate the *Tc-gcl* information of anterior patterning. Moreover, it also indicates the importance of developmental timing for autonomy of SAZ patterning.

5.2.4 Mechanism behind double abdomen formation

Based on the literature and our results, the hypothesis is that *Tc-gcl* controls either the transport and/or the localization of *Tc-axin* which in turn allows activation of *Tc-hbn* and *Tc-zen1* via Wnt pathway repression (See 5.2.2 heading). I tried different combinations to see if *Tc-axin* works alone or in parallel with other factors to repress the double abdomen.

I was not able to get the double abdomen with different combinations of double RNAi (i.e. *Tc-axin+ Tc-zen1/2*, *Tc-axin+ Tc-hbn*, *Tc-hbn+ Tc-zen1/zen2*, *Tc-pan+ Tc-hbn* and *Tc-pan+ Tc-zen1* double RNAi). I assume that there are three possibilities through which *Tc-gcl* information could be translated by the downstream zygotic targets *Tc-hbn* and *Tc-zen1*. Firstly, *Tc-gcl* recruits *Tc-axin* and unknown factors to the anterior to activate the auto-regulatory loop of *Tc-hbn* and *Tc-zen1*. Secondly, *Tc-gcl* directly activates the auto-regulatory loop of *Tc-hbn* and *Tc-zen1* besides the recruitment of *Tc-axin* to the anterior pole. This could be possible because *Tc-gcl* mRNA can be detected until early blastoderm stages. Hence, Tc-Gcl could activate the expression of *Tc-hbn* and *Tc-zen1* via the degradation of a repressor like Dm-Gcl targets Tor receptor for ubiquitination (Pae et al., 2017). Thirdly, *Tc-gcl* might act together with Torso signalling which is active at both poles in freshly laid eggs. *Tc-gcl* could modulate the anterior activity of Torso signalling in such a manner that it allows the activation of *Tc-zen1* but not of the posterior patterning genes *Tc-cad* and *Tc-wg* at the anterior. Weak Torso activity is found at the anterior compare to posterior pole which might allow the activation of *Tc-zen1* but not *Tc-cad* and *Tc-wg* in a concentration specific manner. This hypothesis is in line with the recent finding that Dm-Gcl degrades the Tor receptor in a specific time window in the emerging PGCs (Pae et al., 2017). This could also be true for Tc-Gcl which could degrade the Tor receptor in a specific time window and control the Torso signalling activity. Indeed *Tc-zen1* expression is reduced upon knockdown of *Tc-tor*. However, I found that Torso signalling does not regulate *Tc-hbn* expression which was also confirmed by RNA-seq data of Pridöhl et al. 2017.

5.2.4 Zygotic control of axis specification in insects

Based on double RNAi experiments, I found that *Tc-hbn* and *Tc-zen1* are mutually dependent for their expression and together define anterior structures. Similarly, the posterior patterning genes *Tc-cad* and *Tc-wg* probably form an autoregulatory loop to

establish posterior structures (Oberhofer et al., 2014b). Both auto-regulatory loops, *Tc-hbn* and *Tc-zen1* and *Tc-cad* and *Tc-wg*, could work as two global organizing centres for the anterior and the posterior pole, respectively. This is consistent with the observation that double knockdown of *Tc-hbn* and *Tc-zen1* was able to phenocopy the *Tc-gcl* phenotype and produce double abdomen with high penetrance and expressivity. Similarly, double knockdown of *Tc-cad* and *Tc-pan* (but not *Tc-pan + Tc-torso*, *Tc-arrow + Tc-torso* and *Tc-arrow + Tc-cad* double RNAi) resulted in the replacement of the SAZ with anterior head primordia. However, I was not able to get a double head larval cuticle because the embryos died prior to the secretion of cuticle. This could be primarily because Wnt signalling is involved in many processes like cell fate specification, morphogenesis, and proliferation (Wodarz and Nusse, 1998).

5.2.5 Outlook

Many details remain to be answered to understand A-P axis specification and patterning in *Tribolium castaneum*. Some of the questions which I think we should address are the following:

1. The Tc-Gcl orthologs are present from *C. elegans* to humans. Dm-Gcl is exclusively involved in germ cell development (Cinalli and Lehmann, 2013b; Lerit et al., 2017; Pae et al., 2017). This is the first report where a Gcl ortholog is involved in axis specification and patterning. It would be interesting to identify the function of Tc-Gcl orthologs in other organisms and find out when and how did Gcl evolve its role in A-P patterning.
2. A-P and D-V patterning are quite independent in *Drosophila*. However, A-P and D-V patterning seem to communicate with each other in *Tribolium* (Kotkamp et al., 2010). It would be interesting to further analyse the role of *Tc-gcl* and *Tc-hbn* in D-V patterning. There is already indication that *Tc-gcl* and *Tc-hbn* influence D-V patterning. For example, after *Tc-hbn* RNAi, *Tc-zen1/2* expression boundaries are no longer oblique.

3. Generation and analysis of mutants of *Tc-gcl* and *Tc-hbn* to see the null phenotype. This is important because with RNAi there are always doubts about efficient knockdown of *Tc-gcl* and *Tc-hbn*.
4. The molecular mechanism of Tc-Gcl and Tc-Hbn functions. What are the downstream targets (or binding partners) of Tc-Gcl and Tc-Hbn and any upstream factors which regulate *Tc-gcl* and *Tc-hbn*?
5. What is the mechanism of *Tc-gcl* mRNA localization? How does maternal *Tc-axin* mRNA localize anteriorly?
6. A role of Torso signalling in the anterior patterning besides serosa formation. Is there modulation of Torso signalling by Tc-Gcl?
7. Does *Tc-gcl* function in the development of male PGCs?

6 References

Arakane, Y., Muthukrishnan, S., Kramer, K.J., Specht, C.A., Tomoyasu, Y., Lorenzen, M.D., Kanost, M., and Beeman, R.W. (2005). The *Tribolium* chitin synthase genes TcCHS1 and TcCHS2 are specialized for synthesis of epidermal cuticle and midgut peritrophic matrix. *Insect Mol Biol* *14*, 453–463.

Baird-Titus, J.M., Clark-Baldwin, K., Dave, V., Caperelli, C.A., Ma, J., and Rance, M. (2006). The solution structure of the native K50 Bicoid homeodomain bound to the consensus TAATCC DNA-binding site. *J. Mol. Biol.* *356*, 1137–1151.

Baker, N.E. (1988). Localization of transcripts from the wingless gene in whole *Drosophila* embryos. *Dev. Camb. Engl.* *103*, 289–298.

Bäumer, D., Trauner, J., Hollfelder, D., Cerny, A., and Schoppmeier, M. (2011). JAK-STAT signalling is required throughout telotrophic oogenesis and short-germ embryogenesis of the beetle *Tribolium*. *Dev Biol* *350*, 169–182.

Benton, M.A., Akam, M., and Pavlopoulos, A. (2013). Cell and tissue dynamics during *Tribolium* embryogenesis revealed by versatile fluorescence labeling approaches. *Dev. Camb. Engl.* *140*, 3210–3220.

Berghammer, A., Bucher, G., Maderspacher, F., and Klingler, M. (1999). A system to efficiently maintain embryonic lethal mutations in the flour beetle *Tribolium castaneum*. *Dev Genes Evol* *209*, 382–389.

Berghammer, A.J., Weber, M., Trauner, J., and Klingler, M. (2009a). Red flour beetle (*Tribolium*) germline transformation and insertional mutagenesis. *Cold Spring Harb. Protoc.* *2009*, pdb.prot5259.

Berghammer, A.J., Weber, M., Trauner, J., and Klingler, M. (2009b). Red flour beetle (*Tribolium*) germline transformation and insertional mutagenesis. *Cold Spring Harb. Protoc.* *2009*, pdb.prot5259.

- Bergsten, S.E., and Gavis, E.R. (1999). Role for mRNA localization in translational activation but not spatial restriction of nanos RNA. *Dev. Camb. Engl.* *126*, 659–669.
- Bolognesi, R., Farzana, L., Fischer, T.D., and Brown, S.J. (2008). Multiple Wnt genes are required for segmentation in the short-germ embryo of *Tribolium castaneum*. *Curr Biol* *18*, 1624–1629.
- Brent, A.E., Yucel, G., Small, S., and Desplan, C. (2007). Permissive and instructive anterior patterning rely on mRNA localization in the wasp embryo. *Science* *315*, 1841–1843.
- Bronner, G., and Jackle, H. (1991). Control and function of terminal gap gene activity in the posterior pole region of the *Drosophila* embryo. *Mech. Dev.* *35*, 205–211.
- Brown, S., Fellers, J., Shippy, T., Denell, R., Stauber, M., and Schmidt-Ott, U. (2001). A strategy for mapping bicoid on the phylogenetic tree. *Curr Biol* *11*, R43-4.
- Brown, S.J., Patel, N.H., and Denell, R.E. (1994). Embryonic expression of the single *Tribolium* engrailed homolog. *Dev Genet* *15*, 7–18.
- Brown, S.J., Mahaffey, J.P., Lorenzen, M.D., Denell, R.E., and Mahaffey, J.W. (1999). Using RNAi to investigate orthologous homeotic gene function during development of distantly related insects. *Evol. Dev.* *1*, 11–15.
- Brown, S.J., Shippy, T.D., Miller, S., Bolognesi, R., Beeman, R.W., Lorenzen, M.D., Bucher, G., Wimmer, E.A., and Klingler, M. (2009a). The Red Flour Beetle, *Tribolium castaneum* (Coleoptera): A Model for Studies of Development and Pest Biology. *Cold Spring Harb. Protoc.* *2009*, pdb.emo126.
- Brown, S.J., Shippy, T.D., Miller, S., Bolognesi, R., Beeman, R.W., Lorenzen, M.D., Bucher, G., Wimmer, E.A., and Klingler, M. (2009b). The red flour beetle, *Tribolium castaneum* (Coleoptera): a model for studies of development and pest biology. *Cold Spring Harb. Protoc.* *2009*, pdb.emo126.
- Bucher, G., and Klingler, M. (2004). Divergent segmentation mechanism in the short germ insect *Tribolium* revealed by giant expression and function. *Development* *131*, 1729–1740.

- Bucher, G., Scholten, J., and Klingler, M. (2002). Parental RNAi in *Tribolium* (Coleoptera). *Curr. Biol.* *12*, R85–R86.
- Bucher, G., Farzana, L., Brown, S.J., and Klingler, M. (2005). Anterior localization of maternal mRNAs in a short germ insect lacking bicoid. *Evol Dev* *7*, 142–149.
- Bull, A.L. (1966). Bicaudal, a genetic factor which affects the polarity of the embryo in *Drosophila melanogaster*. *J. Exp. Zool.* *161*, 221–241.
- Carroll, S.B., Laughon, A., and Thalley, B.S. (1988). Expression, function, and regulation of the hairy segmentation protein in the *Drosophila* embryo. *Genes Dev.* *2*, 883–890.
- Cerny, A.C., Bucher, G., Schroder, R., and Klingler, M. (2005). Breakdown of abdominal patterning in the *Tribolium* Kruppel mutant jaws. *Development* *132*, 5353–5363.
- Cerny, A.C., Grossmann, D., Bucher, G., and Klingler, M. (2008). The *Tribolium* ortholog of knirps and knirps-related is crucial for head segmentation but plays a minor role during abdominal patterning. *Dev Biol* *321*, 284–294.
- Chen, C.K., Kühnlein, R.P., Eulenberg, K.G., Vincent, S., Affolter, M., and Schuh, R. (1998). The transcription factors KNIRPS and KNIRPS RELATED control cell migration and branch morphogenesis during *Drosophila* tracheal development. *Dev. Camb. Engl.* *125*, 4959–4968.
- Cho, K.W., Blumberg, B., Steinbeisser, H., and De Robertis, E.M. (1991). Molecular nature of Spemann's organizer: the role of the *Xenopus* homeobox gene goosecoid. *Cell* *67*, 1111–1120.
- Choe, C.P., and Brown, S.J. (2007). Evolutionary flexibility of pair-rule patterning revealed by functional analysis of secondary pair-rule genes, paired and sloppy-paired in the short-germ insect, *Tribolium castaneum*. *Dev Biol* *302*, 281–294.
- Choe, C.P., Miller, S.C., and Brown, S.J. (2006). A pair-rule gene circuit defines segments sequentially in the short-germ insect *Tribolium castaneum*. *Proc Natl Acad Sci U S A* *103*, 6560–6564.
- Cinalli, R.M., and Lehmann, R. (2013a). A spindle-independent cleavage pathway controls germ cell formation in *Drosophila*. *Nat. Cell Biol.* *15*, 839–845.

- Cinalli, R.M., and Lehmann, R. (2013b). A spindle-independent cleavage pathway controls germ cell formation in *Drosophila*. *Nat. Cell Biol.* *15*, 839–845.
- Cohen, S.M., and Jürgens, G. (1990). Mediation of *Drosophila* head development by gap-like segmentation genes. *Nature* *346*, 482–485.
- Copf, T., Schroder, R., and Averof, M. (2004). Ancestral role of caudal genes in axis elongation and segmentation. *Proc Natl Acad Sci U A* *101*, 17711–17715.
- Davis, G.K., and Patel, N.H. (2002). SHORT, LONG, AND BEYOND: Molecular and Embryological Approaches to Insect Segmentation. *Annu. Rev. Entomol.* *47*, 669–699.
- De Robertis, E.M. (2009). Spemann’s organizer and the self-regulation of embryonic fields. *Mech. Dev.* *126*, 925–941.
- Dearden, P., and Akam, M. (1999). Developmental evolution: Axial patterning in insects. *Curr. Biol. CB* *9*, R591-594.
- Dearden, P.K., Wilson, M.J., Sablan, L., Osborne, P.W., Havler, M., McNaughton, E., Kimura, K., Milshina, N.V., Hasselmann, M., Gempe, T., et al. (2006). Patterns of conservation and change in honey bee developmental genes. *Genome Res* *16*, 1376–1384.
- DiNardo, S., Kuner, J.M., Theis, J., and O’Farrell, P.H. (1985). Development of embryonic pattern in *D. melanogaster* as revealed by accumulation of the nuclear engrailed protein. *Cell* *43*, 59–69.
- Dönitz, J., Grossmann, D., Schild, I., Schmitt-Engel, C., Bradler, S., Prpic, N.-M., and Bucher, G. (2013). TrOn: an anatomical ontology for the beetle *Tribolium castaneum*. *PLoS One* *8*, e70695.
- Dönitz, J., Schmitt-Engel, C., Grossmann, D., Gerischer, L., Tech, M., Schoppmeier, M., Klingler, M., and Bucher, G. (2015). iBeetle-Base: a database for RNAi phenotypes in the red flour beetle *Tribolium castaneum*. *Nucleic Acids Res.* *43*, D720–D725.

- Driever, W. (1993). Maternal control of anterior development in the *Drosophila* embryo. In *The Development of Drosophila Melanogaster*, M. Bate, and A. Martinez Arias, eds. (NY: Cold Spring Harbor Laboratory Press), pp. 301–324.
- Driever, W., and Nüsslein-Volhard, C. (1988a). A gradient of bicoid protein in *Drosophila* embryos. *Cell* *54*, 83–93.
- Driever, W., and Nüsslein-Volhard, C. (1988b). The bicoid protein determines position in the *Drosophila* embryo in a concentration-dependent manner. *Cell* *54*, 95–104.
- Driever, W., and Nüsslein-Volhard, C. (1988). The bicoid protein determines position in the *Drosophila* embryo in a concentration-dependent manner. *Cell* *54*, 95–104.
- Driever, W., Siegel, V., and Nüsslein-Volhard, C. (1990). Autonomous determination of anterior structures in the early *Drosophila* embryo by the bicoid morphogen. *Dev. Camb. Engl.* *109*, 811–820.
- Dubnau, J., and Struhl, G. (1996). RNA recognition and translational regulation by a homeodomain protein. *Nature* *379*, 694–699.
- Dubrulle, J., and Pourquié, O. (2004). Coupling segmentation to axis formation. *Dev. Camb. Engl.* *131*, 5783–5793.
- Ellwanger, K., Pfizenmaier, K., Lutz, S., and Hausser, A. (2008). Expression patterns of protein kinase D 3 during mouse development. *BMC Dev. Biol.* *8*, 47.
- El-Sherif, E., Zhu, X., Fu, J., and Brown, S.J. (2014). Caudal Regulates the Spatiotemporal Dynamics of Pair-Rule Waves in *Tribolium*. *PLOS Genet.* *10*, e1004677.
- Ephrussi, A., Dickinson, L.K., and Lehmann, R. (1991). Oskar organizes the germ plasm and directs localization of the posterior determinant nanos. *Cell* *66*, 37–50.
- Felsenstein, J. (1985). Confidence Limits on Phylogenies: An Approach Using the Bootstrap. *Evolution* *39*, 783.

Frohnhofer, H.G., and Christiane Niisslein-Volhard, H.G.F. (1987). Maternal genes required for the anterior localization of bicoid activity in the embryo of *Drosophila*. *Genes Dev.* *1*, 880–890.

Frohnhofer, H.G., and Nüsslein-Volhard, C. (1986). Organization of anterior pattern in the *Drosophila* embryo by the maternal gene bicoid. *Nature* *324*, 120–125.

Frohnhofer, H.G., Lehmann, R., and Nüsslein-Volhard, C. (1986). Manipulating the anteroposterior pattern of the *Drosophila* embryo. *J. Embryol. Exp. Morphol.* *97 Suppl*, 169–179.

Fu, J., Posnien, N., Bolognesi, R., Fischer, T.D., Rayl, P., Oberhofer, G., Kitzmann, P., Brown, S.J., and Bucher, G. (2012a). Asymmetrically expressed axin required for anterior development in *Tribolium*.

Fu, J., Posnien, N., Bolognesi, R., Fischer, T.D., Rayl, P., Oberhofer, G., Kitzmann, P., Brown, S.J., and Bucher, G. (2012b). Asymmetrically expressed axin required for anterior development in *Tribolium*. *Proc. Natl. Acad. Sci. U. S. A.* *109*, 7782–7786.

Fu, J., Posnien, N., Bolognesi, R., Fischer, T.D., Rayl, P., Oberhofer, G., Kitzmann, P., Brown, S.J., and Bucher, G. (2012c). Asymmetrically expressed axin required for anterior development in *Tribolium*.

Fujioka, M., Emi-Sarker, Y., Yusibova, G.L., Goto, T., and Jaynes, J.B. (1999). Analysis of an even-skipped rescue transgene reveals both composite and discrete neuronal and early blastoderm enhancers, and multi-stripe positioning by gap gene repressor gradients. *Dev. Camb. Engl.* *126*, 2527–2538.

Furriols, M., and Casanova, J. (2003). In and out of Torso RTK signalling. *EMBO J.* *22*, 1947–1952.

Gallitano-Mendel, A., and Finkelstein, R. (1997). Novel segment polarity gene interactions during embryonic head development in *Drosophila*. *Dev Biol* *192*, 599–613.

Garcia-Fernandez, J. (2005). The genesis and evolution of homeobox gene clusters. *Nat Rev Genet* *6*, 881–892.

- Gavis, E.R., and Lehmann, R. (1992). Localization of nanos RNA controls embryonic polarity. *Cell* *71*, 301–313.
- Genschik, P., Sumara, I., and Lechner, E. (2013). The emerging family of CULLIN3-RING ubiquitin ligases (CRL3s): cellular functions and disease implications. *EMBO J.* *32*, 2307–2320.
- Gilles, A.F., Schinko, J.B., and Averof, M. (2015). Efficient CRISPR-mediated gene targeting and transgene replacement in the beetle *Tribolium castaneum*. *Dev. Camb. Engl.* *142*, 2832–2839.
- Guder, C., Pinho, S., Nacak, T.G., Schmidt, H.A., Hobmayer, B., Niehrs, C., and Holstein, T.W. (2006). An ancient Wnt-Dickkopf antagonism in Hydra. *Dev. Camb. Engl.* *133*, 901–911.
- Hales, K.G., Korey, C.A., Larracuente, A.M., and Roberts, D.M. (2015). Genetics on the Fly: A Primer on the Drosophila Model System. *Genetics* *201*, 815–842.
- Hanington, P.C., Barreda, D.R., and Belosevic, M. (2006). A Novel Hematopoietic Granulin Induces Proliferation of Goldfish (*Carassius auratus* L.) Macrophages. *J. Biol. Chem.* *281*, 9963–9970.
- Harding, K., and Levine, M. (1988). Gap genes define the limits of antennapedia and bithorax gene expression during early development in Drosophila. *EMBO J.* *7*, 205–214.
- de las Heras, J.M., and Casanova, J. (2006). Spatially distinct downregulation of Capicua repression and tailless activation by the Torso RTK pathway in the Drosophila embryo. *Mech. Dev.* *123*, 481–486.
- Hülskamp, M., Pfeifle, C., and Tautz, D. (1990). A morphogenetic gradient of hunchback protein organizes the expression of the gap genes Krüppel and knirps in the early Drosophila embryo. *Nature* *346*, 577–580.
- Ingham, P.W., Baker, N.E., and Martinez-Arias, A. (1988). Regulation of segment polarity genes in the Drosophila blastoderm by fushi tarazu and even skipped. *Nature* *337*, 73–75.
- Irish, V., Lehmann, R., and Akam, M. (1989a). The Drosophila posterior-group gene nanos functions by repressing hunchback activity. *Nature* *338*, 646–648.

- Irish, V.F., Martinez-Arias, A., and Akam, M. (1989b). Spatial regulation of the Antennapedia and Ultrabithorax homeotic genes during *Drosophila* early development. *EMBO J.* *8*, 1527–1537.
- Jongens, T.A., Hay, B., Jan, L.Y., and Jan, Y.N. (1992). The germ cell-less gene product: a posteriorly localized component necessary for germ cell development in *Drosophila*. *Cell* *70*, 569–584.
- Jongens, T.A., Ackerman, L.D., Swedlow, J.R., Jan, L.Y., and Jan, Y.N. (1994). Germ cell-less encodes a cell type-specific nuclear pore-associated protein and functions early in the germ-cell specification pathway of *Drosophila*. *Genes Dev.* *8*, 2123–2136.
- Kalthoff, K. (1971). Photoreversion of UV induction of the malformation “double abdomen” in the egg of *Smittia spec.* (Diptera, Chironomidae). *Dev. Biol.* *25*, 119–132.
- Kalthoff, K., and Sander, K. (1968). Der Entwicklungsgang der Mißsbildung „Doppelabdomen“ im partiell UV-bestrahlten Ei von *Smittia parthenogenetica* (Dipt., Chironomidae). *Dev. Genes Evol.* *161*, 129–146.
- Kimura, T., Yomogida, K., Iwai, N., Kato, Y., and Nakano, T. (1999). Molecular cloning and genomic organization of mouse homologue of *Drosophila* germ cell-less and its expression in germ lineage cells. *Biochem. Biophys. Res. Commun.* *262*, 223–230.
- Kimura, T., Ito, C., Watanabe, S., Takahashi, T., Ikawa, M., Yomogida, K., Fujita, Y., Ikeuchi, M., Asada, N., Matsumiya, K., et al. (2003). Mouse germ cell-less as an essential component for nuclear integrity. *Mol. Cell. Biol.* *23*, 1304–1315.
- Kittelmann, S. (2012). Formation of the clypeolabral region during embryonic head development of the red flour beetle *Tribolium castaneum*.
- Kitzmann, P., Schwirz, J., Schmitt-Engel, C., and Bucher, G. (2013). RNAi phenotypes are influenced by the genetic background of the injected strain. *BMC Genomics* *14*, 5.

- Kleiman, S.E., Yogev, L., Gal-Yam, E.N., Hauser, R., Gamzu, R., Botchan, A., Paz, G., Yavetz, H., Maymon, B.B.-S., Schreiber, L., et al. (2003). Reduced human germ cell-less (HGCL) expression in azoospermic men with severe germinal cell impairment. *J. Androl.* *24*, 670–675.
- Klingler, M., Erdelyi, M., Szabad, J., and Nüsslein-Volhard, C. (1988). Function of torso in determining the terminal Anlagen of the *Drosophila* embryo. *Nature* *335*, 275–277.
- Klomp, J., Athy, D., Kwan, C.W., Bloch, N.I., Sandmann, T., Lemke, S., and Schmidt-Ott, U. (2015). Embryo development. A cysteine-clamp gene drives embryo polarity in the midge *Chironomus*. *Science* *348*, 1040–1042.
- Kotkamp, K., Klingler, M., and Schoppmeier, M. (2010). Apparent role of *Tribolium* orthodenticle in anteroposterior blastoderm patterning largely reflects novel functions in dorsoventral axis formation and cell survival. *Development* *137*, 1853–1862.
- Krause, G. (1939). *Die Eitypen der Insekten* (Thieme).
- Kuta, A., Mao, Y., Martin, T., Ferreira de Sousa, C., Whiting, D., Zakaria, S., Crespo-Enriquez, I., Evans, P., Balczerski, B., Mankoo, B., et al. (2016). Fat4-Dchs1 signalling controls cell proliferation in developing vertebrae. *Dev. Camb. Engl.* *143*, 2367–2375.
- Leatherman, J.L., Levin, L., Boero, J., and Jongens, T.A. (2002a). germ cell-less acts to repress transcription during the establishment of the *Drosophila* germ cell lineage. *12*, 1681–1685.
- Leatherman, J.L., Levin, L., Boero, J., and Jongens, T.A. (2002b). germ cell-less acts to repress transcription during the establishment of the *Drosophila* germ cell lineage. *Curr. Biol. CB* *12*, 1681–1685.
- Lehmann, R., and Frohnhofer, H.G. (1989). Segmental polarity and identity in the abdomen of *Drosophila* is controlled by the relative position of gap gene expression. *Dev. Camb. Engl.* *107 Suppl*, 21–29.
- Lerit, D.A., Shebelut, C.W., Lawlor, K.J., Rusan, N.M., Gavis, E.R., Schedl, P., and Deshpande, G. (2017). Germ Cell-less Promotes Centrosome Segregation to Induce Germ Cell Formation. *Cell Rep.* *18*, 831–839.

- Lewis, S.L., Khoo, P.-L., De Young, R.A., Steiner, K., Wilcock, C., Mukhopadhyay, M., Westphal, H., Jamieson, R.V., Robb, L., and Tam, P.P.L. (2008). Dkk1 and Wnt3 interact to control head morphogenesis in the mouse. *Dev. Camb. Engl.* *135*, 1791–1801.
- Li, J., Lehmann, S., Weißbecker, B., Ojeda Naharros, I., Schütz, S., Joop, G., and Wimmer, E.A. (2013). Odoriferous Defensive Stink Gland Transcriptome to Identify Novel Genes Necessary for Quinone Synthesis in the Red Flour Beetle, *Tribolium castaneum*. *PLoS Genet* *9*, e1003596.
- Livak, K.J., and Schmittgen, T.D. (2001). Analysis of Relative Gene Expression Data Using Real-Time Quantitative PCR and the $2^{-\Delta\Delta CT}$ Method. *Methods* *25*, 402–408.
- Lorenzen, M.D., Kimzey, T., Shippy, T.D., Brown, S.J., Denell, R.E., and Beeman, R.W. (2007). piggyBac-based insertional mutagenesis in *Tribolium castaneum* using donor/helper hybrids. *Insect Mol Biol* *16*, 265–275.
- Lu, X., Perkins, L.A., and Perrimon, N. (1993). The torso pathway in *Drosophila*: a model system to study receptor tyrosine kinase signal transduction. *Dev Suppl* 47–56.
- de la Luna, S., Allen, K.E., Mason, S.L., and La Thangue, N.B. (1999). Integration of a growth-suppressing BTB/POZ domain protein with the DP component of the E2F transcription factor. *EMBO J.* *18*, 212–228.
- Luschnig, S., Moussian, B., Krauss, J., Desjeux, I., Perkovic, J., and Nüsslein-Volhard, C. (2004). An F1 genetic screen for maternal-effect mutations affecting embryonic pattern formation in *Drosophila melanogaster*. *Genetics* *167*, 325–342.
- Lynch, J.A., Brent, A.E., Leaf, D.S., Pultz, M.A., and Desplan, C. (2006). Localized maternal orthodenticle patterns anterior and posterior in the long germ wasp *Nasonia*. *Nature* *439*, 728–732.
- Lynch, J.A., Peel, A.D., Drechsler, A., Averof, M., and Roth, S. (2010). EGF signaling and the origin of axial polarity among the insects. *Curr. Biol. CB* *20*, 1042–1047.

- Lynch, J.A., Ozüak, O., Khila, A., Abouheif, E., Desplan, C., and Roth, S. (2011). The phylogenetic origin of oskar coincided with the origin of maternally provisioned germ plasm and pole cells at the base of the Holometabola. *PLoS Genet.* *7*, e1002029.
- Lynch, J.A., El-Sherif, E., and Brown, S.J. (2012). Comparisons of the embryonic development of *Drosophila*, *Nasonia*, and *Tribolium*. *Wiley Interdiscip. Rev. Dev. Biol.* *7*, 16–39.
- Manoukian, A.S., and Krause, H.M. (1992). Concentration-dependent activities of the even-skipped protein in *Drosophila* embryos. *Genes Dev.* *6*, 1740–1751.
- Marques-Souza, H., Aranda, M., and Tautz, D. (2008a). Delimiting the conserved features of hunchback function for the trunk organization of insects. *Development* *135*, 881–888.
- Marques-Souza, H., Aranda, M., and Tautz, D. (2008b). Delimiting the conserved features of hunchback function for the trunk organization of insects. *Dev. Camb. Engl.* *135*, 881–888.
- Martin, J.R., Raibaud, A., and Olló, R. (1994). Terminal pattern elements in *Drosophila* embryo induced by the torso-like protein. *Nature* *367*, 741–745.
- Masuhara, M., Nagao, K., Nishikawa, M., Kimura, T., and Nakano, T. (2003). Enhanced degradation of MDM2 by a nuclear envelope component, mouse germ cell-less. *Biochem. Biophys. Res. Commun.* *308*, 927–932.
- Mazza, M.E., Pang, K., Reitzel, A.M., Martindale, M.Q., and Finnerty, J.R. (2010). A conserved cluster of three PRD-class homeobox genes (homeobrain, rx and orthopedia) in the Cnidaria and Protostomia. *Evodevo* *1*, 3.
- McGregor, A.P. (2005). How to get ahead: the origin, evolution and function of bicoid. *BioEssays News Rev. Mol. Cell. Dev. Biol.* *27*, 904–913.
- Meinhardt, H. (1977). A Model of Pattern Formation in Insect Embryogenesis. *J. Cell Sci.* *23*, 117–139.
- Miller, S.C., Miyata, K., Brown, S.J., and Tomoyasu, Y. (2012). Dissecting systemic RNA interference in the red flour beetle *Tribolium castaneum*: parameters affecting the efficiency of RNAi. *PLoS One* *7*, e47431.

- Mineo, A., Furriols, M., and Casanova, J. (2015). Accumulation of the *Drosophila* Torso-like protein at the blastoderm plasma membrane suggests that it translocates from the eggshell. *Dev. Camb. Engl.* *142*, 1299–1304.
- Mohler, J., and Wieschaus, E.F. (1986). Dominant maternal-effect mutations of *Drosophila melanogaster* causing the production of double-abdomen embryos. *Genetics* *112*, 803–822.
- Monecke, T., Güttler, T., Neumann, P., Dickmanns, A., Görlich, D., and Ficner, R. (2009). Crystal Structure of the Nuclear Export Receptor CRM1 in Complex with Snurportin1 and RanGTP. *Science* *324*, 1087–1091.
- Moore, J., Han, H., and Lasko, P. (2009). Bruno negatively regulates germ cell-less expression in a BRE-independent manner. *Mech. Dev.* *126*, 503–516.
- Nagy, L.M., and Carroll, S. (1994). Conservation of wingless patterning functions in the short-germ embryos of *Tribolium castaneum*. *Nature* *367*, 460–463.
- Nayak, A., Berry, B., Tassetto, M., Kunitomi, M., Acevedo, A., Deng, C., Krutchinsky, A., Gross, J., Antoniewski, C., and Andino, R. (2010). Cricket paralysis virus antagonizes Argonaute 2 to modulate antiviral defense in *Drosophila*. *Nat. Struct. Mol. Biol.* *17*, 547–554.
- Nie, W., Stronach, B., Panganiban, G., Shippy, T., Brown, S., and Denell, R. (2001). Molecular characterization of Tclabial and the 3' end of the *Tribolium* homeotic complex. *Dev Genes Evol* *211*, 244–251.
- Niehrs, C. (1999). Head in the WNT: the molecular nature of Spemann's head organizer. *Trends Genet* *15*, 314–319.
- Nili, E., Cojocar, G.S., Kalma, Y., Ginsberg, D., Copeland, N.G., Gilbert, D.J., Jenkins, N.A., Berger, R., Shaklai, S., Amariglio, N., et al. (2001). Nuclear membrane protein LAP2beta mediates transcriptional repression alone and together with its binding partner GCL (germ-cell-less). *J. Cell Sci.* *114*, 3297–3307.
- Nüsslein-Volhard, C. (1977). Genetic analysis of pattern-formation in the embryo of *Drosophila melanogaster*. *Dev. Genes Evol.* *183*, 249–268.

- Nüsslein-Volhard, C., and Wieschaus, E. (1980). Mutations affecting segment number and polarity in *Drosophila*. *Nature* *287*, 795–801.
- Nüsslein-Volhard, C., Frohnhofer, H., and Lehmann, R. (1987). Determination of anteroposterior polarity in *Drosophila*. *Science* *238*, 1675–1681.
- Oberhofer, G., Grossmann, D., Siemanowski, J.L., Beissbarth, T., and Bucher, G. (2014a). Wnt/ β -catenin signaling integrates patterning and metabolism of the insect growth zone. *Development* dev.112797.
- Oberhofer, G., Grossmann, D., Siemanowski, J.L., Beissbarth, T., and Bucher, G. (2014b). Wnt/ β -catenin signaling integrates patterning and metabolism of the insect growth zone. *Dev. Camb. Engl.* *141*, 4740–4750.
- Pae, J., Cinalli, R.M., Marzio, A., Pagano, M., and Lehmann, R. (2017). GCL and CUL3 Control the Switch between Cell Lineages by Mediating Localized Degradation of an RTK. *Dev. Cell* *42*, 130–142.e7.
- Panfilio, K.A. (2008). Extraembryonic development in insects and the acrobatics of blastokinesis. *Dev. Biol.* *313*, 471–491.
- Pankratz, M.J., and Jackle, H. (1990). Making stripes in the *Drosophila* embryo. *Trends Genet* *6*, 287–92.
- Peel, A.D., and Averof, M. (2010). Early asymmetries in maternal transcript distribution associated with a cortical microtubule network and a polar body in the beetle *Tribolium castaneum*. *Dev. Dyn. Off. Publ. Am. Assoc. Anat.* *239*, 2875–2887.
- Perez-Torrado, R., Yamada, D., and Defossez, P.-A. (2006). Born to bind: the BTB protein-protein interaction domain. *BioEssays News Rev. Mol. Cell. Dev. Biol.* *28*, 1194–1202.
- Petersen, C.P., and Reddien, P.W. (2009). Wnt signaling and the polarity of the primary body axis. *Cell* *139*, 1056–1068.
- Pirrotta, V. (1997). PcG complexes and chromatin silencing. *Curr. Opin. Genet. Dev.* *7*, 249–258.

- Posnien, N., Schinko, J., Grossmann, D., Shippy, T.D., Konopova, B., and Bucher, G. (2009). RNAi in the red flour beetle (*Tribolium*). *Cold Spring Harb. Protoc.* *2009*, pdb.prot5256.
- Posnien, N., Schinko, J.B., Kittelmann, S., and Bucher, G. (2010). Genetics, development and composition of the insect head - A beetle's view. *Arthropod Struct Dev* *39*, 399–410.
- Posnien, N., Koniszewski, N.D.B., Hein, H.J., and Bucher, G. (2011). Candidate Gene Screen in the Red Flour Beetle *Tribolium* Reveals Six3 as Ancient Regulator of Anterior Median Head and Central Complex Development. *PLoS Genet.* *7*, e1002418.
- Pridöhl, F., Weis kopf, M., Koniszewski, N., Sulzmaier, A., Uebe, S., Ekici, A.B., and Schoppmeier, M. (2017a). Transcriptome sequencing reveals maelstrom as a novel target gene of the terminal-system in the red flour beetle *Tribolium castaneum*. *Dev. Camb. Engl.*
- Pridöhl, F., Weis kopf, M., Koniszewski, N., Sulzmaier, A., Uebe, S., Ekici, A.B., and Schoppmeier, M. (2017b). Transcriptome sequencing reveals maelstrom as a novel target gene of the terminal-system in the red flour beetle *Tribolium castaneum*. *Dev. Camb. Engl.*
- Pultz, M.A., Zimmerman, K.K., Alto, N.M., Kaeberlein, M., Lange, S.K., Pitt, J.N., Reeves, N.L., and Zehrung, D.L. (2000). A Genetic Screen for Zygotic Embryonic Lethal Mutations Affecting Cuticular Morphology in the Wasp *Nasonia vitripennis*. *Genetics* *154*, 1213–1229.
- Reinitz, J., and Sharp, D.H. (1995). Mechanism of eve stripe formation. *Mech. Dev.* *49*, 133–158.
- Rivera-Pomar, R., Niessing, D., Schmidt-Ott, U., Gehring, W.J., and Jackle, H. (1996). RNA binding and translational suppression by bicoid. *Nature* *379*, 746–749.
- Robertson, S.E., Dockendorff, T.C., Leatherman, J.L., Faulkner, D.L., and Jongens, T.A. (1999). germ cell-less is required only during the establishment of the germ cell lineage of *Drosophila* and has activities which are dependent and independent of its localization to the nuclear envelope. *Dev. Biol.* *215*, 288–297.

- Rossi, A., Kontarakis, Z., Gerri, C., Nolte, H., Hölper, S., Krüger, M., and Stainier, D.Y.R. (2015). Genetic compensation induced by deleterious mutations but not gene knockdowns. *Nature* *524*, 230–233.
- Roth, S., and Lynch, J.A. (2009). Symmetry breaking during *Drosophila* oogenesis. *Cold Spring Harb. Perspect. Biol.* *7*, a001891.
- Saburi, S., Hester, I., Fischer, E., Pontoglio, M., Eremina, V., Gessler, M., Quaggin, S.E., Harrison, R., Mount, R., and McNeill, H. (2008). Loss of Fat4 disrupts PCP signaling and oriented cell division and leads to cystic kidney disease. *Nat. Genet.* *40*, 1010–1015.
- Sander, K. (1961). [Reversal of the germ band polarity in egg fragments of *Euscelis* (Cicadina)]. *Experientia* *17*, 179–180.
- Sanson, B. (2001). Generating patterns from fields of cells. Examples from *Drosophila* segmentation. *EMBO Rep.* *2*, 1083–1088.
- Sarrazin, A.F., Peel, A.D., and Averof, M. (2012). A Segmentation Clock with Two-Segment Periodicity in Insects. *Science*.
- Savant-Bhonsale, S., and Montell, D.J. (1993). torso-like encodes the localized determinant of *Drosophila* terminal pattern formation. *Genes Dev.* *7*, 2548–2555.
- Savard, J., Marques-Souza, H., Aranda, M., and Tautz, D. (2006). A segmentation gene in *tribolium* produces a polycistronic mRNA that codes for multiple conserved peptides. *Cell* *126*, 559–569.
- Schinko, J., Posnien, N., Kittelmann, S., Koniszewski, N., and Bucher, G. (2009). Single and Double Whole-Mount *In situ* Hybridization in Red Flour Beetle (*Tribolium*) Embryos. *Cold Spring Harb. Protoc.* *2009*, pdb.prot5258-pdb.prot5258.
- Schinko, J.B., Kreuzer, N., Offen, N., Posnien, N., Wimmer, E.A., and Bucher, G. (2008). Divergent functions of orthodenticle, empty spiracles and buttonhead in early head patterning of the beetle *Tribolium castaneum* (Coleoptera). *Dev Biol* *317*, 600–613.

- Schinko, J.B., Weber, M., Viktorinova, I., Kiupakis, A., Averof, M., Klingler, M., Wimmer, E.A., and Bucher, G. (2010). Functionality of the GAL4/UAS system in *Tribolium* requires the use of endogenous core promoters. *BMC Dev Biol* *10*, 53.
- Schmitt-Engel, C., Cerny, A.C., and Schoppmeier, M. (2012a). A dual role for nanos and pumilio in anterior and posterior blastodermal patterning of the short-germ beetle *Tribolium castaneum*. *Dev. Biol.*
- Schmitt-Engel, C., Cerny, A.C., and Schoppmeier, M. (2012b). A dual role for nanos and pumilio in anterior and posterior blastodermal patterning of the short-germ beetle *Tribolium castaneum*. *Dev. Biol.* *364*, 224–235.
- Schmitt-Engel, C., Schultheis, D., Schwirz, J., Ströhlein, N., Troelenberg, N., Majumdar, U., Dao, V.A., Grossmann, D., Richter, T., Tech, M., et al. (2015a). The iBeetle large-scale RNAi screen reveals gene functions for insect development and physiology. *Nat. Commun.* *6*, 7822.
- Schmitt-Engel, C., Schultheis, D., Schwirz, J., Ströhlein, N., Troelenberg, N., Majumdar, U., Dao, V.A., Grossmann, D., Richter, T., Tech, M., et al. (2015b). The iBeetle large-scale RNAi screen reveals gene functions for insect development and physiology. *Nat. Commun.* *6*, 7822.
- Schmitt-Engel, C., Schultheis, D., Schwirz, J., Ströhlein, N., Troelenberg, N., Majumdar, U., Dao, V.A., Grossmann, D., Richter, T., Tech, M., et al. (2015c). The iBeetle large-scale RNAi screen reveals gene functions for insect development and physiology. *Nat. Commun.* *6*, 7822.
- Schmittgen, T.D., and Livak, K.J. (2008). Analyzing real-time PCR data by the comparative CT method. *Nat. Protoc.* *3*, 1101–1108.
- Schönauer, A., Paese, C.L.B., Hilbrant, M., Leite, D.J., Schwager, E.E., Feitosa, N.M., Eibner, C., Damen, W.G.M., and McGregor, A.P. (2016). The Wnt and Delta-Notch signalling pathways interact to direct pair-rule gene expression via caudal during segment addition in the spider *Parasteatoda tepidariorum*. *Dev. Camb. Engl.* *143*, 2455–2463.
- Schoppmeier, M., and Schröder, R. (2005). Maternal torso signaling controls body axis elongation in a short germ insect. *Curr Biol* *15*, 2131–2136.

- Schoppmeier, M., Fischer, S., Schmitt-Engel, C., Löhr, U., and Klingler, M. (2009a). An Ancient Anterior Patterning System Promotes Caudal Repression and Head Formation in Ecdysozoa. *Curr. Biol.* *19*, 1811–1815.
- Schoppmeier, M., Fischer, S., Schmitt-Engel, C., Löhr, U., and Klingler, M. (2009b). An ancient anterior patterning system promotes caudal repression and head formation in ecdysozoa. *Curr. Biol. CB* *19*, 1811–1815.
- Schröder, R. (2003). The genes *orthodenticle* and *hunchback* substitute for *bicoid* in the beetle *Tribolium*. *Nature* *422*, 621–625.
- Schröder, R. (2006). *vasa* mRNA accumulates at the posterior pole during blastoderm formation in the flour beetle *Tribolium castaneum*. *Dev. Genes Evol.* *216*, 277–283.
- Schroder, R., Eckert, C., Wolff, C., and Tautz, D. (2000). Conserved and divergent aspects of terminal patterning in the beetle *Tribolium castaneum*. *Proc. Natl. Acad. Sci.* *97*, 6591–6596.
- Schröder, R., Eckert, C., Wolff, C., and Tautz, D. (2000). Conserved and divergent aspects of terminal patterning in the beetle *Tribolium castaneum*. *Proc. Natl. Acad. Sci. U. S. A.* *97*, 6591–6596.
- Schröder, R., Beermann, A., Wittkopp, N., and Lutz, R. (2008). From development to biodiversity--*Tribolium castaneum*, an insect model organism for short germband development. *Dev. Genes Evol.* *218*, 119–126.
- Schulz, C., Schroder, R., Hausdorf, B., Wolff, C., and Tautz, D. (1998). A caudal homologue in the short germ band beetle *Tribolium* shows similarities to both, the *Drosophila* and the vertebrate caudal expression patterns. *Dev Genes Evol* *208*, 283–289.
- Schupbach, T., and Wieschaus, E. (1986). Germline autonomy of maternal-effect mutations altering the embryonic body pattern of *Drosophila*. *Dev. Biol.* *113*, 443–448.
- Shalaby, N.A., Parks, A.L., Morreale, E.J., Osswald, M.C., Pfau, K.M., Pierce, E.L., and Muskavitch, M.A.T. (2009). A screen for modifiers of notch signaling uncovers Amun, a protein with a critical role in sensory organ development. *Genetics* *182*, 1061–1076.

- Shapiro, R.S., and Anderson, K.V. (2006). *Drosophila* Ik2, a member of the I kappa B kinase family, is required for mRNA localization during oogenesis. *Dev. Camb. Engl.* *133*, 1467–1475.
- Shi, Z.R., Itzkowitz, S.H., and Kim, Y.S. (1988). A comparison of three immunoperoxidase techniques for antigen detection in colorectal carcinoma tissues. *J. Histochem. Cytochem.* *36*, 317–322.
- Shinmyo, Y., Mito, T., Matsushita, T., Sarashina, I., Miyawaki, K., Ohuchi, H., and Noji, S. (2005). *caudal* is required for gnathal and thoracic patterning and for posterior elongation in the intermediate-germband cricket *Gryllus bimaculatus*. *Mech Dev* *122*, 231–239.
- Shippy, T.D., Ronshaugen, M., Cande, J., He, J., Beeman, R.W., Levine, M., Brown, S.J., and Denell, R.E. (2008). Analysis of the *Tribolium* homeotic complex: insights into mechanisms constraining insect Hox clusters. *Dev Genes Evol* *218*, 127–139.
- Siebert, K.S., Lorenzen, M.D., Brown, S.J., Park, Y., and Beeman, R.W. (2008). Tubulin superfamily genes in *Tribolium castaneum* and the use of a Tubulin promoter to drive transgene expression. *Insect Biochem. Mol. Biol.* *38*, 749–755.
- Siemanowski, J., Richter, T., Dao, V.A., and Bucher, G. (2015). Notch signaling induces cell proliferation in the labrum in a regulatory network different from the thoracic legs. *Dev. Biol.* *408*, 164–177.
- Simpson-Brose, M., Treisman, J., and Desplan, C. (1994). Synergy between the hunchback and bicoid morphogens is required for anterior patterning in *Drosophila*. *Cell* *78*, 855–865.
- Snodgrass, R. (1954). *Insect Metamorphosis*: Smithsonian Miscellaneous Collections, V122, No. 9 (Washington: Literary Licensing).
- Sokoloff, A. (1972). *The biology of Tribolium: with special emphasis on genetic aspects* (Oxford: Clarendon Press).
- Sokoloff, A. (1974). *The biology of Tribolium: with special emphasis on genetic aspects* (Clarendon Press).

- St Johnston, D. (2002). The art and design of genetic screens: *Drosophila melanogaster*. *Nat Rev Genet* *3*, 176–188.
- St Johnston, D., and Nüsslein-Volhard, C. (1992). The origin of pattern and polarity in the *Drosophila* embryo. *Cell* *68*, 201–219.
- Stauber, M., Jackle, H., and Schmidt-Ott, U. (1999). The anterior determinant bicoid of *Drosophila* is a derived Hox class 3 gene. *Proc Natl Acad Sci U S A* *96*, 3786–3789.
- Stogios, P.J., Downs, G.S., Jauhal, J.J.S., Nandra, S.K., and Privé, G.G. (2005). Sequence and structural analysis of BTB domain proteins. *Genome Biol.* *6*, R82.
- Strecker, T.R., Kongsuwan, K., Lengyel, J.A., and Merriam, J.R. (1986). The zygotic mutant tailless affects the anterior and posterior ectodermal regions of the *Drosophila* embryo. *Dev Biol* *113*, 64–76.
- Sulston, I.A., and Anderson, K.V. (1996). Embryonic patterning mutants of *Tribolium castaneum*. *Development* *122*, 805–814.
- Tamura, K., Stecher, G., Peterson, D., Filipski, A., and Kumar, S. (2013). MEGA6: Molecular Evolutionary Genetics Analysis Version 6.0. *Mol. Biol. Evol.* *30*, 2725–2729.
- Tanaka, S.S., Toyooka, Y., Akasu, R., Katoh-Fukui, Y., Nakahara, Y., Suzuki, R., Yokoyama, M., and Noce, T. (2000). The mouse homolog of *Drosophila* Vasa is required for the development of male germ cells. *Genes Dev.* *14*, 841–853.
- Trauner, J., and Büning, J. (2007). Germ-cell cluster formation in the telotrophic meroistic ovary of *Tribolium castaneum* (Coleoptera, Polyphaga, Tenebrionidae) and its implication on insect phylogeny. *Dev. Genes Evol.* *217*, 13–27.
- Trauner, J., and Buning, J. (2007). Germ-cell cluster formation in the telotrophic meroistic ovary of *Tribolium castaneum* (Coleoptera, Polyphaga, Tenebrionidae) and its implication on insect phylogeny. *Dev Genes Evol* *217*, 13–27.
- Trauner, J., Schinko, J., Lorenzen, M.D., Shippy, T.D., Wimmer, E.A., Beeman, R.W., Klingler, M., Bucher, G., and Brown, S.J. (2009). Large-scale insertional mutagenesis of a

- coleopteran stored grain pest, the red flour beetle *Tribolium castaneum*, identifies embryonic lethal mutations and enhancer traps. *BMC Biol* 7, 73.
- Tribolium Genome Sequencing Consortium, Richards, S., Gibbs, R.A., Weinstock, G.M., Brown, S.J., Denell, R., Beeman, R.W., Gibbs, R., Beeman, R.W., Brown, S.J., et al. (2008). The genome of the model beetle and pest *Tribolium castaneum*. *Nature* 452, 949–955.
- Twigg, S.R.F., Lloyd, D., Jenkins, D., Elçioğlu, N.E., Cooper, C.D.O., Al-Sannaa, N., Annagür, A., Gillessen-Kaesbach, G., Hüning, I., Knight, S.J.L., et al. (2012). Mutations in multidomain protein MEGF8 identify a Carpenter syndrome subtype associated with defective lateralization. *Am. J. Hum. Genet.* 91, 897–905.
- Van der Zee, M., Berns, N., and Roth, S. (2005). Distinct functions of the *Tribolium* *zerknüllt* genes in serosa specification and dorsal closure. *15*, 624–636.
- Walldorf, U., Kiewe, A., Wickert, M., Ronshaugen, M., and McGinnis, W. (2000a). Homeobrain, a novel paired-like homeobox gene is expressed in the *Drosophila* brain. *Mech Dev* 96, 141–144.
- Walldorf, U., Kiewe, A., Wickert, M., Ronshaugen, M., and McGinnis, W. (2000b). Homeobrain, a novel paired-like homeobox gene is expressed in the *Drosophila* brain. *Mech. Dev.* 96, 141–144.
- Wodarz, A., and Nusse, R. (1998). Mechanisms of Wnt signaling in development. *Annu. Rev. Cell Dev. Biol.* 14, 59–88.
- Wolff, C., Schröder, R., Schulz, C., Tautz, D., and Klingler, M. (1998). Regulation of the *Tribolium* homologues of caudal and hunchback in *Drosophila*: evidence for maternal gradient systems in a short germ embryo. *Dev. Camb. Engl.* 125, 3645–3654.
- Yajima (1960). Studies on embryonic determination of the harlequin-fly, *Chironomus dorsalis*. I. Effects of centrifugation and of its combination with constriction and puncturing. *J. Embryol. Exp. Morphol.* 8, 198–215.

- Yajima, H. (1964). Studies on embryonic determination of the harlequin-fly, *Chironomus dorsalis*. II. Effects of partial irradiation of the egg by ultra-violet light. *Development* *12*, 89–100.
- van der Zee, M., Berns, N., and Roth, S. (2005). Distinct functions of the *Tribolium zerknullt* genes in serosa specification and dorsal closure. *Curr Biol* *15*, 624–636.
- Zhang, T., Braun, U., and Leitges, M. (2016). PKD3 deficiency causes alterations in microtubule dynamics during the cell cycle. *Cell Cycle Georget. Tex* *15*, 1844–1854.
- Zhang, Z., Alpert, D., Francis, R., Chatterjee, B., Yu, Q., Tansey, T., Sabol, S.L., Cui, C., Bai, Y., Koriabine, M., et al. (2009). Massively parallel sequencing identifies the gene *Megf8* with ENU-induced mutation causing heterotaxy. *Proc. Natl. Acad. Sci. U. S. A.* *106*, 3219–3224.
- Zollman, S., Godt, D., Privé, G.G., Couderc, J.L., and Laski, F.A. (1994). The BTB domain, found primarily in zinc finger proteins, defines an evolutionarily conserved family that includes several developmentally regulated genes in *Drosophila*. *Proc. Natl. Acad. Sci. U. S. A.* *91*, 10717–10721.
- (1987). Maternal genes required for the anterior localization of bicoid activity in the embryo of *Drosophila*. *Genes Dev.* *1*, 880–890.

7 Appendix

7.1 List of *Tc* genes

Table 7.1 Known *Tc* genes found during the rescreening

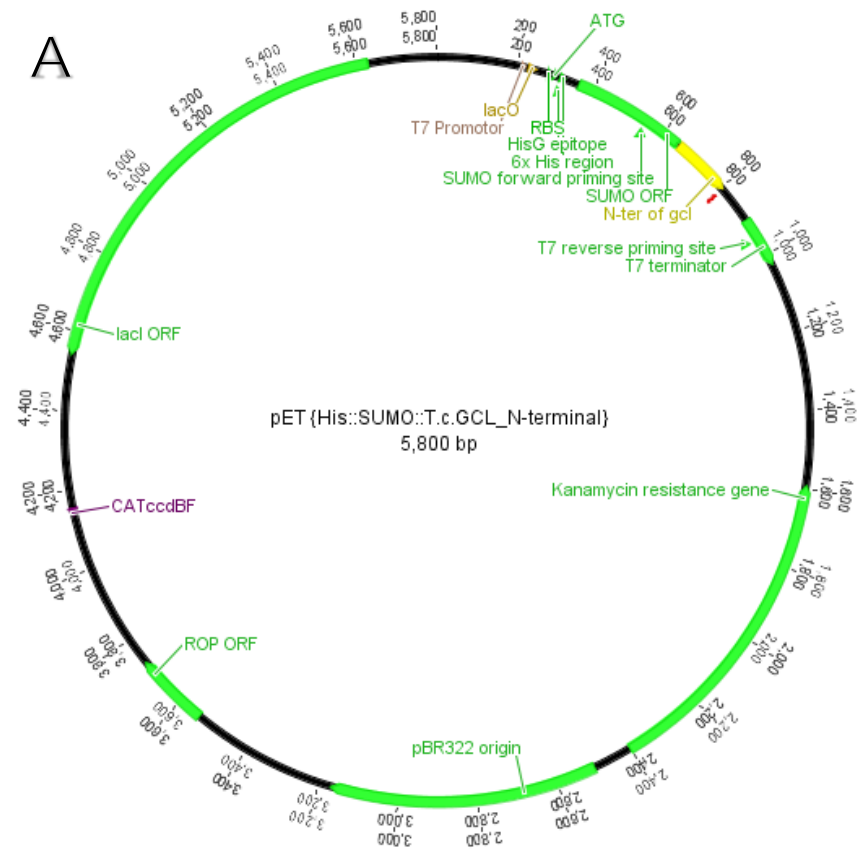
dsRNA_ID	Gene ID	dsRNA_ID	Gene ID
6816	<i>six3/optix</i>	7208	<i>krüppel</i>
3011	<i>six 3/optix</i>	3105	<i>proboscipedia</i>
4564	<i>homeobrain</i>	9082	<i>pannier</i>
7188	<i>eyless</i>	7222	<i>eyegone</i>
5898	<i>paired</i>	6941	<i>spineless (ss)</i>
7983	<i>crocodile</i>	5264	<i>DSCAM</i>
8747	<i>scarecrow</i>	3837	<i>foxQ2</i>
7391	<i>orthodenticle</i>	3352	<i>grain</i>
5098	<i>empty spiracles</i>	8824	<i>serrate</i>
2761	<i>sloppy paired</i>	4764	<i>serrate</i>

Table 7.2 *Tc* genes cloned. The name of the gene, the name of the primer, primer sequence and purpose of clones are mentioned.

Gene ID	Primer iD	Sequence	Purpose
<i>germ cell-less</i>	Gcl_GG_Linkers_F	CCAGGTCTCATGGTATGGGGCTGATTTACTCCAGTAGTAG	Protein overexpression
	Gcl_GG_Linkers_R	GGGGTCTCCTCGAGTTAGGAGACAGTTTGACGACC	
<i>germ cell-less</i>	gcl_N-ter_linker_Fw	CCAGGTCTCATGGTATGGGGCTGATTTACTCC	Protein overexpression
	gcl_N-ter_linker_Rv	GGGGTCTCCTCGAGTTCATGCAGTGCTCACTAG	
<i>germ cell-less</i>	Tc_Gcl_F	ATGGGGCTGATTTACTCCAGTAGTAG	in situ probe
	Tc_Gcl_R	TTAGGAGACAGTTTGACGACC	
<i>germ cell-less</i>	gcl_iB_02693_Fw	TCAACCAAAACGACGATAAGG	dsRNA (iB fragment)
	gcl_iB_02693_Rv	TGCACGACCTCTTCTGATT	
<i>homeobrain</i>	hbn_iB_04564_Fw	CGTCTACAGCATCGACCAGA	dsRNA (iB fragment)
	hbn_iB_04564_Rv	CCTTTTCACGCTTCTCCAC	
<i>pangolin</i>	pang_iB_07007_Fw	TGTACGTGTACGACGTGACG	dsRNA (iB fragment)
	pang_iB_07007_Rv	CCCATGTTGAACGAAGAGGTG	
<i>pannier</i>	pannier_CDS_Fw	ATGTTCCATACAAGCGGTGG	in situ probe
	pannier_CDS_Rv	CTAAGACGAGGCCATTAGTTTG	
TC005612	iB_00900_Fw	ATGGCCTCCGCTAAAGACAC	in situ probe
	iB_00900_Rv	TCACTTATCTCGTACGTCCTCCC	
TC032760	iB_4393/6244_Fw	ATTTCCCCGAACTGCAGAGG	in situ probe
	iB_4393/6244_Rv	ATTTCCCCGAACTGCAGAGG	
TC009940	iB_4730_Fw	ATGGATGGTACGGGGCCAG	in situ probe
	iB_4730_Rv	AGCCAGCCCTCTTTGATCAC	
TC031158	iB_5677_Fw	CAACAACCTGCTCCAACCACG	in situ probe
	iB_5677_Rv	ATTTCCGTCCAGTGACGGTC	
TC010832	iB_6600_Fw	ATCTCCGAGTGCATAGCGTC	in situ probe
	iB_6600_Rv	GGCGGCTATTTTTACTGGG	
TC005276	iB_6673_Fw	TGGACGTGCTTACACCTTC	in situ probe
	iB_6673_Rv	TCGAGACTTGGCGTTTCTC	
TC007939	iB_7145_mRNA_Fw	ACTGTGATTATTATTGTAAGACAGCCG	in situ probe
	iB_7145_mRNA_Rv	AATCACATAGAAAAATCTGCTCACAC	
	iB_7145_CDS_Fw	CGAACAACCTGTCAGCCAACG	in situ probe
	iB_7145_CDS_Rv	CTATTCGCTGTCCTCGAACAGC	
TC004152	iB_10029_Fw	CCCACACTGTCACCCTACACAC	in situ probe
	iB_10029_Rv	CACTGCGCTCGATGGAAATG	

7.2 Vectors used during the study

petSUMO vector was used for protein overexpression experiments (Fig. 7.1A). For synthesis of dsRNAs or *in situ* probes, fragments were cloned into the pJet 1.2 vector (Fig. 7.1B). Other vectors were also used for the purpose of dsRNAs and *in situ* probes synthesis but it was not cloned by myself.



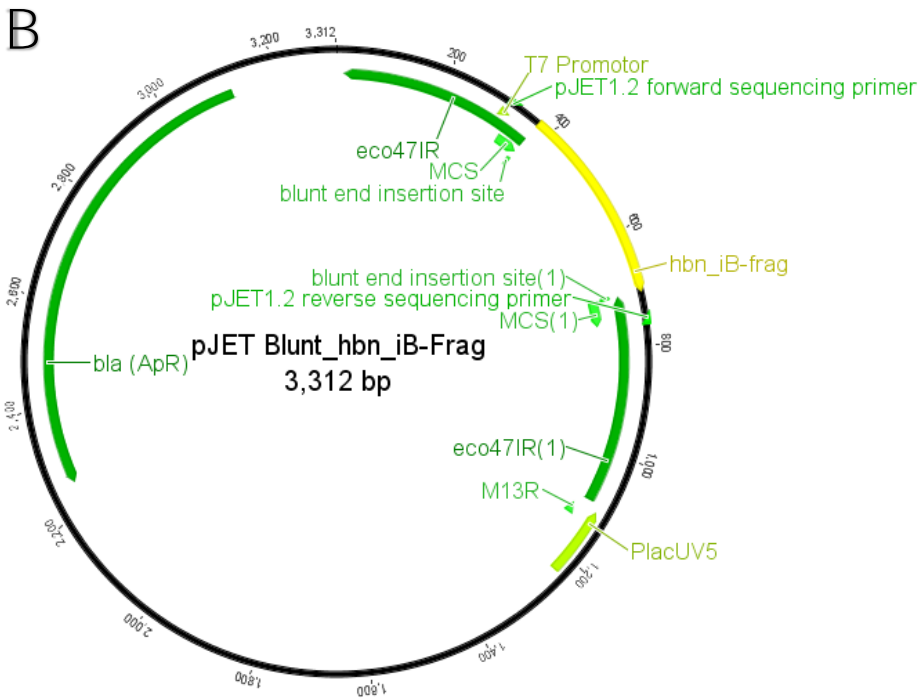


Figure 7.1 Vector maps. (A) N terminal *Tc-gcl* was cloned into petSUMO vector for the overexpression which also tagged the protein with His and SUMO tag. (B) *Tc-hbn* iBeetle fragment was cloned into pjet1.2 vector for dsRNA synthesis.

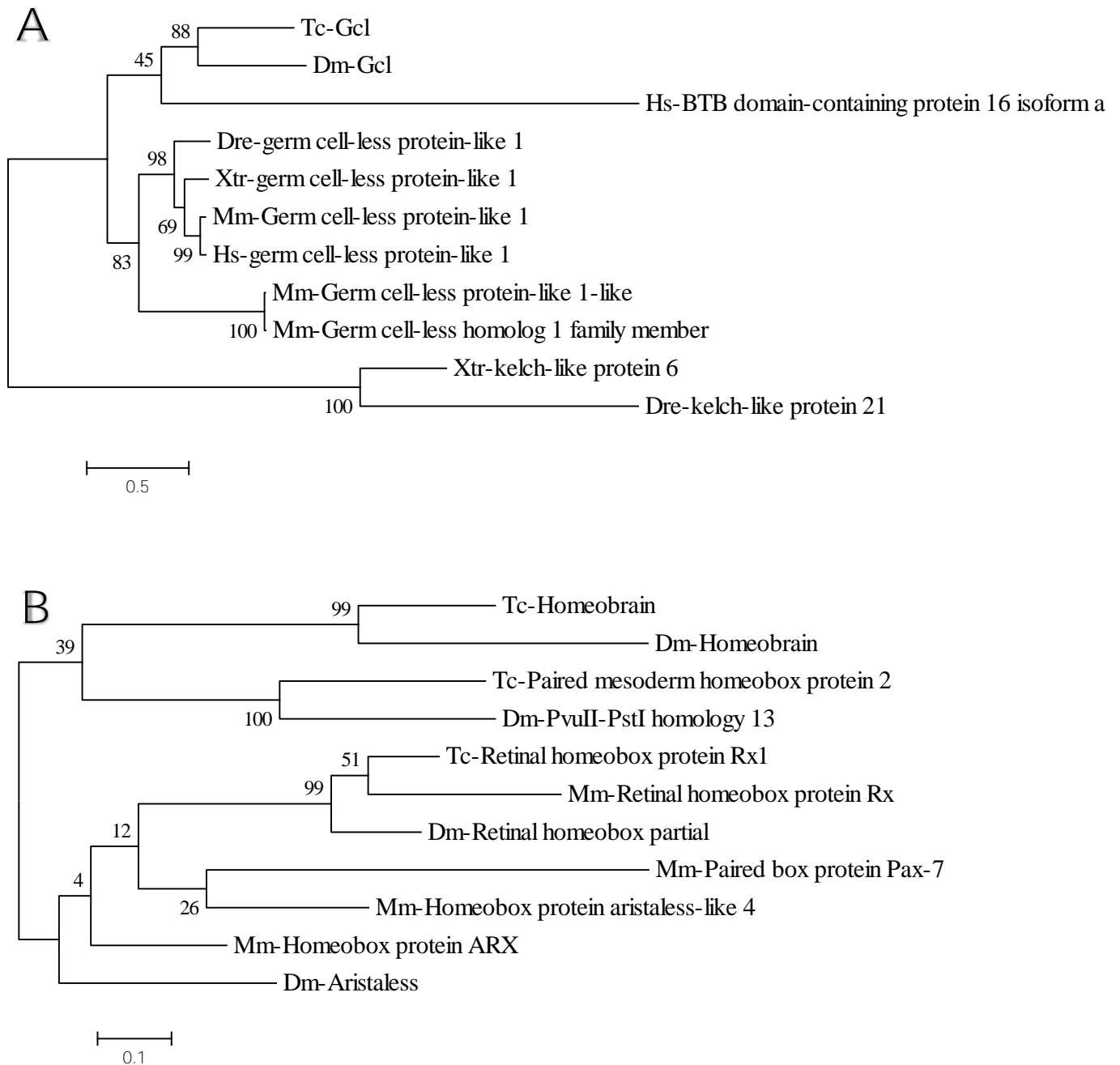
7.3 Phylogenetic trees of *Tc-gcl* and *Tc-hbn*

Figure 7.2 Phylogenetic analysis of *Tc-Gcl* and *Tc-Hbn* based on Maximum Likelihood method and JTT matrix with bootstrap scores at the nodes. (A) *Tc-Gcl* phylogenetic tree. *Tc*= *Tribolium castaneum*, *Dm*= *Drosophila melanogaster*, *Dre*= *Danio rerio*, *Mm*= Mouse; *Xtr*= *Xenopus tropicalis*; *Hsa*= *Homo sapiens*. (B) *Tc-Hbn* phylogenetic tree. The evolutionary history was analyzed by using amino acid sequences.

7.3.1 Tc -Gcl sequence analysis

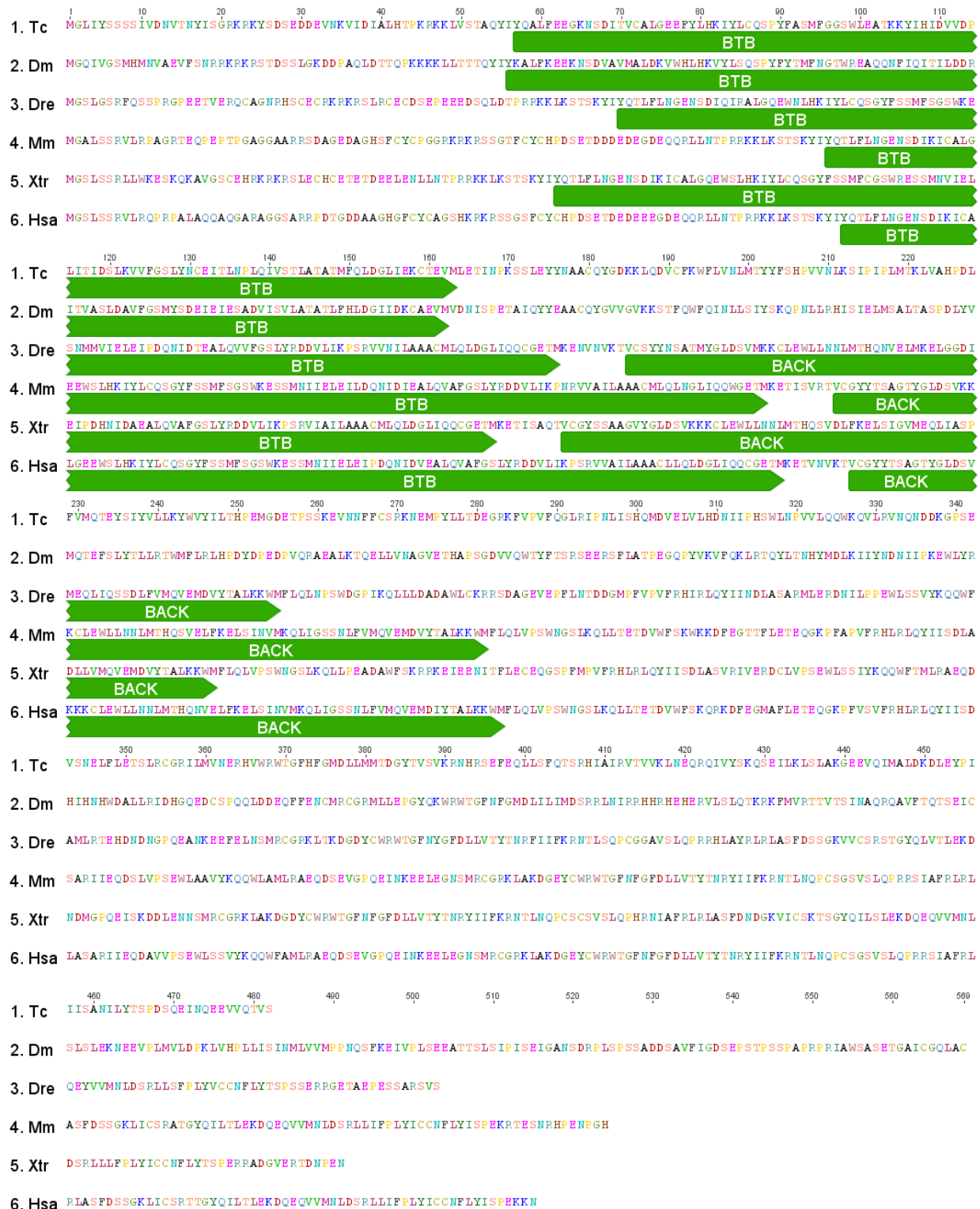


Figure 7.3 Gcl alignment. Comparison of BTB domains of Gcl proteins from different species.

8 Curriculum vitae

Personal Information:

Name	Salim Ansari
Date of birth	03-05-1990
Gender/Marital Status	Male/Single
Nationality	Indian
Address	Kellnerweg 10 Göttingen 37077, Germany
Email Id	sansari@gwdg.de

Publication:

Gurudutta Panda, Pooja Tanwer, Salim Ansari, Devanshi Khare. Regulation and RNA-binding properties of Hfq-like RNA chaperones in *Bacillus anthracis*. *Biochim Biophys Acta*. 2015 Sep;1850(9):1661-8.

Salim Ansari*, Nicole Troelenberg*, Julia Ulrich*, Van Anh Dao, Tobias Richter, Gregor Bucher#, Martin Klingler. Maternal *germ cell-less* and zygotic *homeobrain* and *zen1* in axis formation. **In submission process.**

Research Experience:

PhD project (2013- 2017).

1st. iBeetle screening, Genome-wide RNAi screening in *Tribolium castaneum*

2nd. Head versus tail: *germ cell-less* initiates axis formation via *homeobrain* and *zen1* in a beetle

Supervisor: Prof. Gregor Bucher, Department of Developmental Evolutionary Genetics, Georg-August-Universität Göttingen, Germany.

M.Sc. thesis, Jawaharlal Nehru University, New Delhi (2012-2013).

Title- “Characterization of RNA Chaperones - Hfq & Hf1 in *Bacillus anthracis*”

Supervisor: Prof. Rakesh Bhatnagar, School of Biotechnology, JNU, New Delhi, India.

Education:

<i>Degree</i>	<i>Subjects</i>	<i>Year</i>	<i>University</i>	<i>% Marks / grade</i>
PhD	Functional Genomics	2017	Georg August University, Germany	-----
M.Sc.	Biotechnology	2013	Jawaharlal Nehru University, Delhi, India	7.42 out of 9 / first
B.Sc. (Hons.)	Biotechnology	2011	C.S.J.M. University, Kanpur, India	66 % / first
Intermediate (12 th)	English, Hindi, Biology, Physics, Chemistry	2008	U.P. Board	67 % / first

Supervision:

Guided two bachelor students during the thesis and rotation. Guided group of Master student in the lab course.

Contribution to conferences:

Talk at *Tribolium* satellite meeting and Euro Evo Devo Uppsala 2016: "Instead of *bicoid*, *germ cell-less* is required for axis formation in a beetle", Uppsala, Sweden, 25/07/16 - 29/07/16

Language skills:

Native- Hindi,

Full proficiency- English,

A1.2- German.